Geotechniekdag 2019:
The Future of Geo-Engineering

Dynamic Soil-Structure Interaction:
Understanding the Holocene, instrumenting the Anthropocene

Nick O'Riordan PhD PE CEng

Excerpts from 58th Rankine Lecture re-run
Breda, November 5th, 2019

ARUP

Full 58th Rankine lecture is on Youtube!

https://www.youtube.com/channel/UCdAPBc_wlRBG_708brXabkg

ARUP

1980s photo: Courtesy Heller Manus Architects
2017 photo: Proehl Studios

San Francisco Downtown 1987 > 2017

Anthropocene: the current geological age, during which human activity has been the dominant influence on the environment *(Wikipedia)*

ARUP

Seismic ground displacements imposed on below-ground structures (modified, after Free et al, 2001)

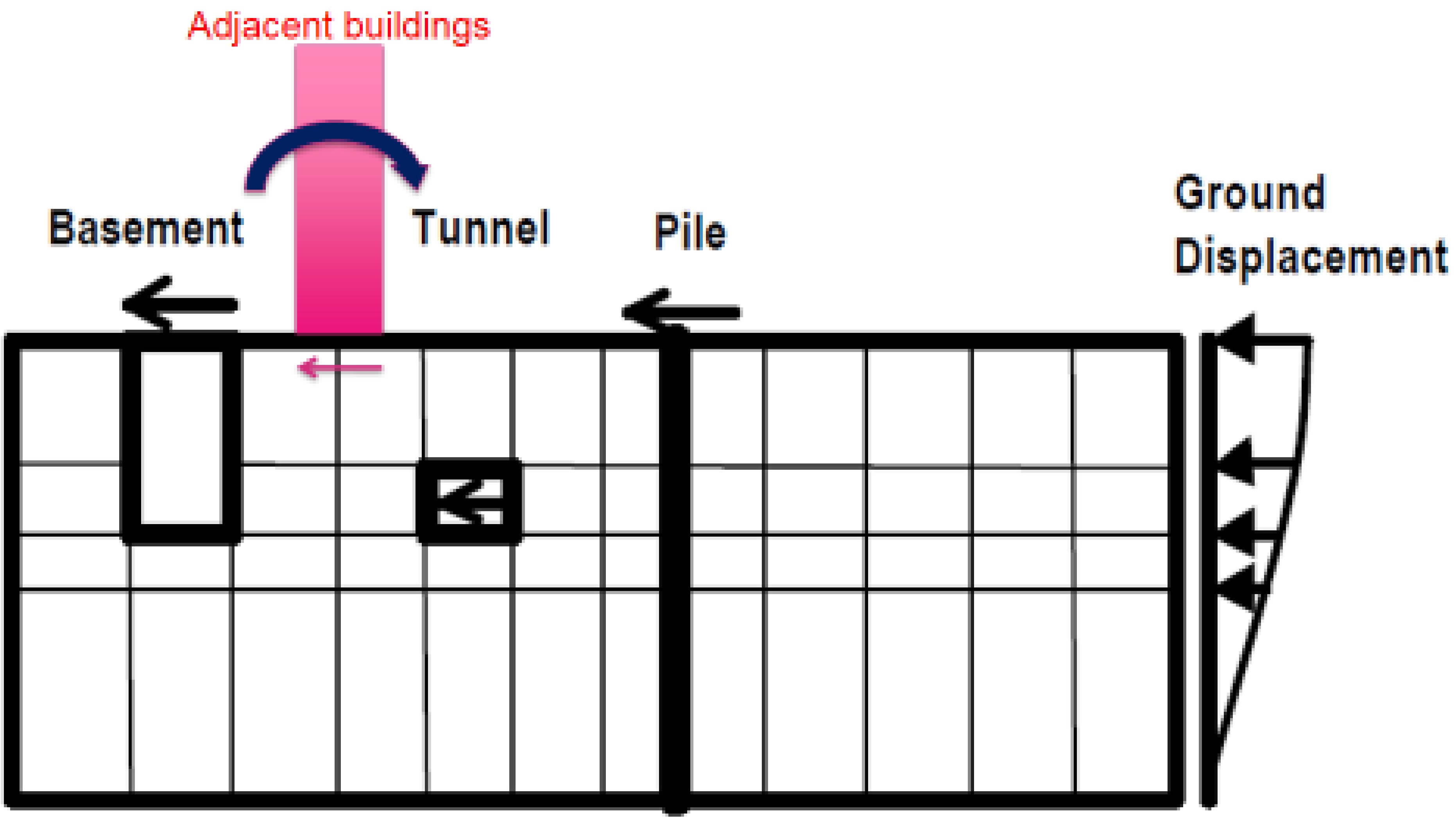

Closed arrows indicate free-field displacement

Open arrows indicate inertial force effects

Main components of dynamic SSI

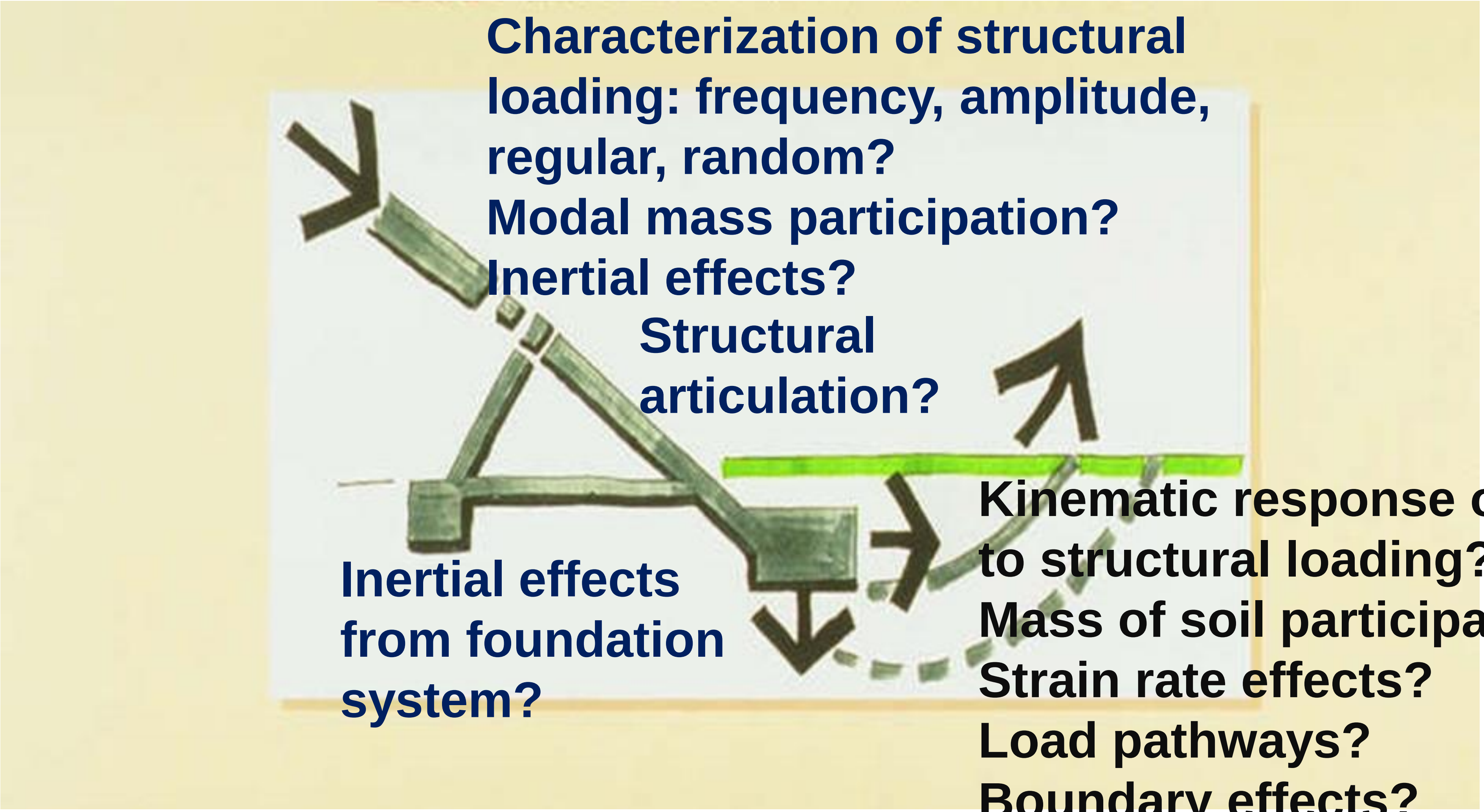

Characterization of structural loading: frequency, amplitude, regular, random?
Modal mass participation?
Inertial effects?

Structural articulation?

Inertial effects from foundation system?

Kinematic response of soil to structural loading?
Mass of soil participating?
Strain rate effects?
Load pathways?
Boundary effects?

The digital ‘twin’

Digital twin refers to a **digital** replica of physical assets (physical **twin**), processes, people, places, systems and devices that can be used for various purposes.
The **digital** representation provides both the elements and the dynamics of how an Internet of things device operates and lives throughout its life cycle.

As Geotechnical Engineers we need to be better at defining the properties of the ground in the time domain: strain rate dependency, destructuration under repetitive loading, in situ tests, long term behaviour and feedback.

A digital twin can be made for a rapid insitu test (CPT, Pressuremeter, DMT), the construction process and completed installation.

ARUP

FE analyses: EuroNCAP Pole Impact 50 km/hr (14 m/s)

Peak Intrusion Depth (mm)		
POINT	TARGET	SLC
1	< 230	110
2	< 230	207
3	< 230	262
4	< 230	297
5	< 230	326
6	< 230	189
7	< 230	294
8	< 230	294
9	< 230	285
10	< 230	296
11	< 230	107
12	< 230	48
13	< 230	51
14	< 230	61

Peak Global Velocity (m/s)		
POINT	TARGET	SLC
3	< 8 m/s	8.3
5	< 8 m/s	8.2
10	< 8 m/s	8.1

Survival Space (Door) (mm)		
POINT	TARGET	SLC
10	> 405	547

Vehicle deformation

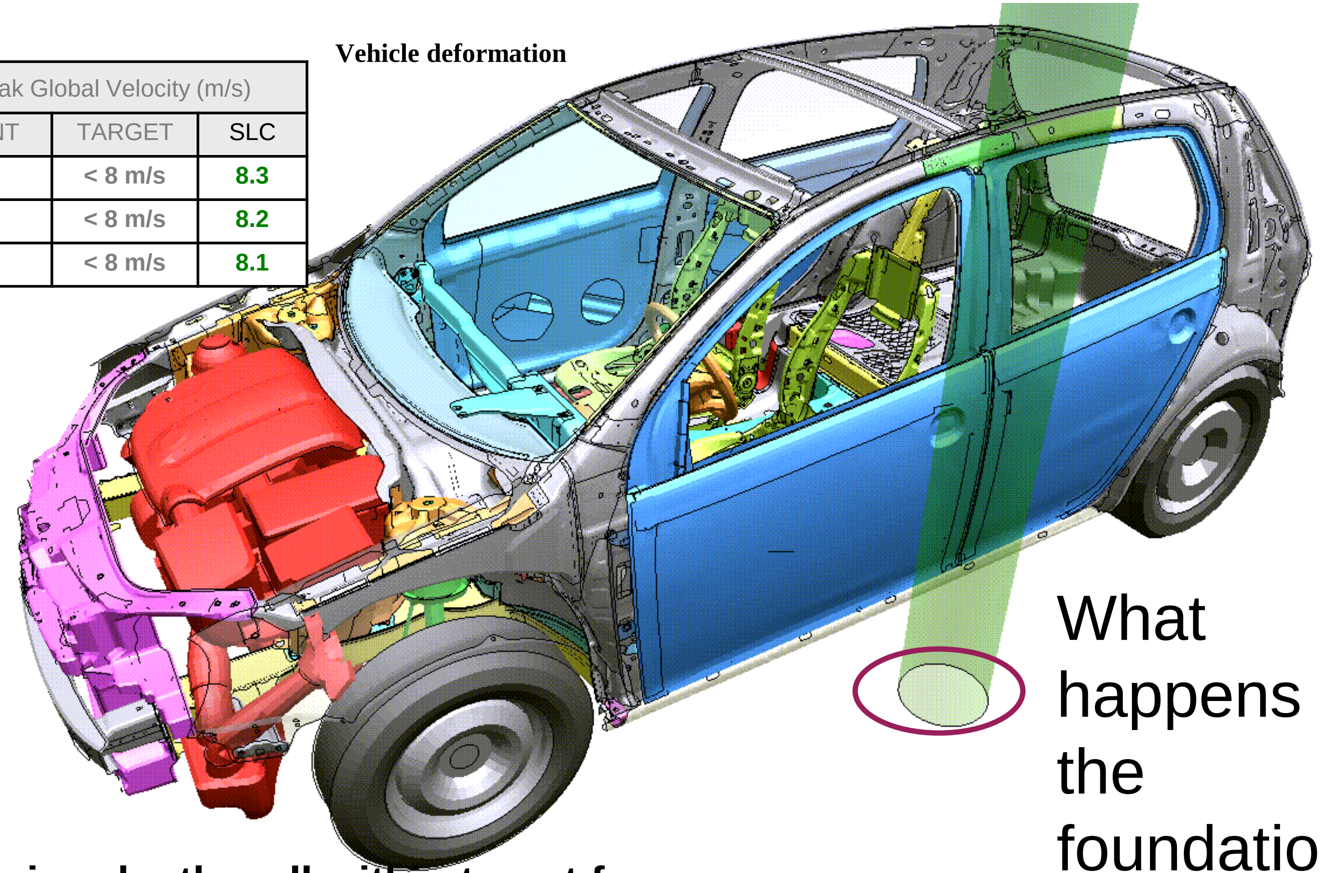

What happens at the foundation?

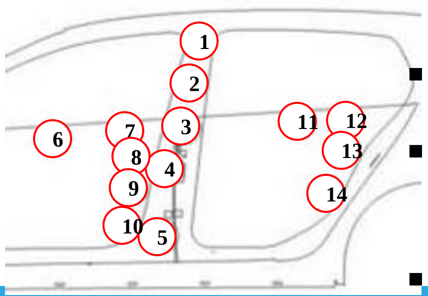

- Intrusion depth well within target for all measuring points ✓
- Survival space well within target ✓
- Intrusion velocity better than reference ✓
- Deformation better than reference ✓

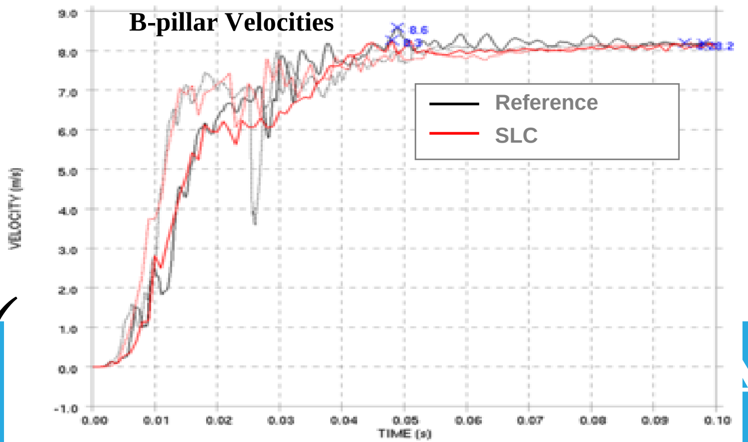

ARUP

181 Fre

Transbay Transit Center, Transbay Tower, 181 Fremont Tower and existing high-rise performance under 1 in 975 Return Period EQ

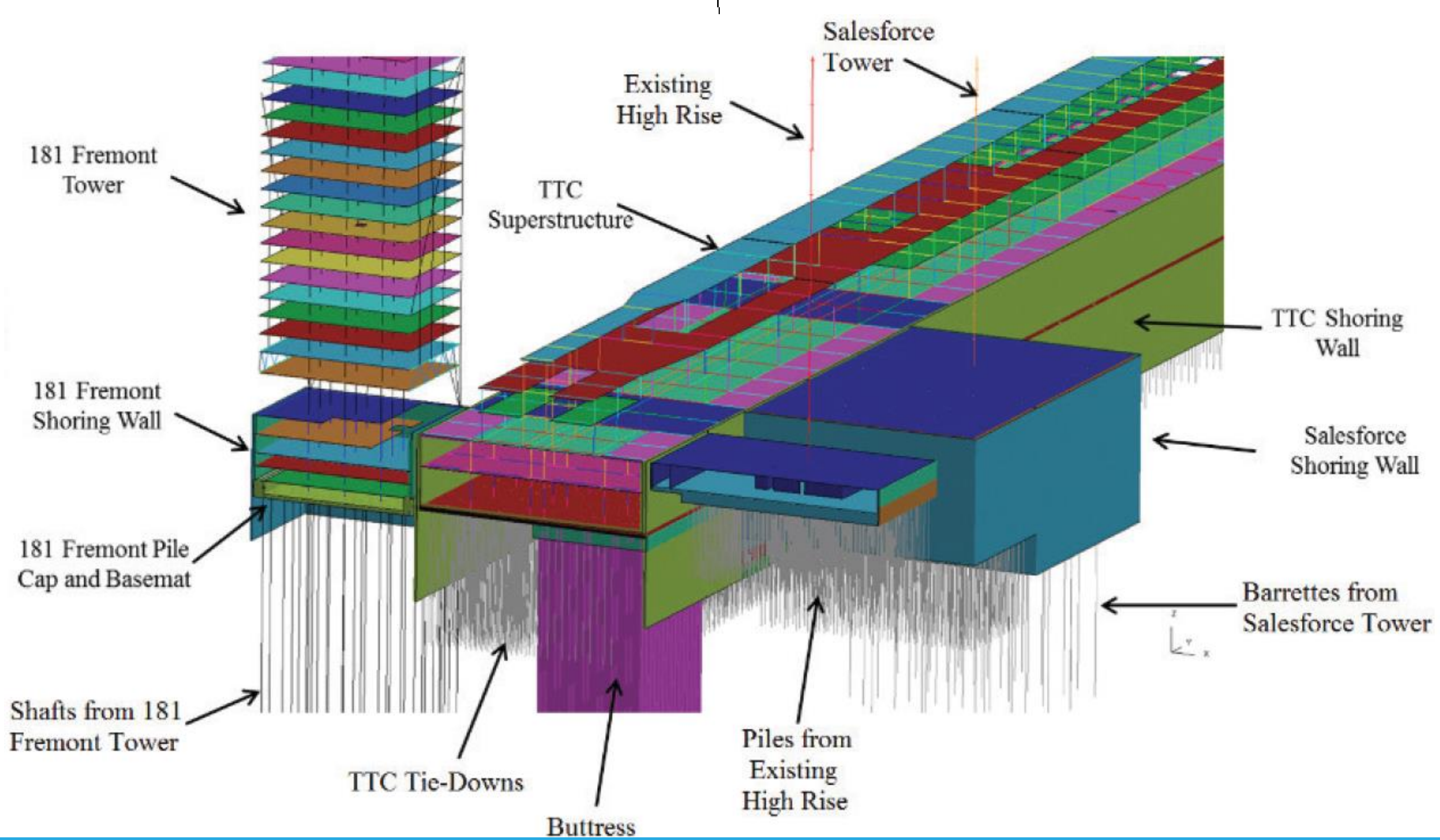

(Ellison et al, 2017)

ARUP

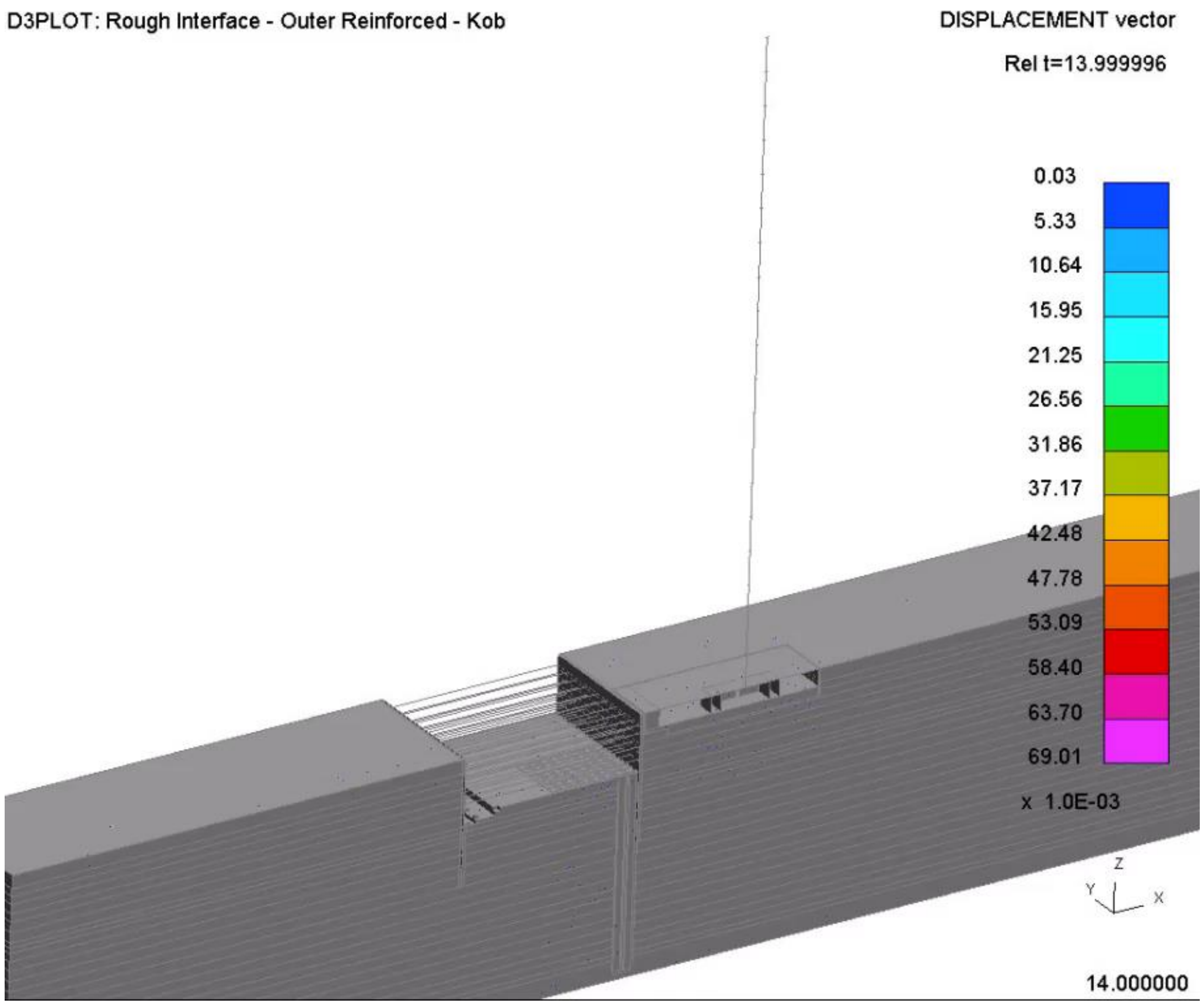

LSDyna analysis reported in O'Riordan & Almufti (2015)

ARUP

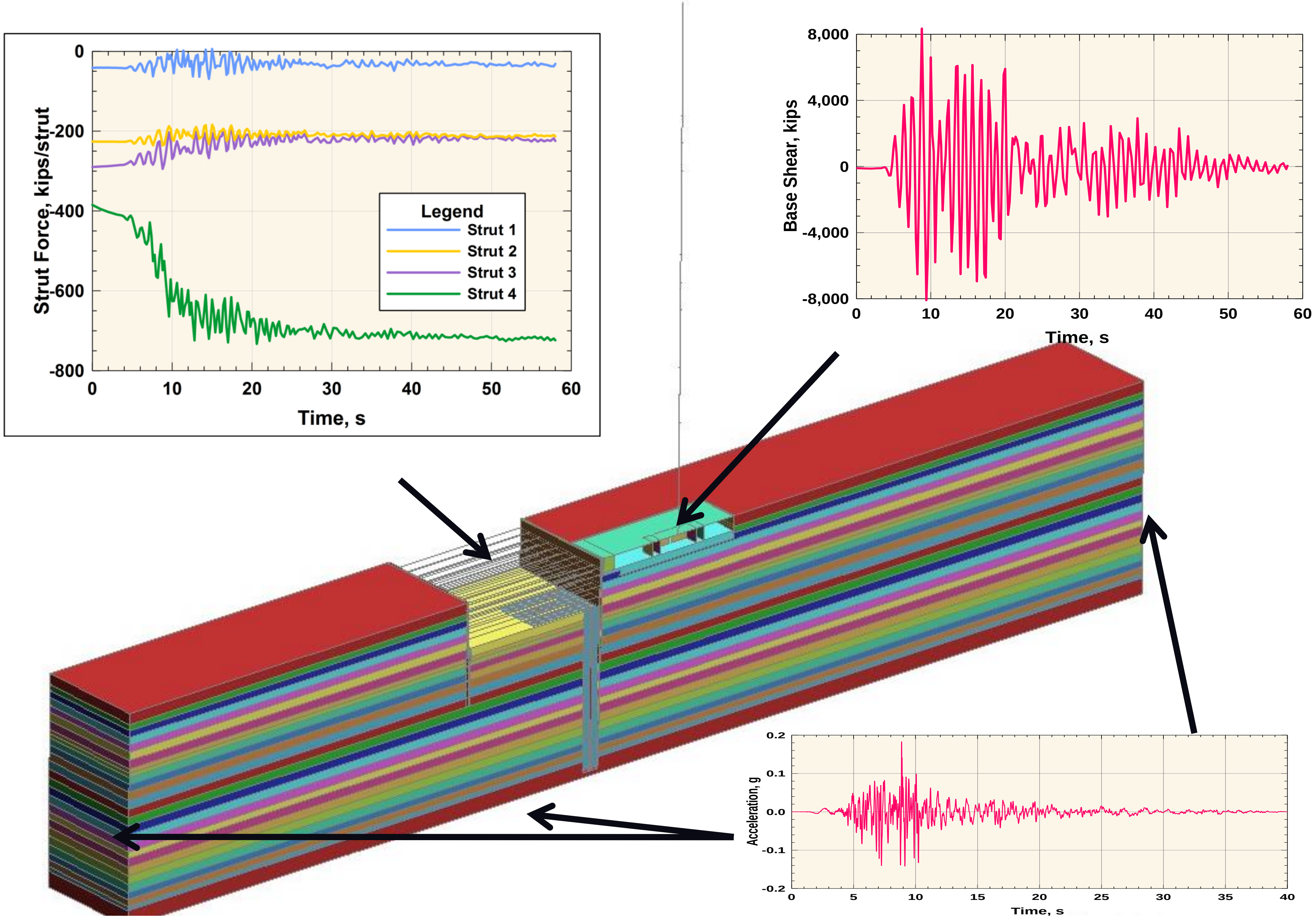

Seismic structure-soil-structure interaction (O'Riordan & Almufti, 2015)

ARUP

Instrumentation of the Transbay regeneration zone

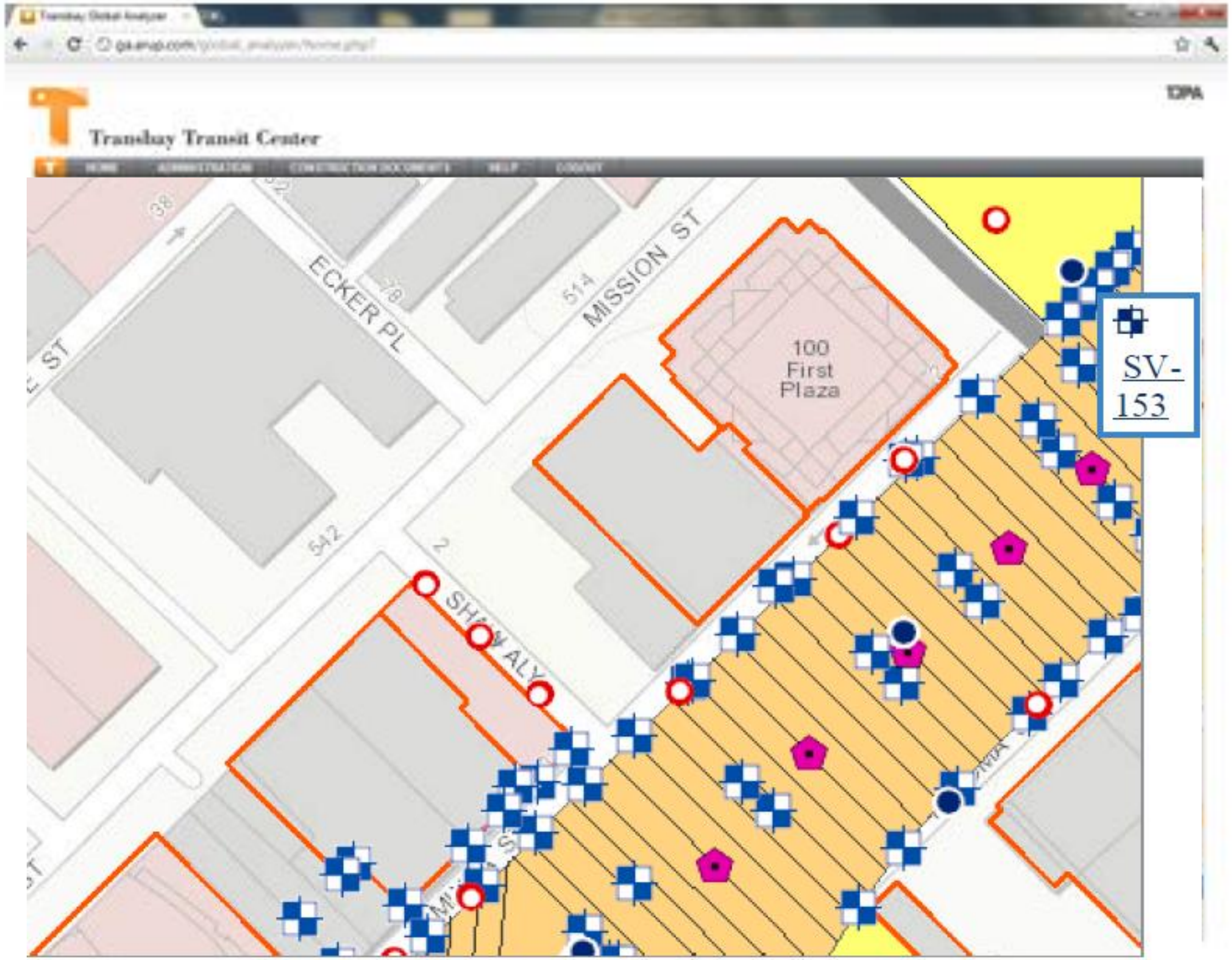

ARUP

Napa earthquake, August 2014, c.60 km from San Francisco, Mw= 6.0

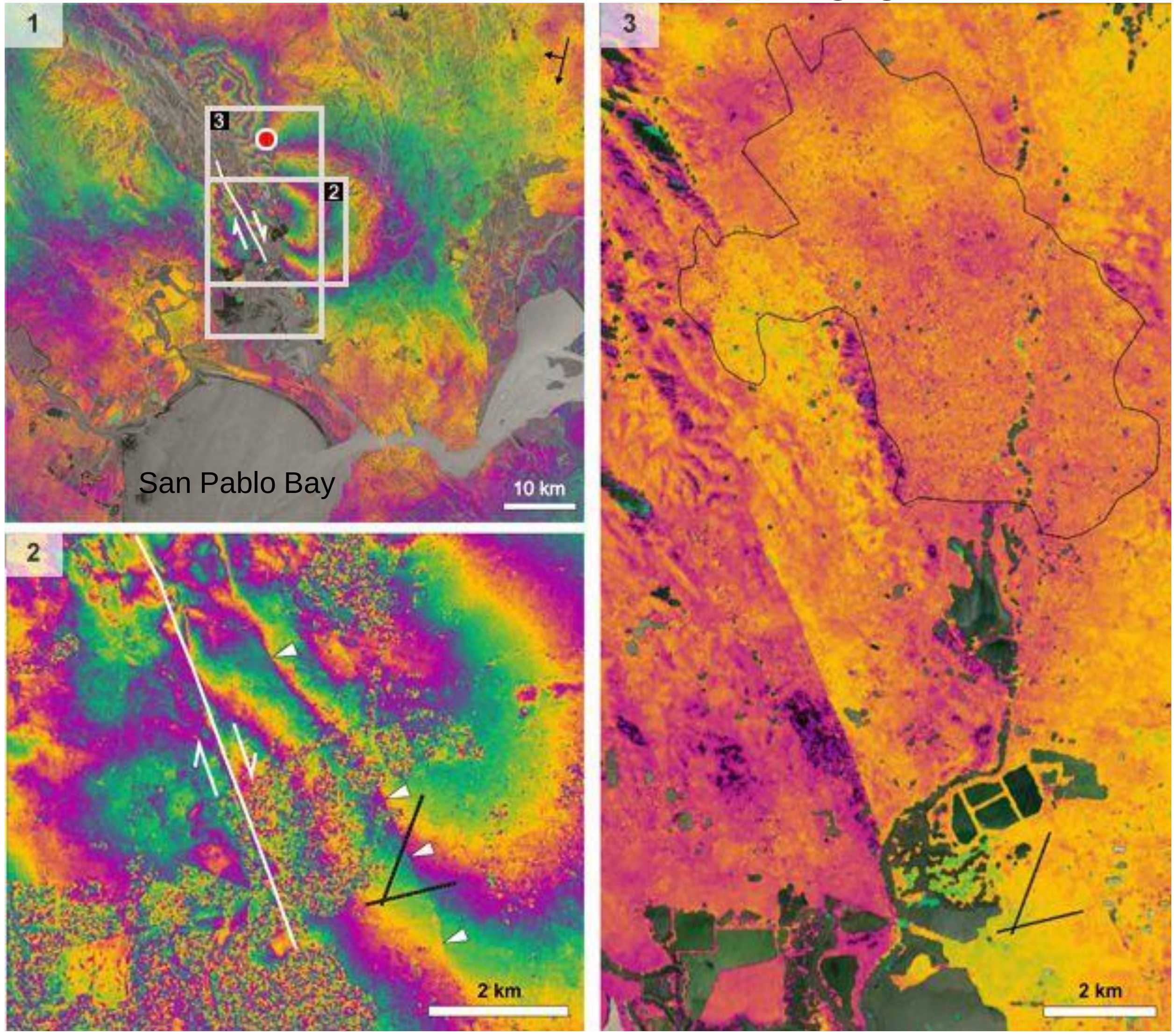

- (1) Sentinel-1a's first interferogram showing widespread ground movement in the aftermath of the August earthquake
- (2) A blow-up from the August image detailing the surface fault rupture (white line) that was mapped by scientists on foot
- (3) A sharp discontinuity is visible in this September interferogram that betrays afterslip on the fault of up to **2cm**

- http://www.bbc.co.uk/news/science-environment-30510268

12 storey low-rise with 5 level, 18m basement: accelerometer data (CA Geol Survey)

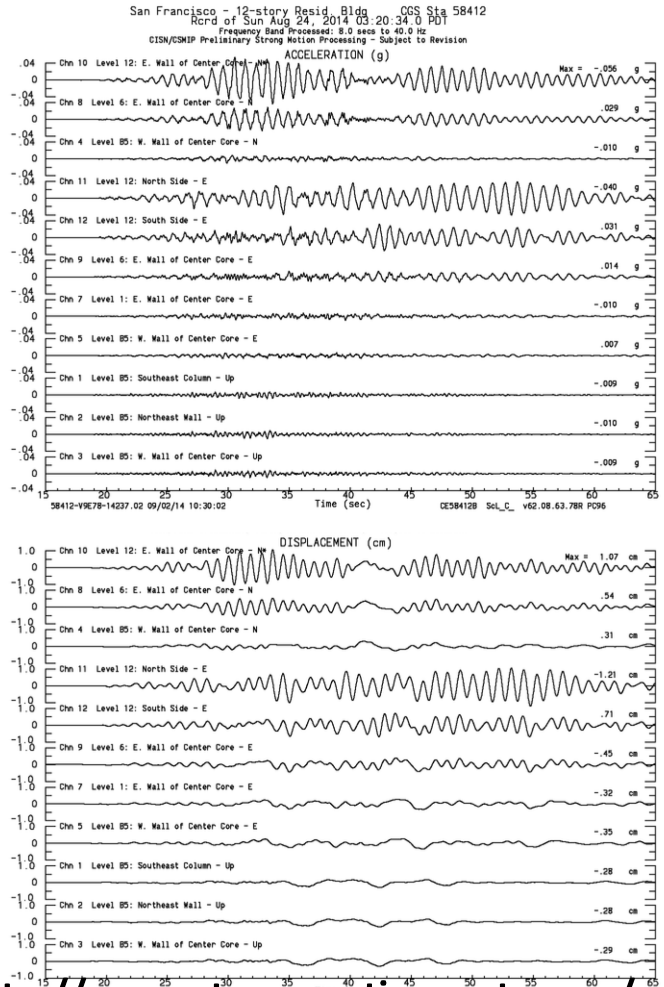

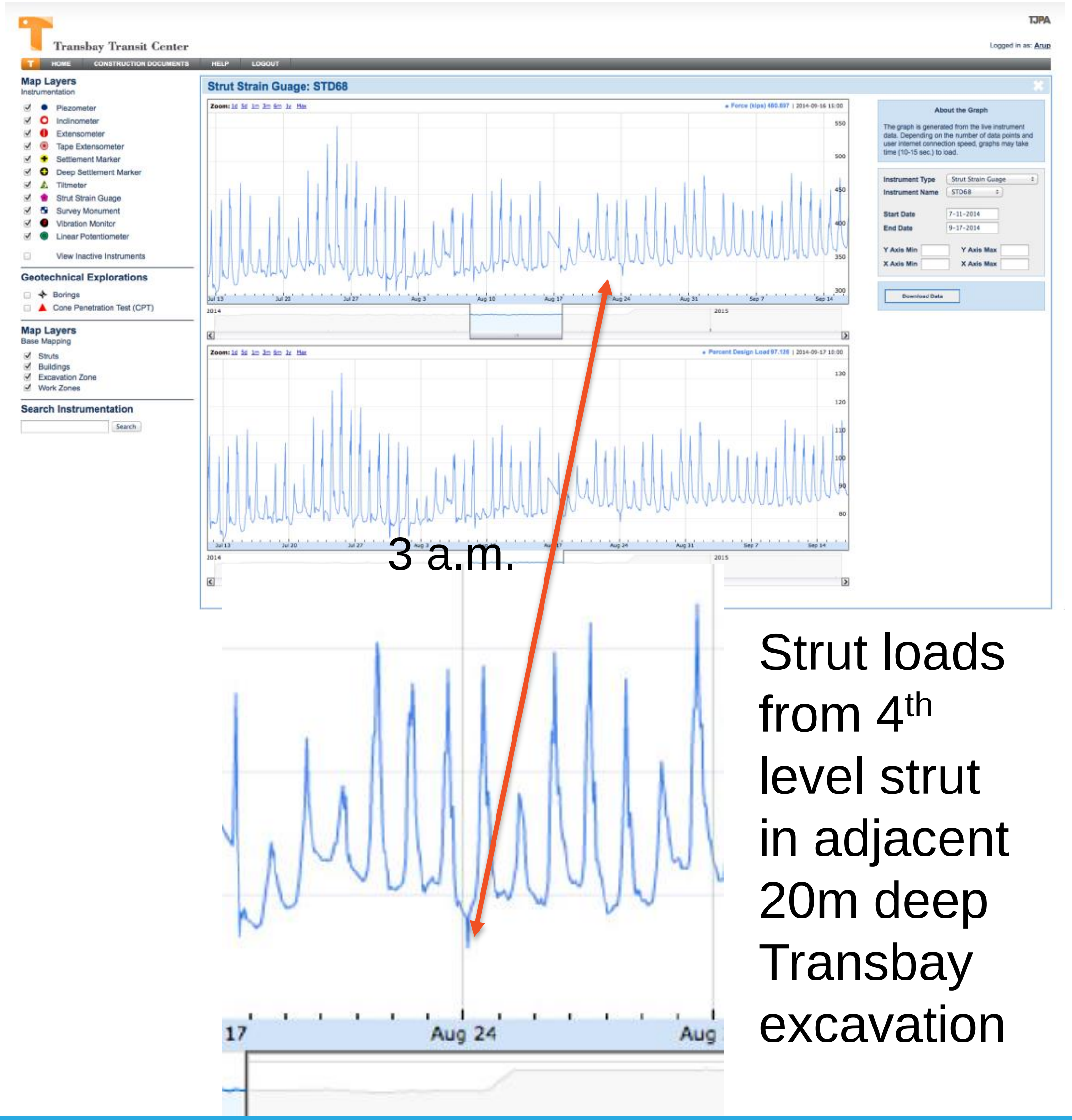

Strut loads from 4th level strut in adjacent 20m deep Transbay excavation

http://www.strongmotioncenter.org/cgi-bin/CESMD/iqrStationMap.pl?ID=SouthNapa_24Aug2014_72282711

ARUP

Mexico City: a mega-city on soft ground

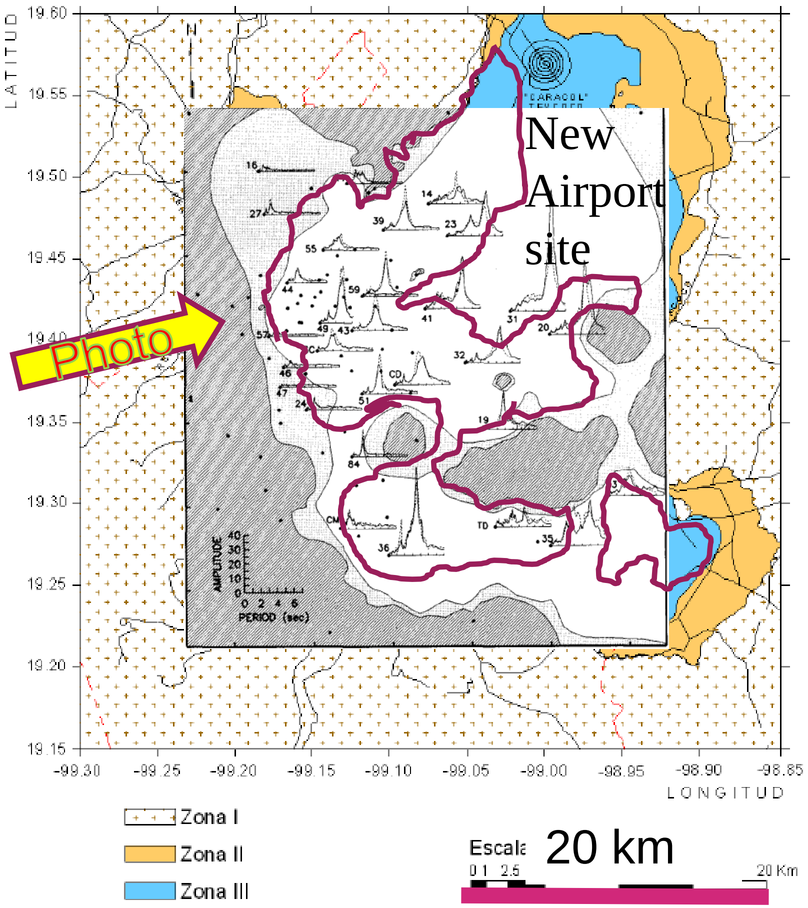

GDF(2004) Geotechnical zoning map of Mexico City Basin

Boundary of the urban area (the Anthropocene) in Zone III, Lakebed Deposits

Spectral amplification at urban recording stations deployed after 19 September 1985 EQ (Reinoso & Ordaz, 1999)

ARUP

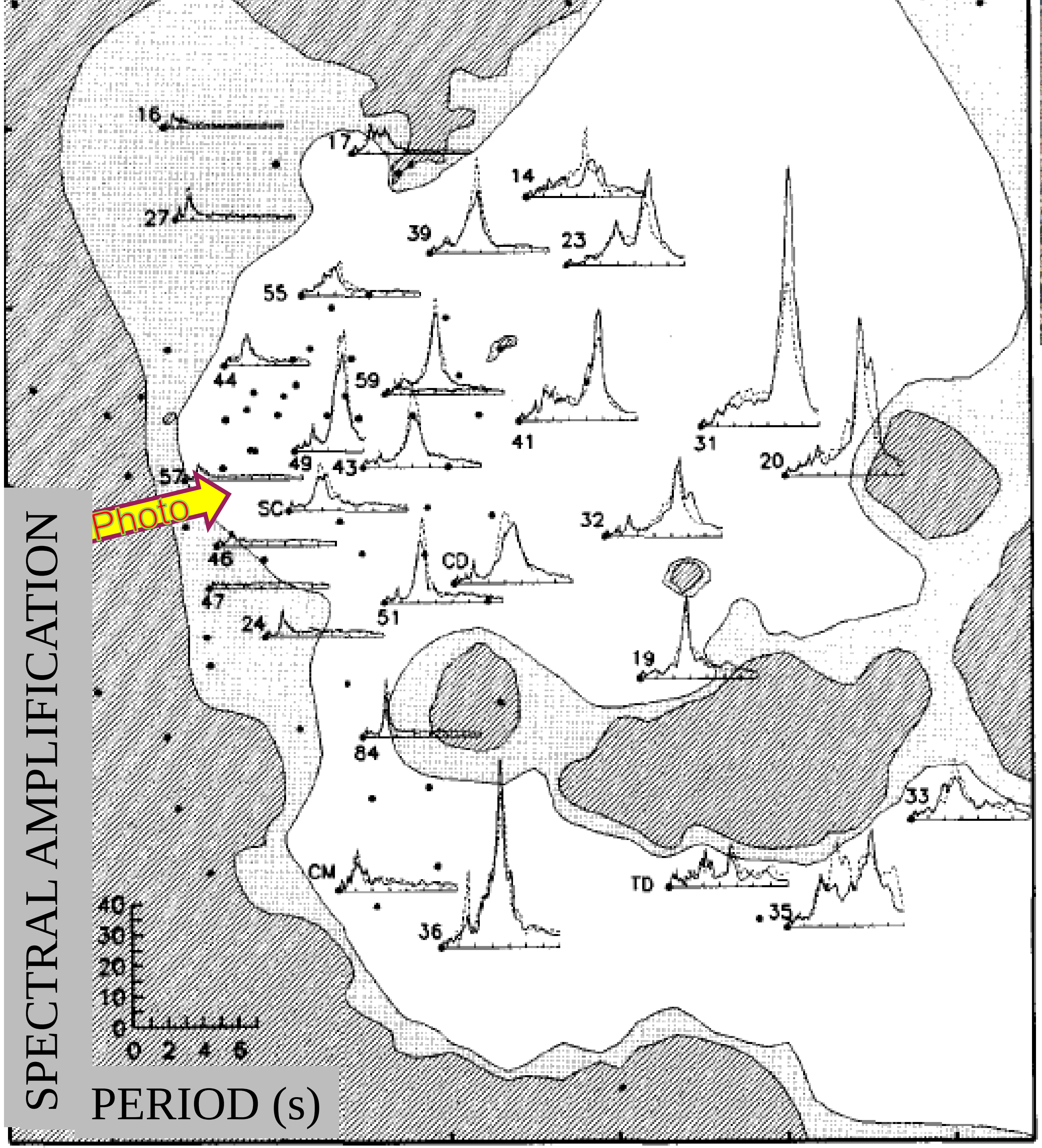

Spectral amplification at urban recording stations deployed after 19 September 1985 EQ (Reinoso & Ordaz, 1999)

Mexico City, Lakebed zone, V_S profiles

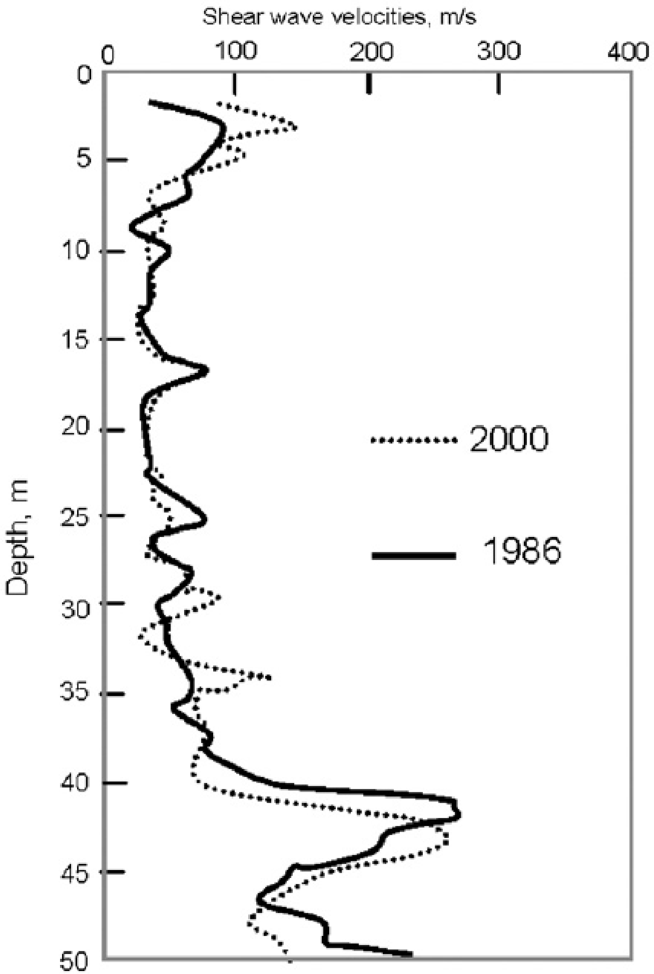

Ovando (2007)

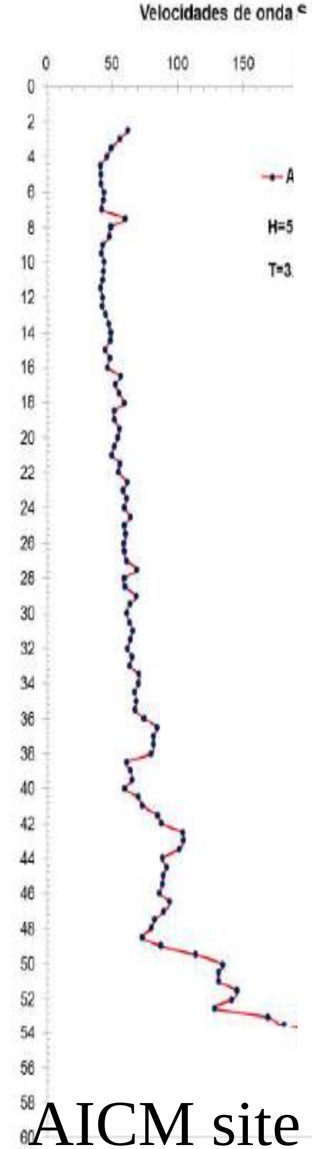

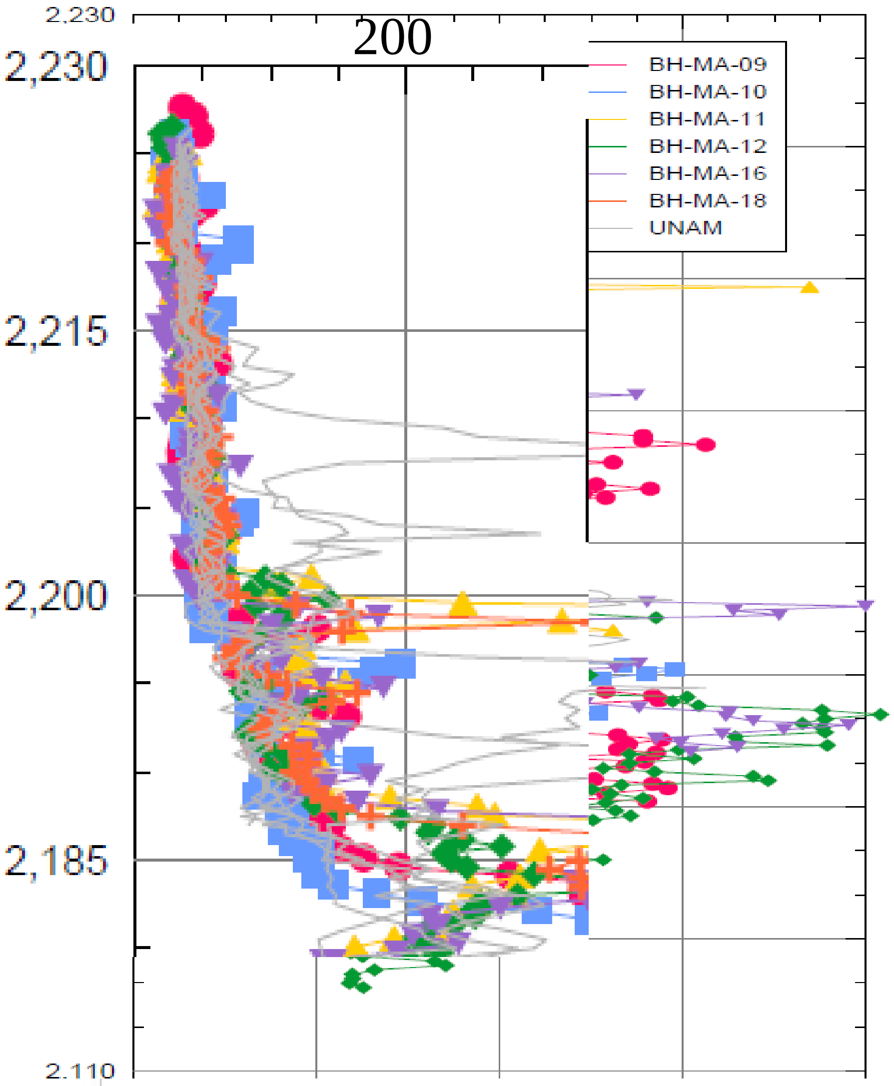

CAO site (West, urban)

AICM site (Central, suburban)

NAIM site (East, undeveloped)

ARUP

New Airport site, Mexico City
Puebla EQ 19 September 2017

(Under construction)
undeveloped lakebed

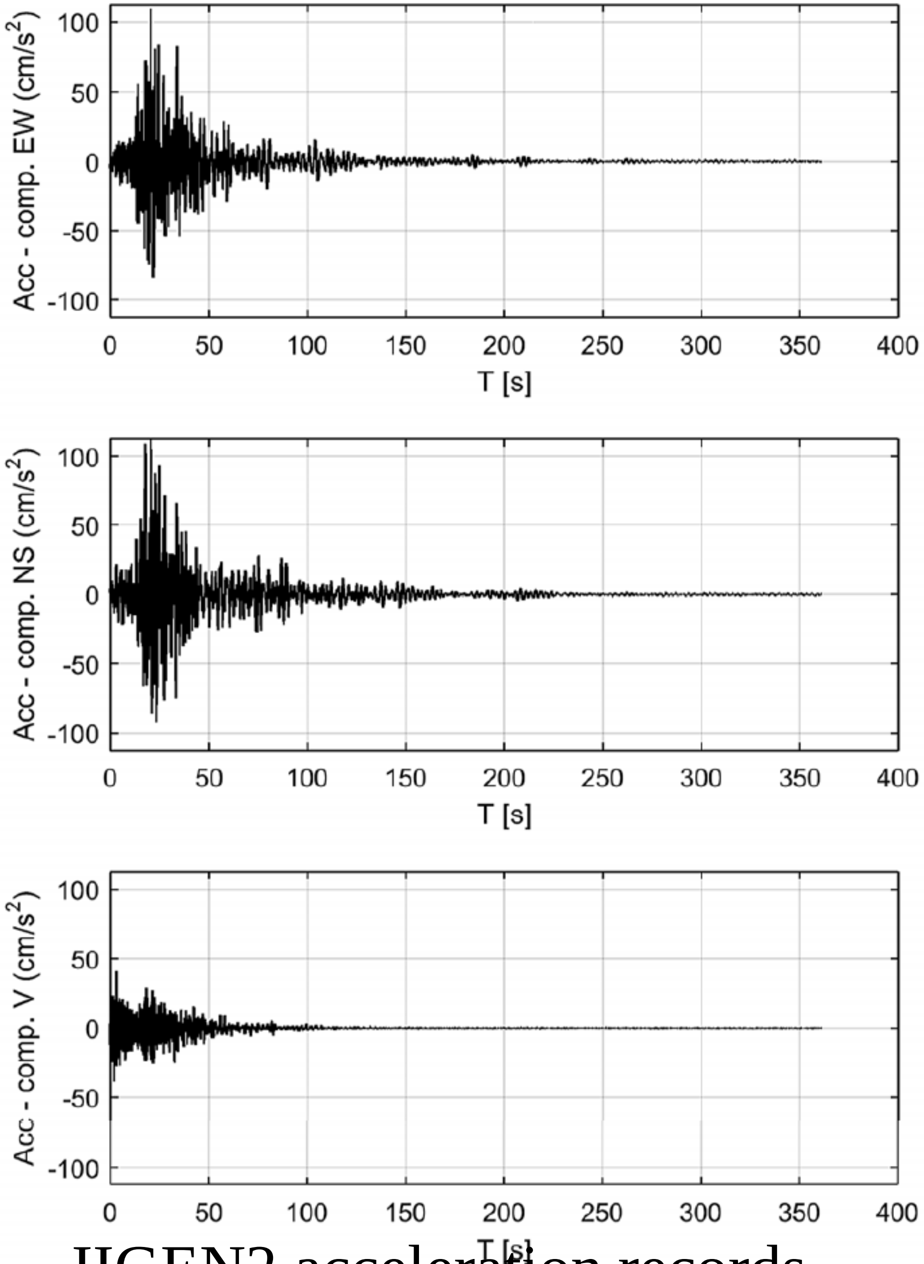

IIGEN2 acceleration records
(UNAM,2017)

ARUP

Aux. Station, urban lakebed zone, Mexico City – Beating (2nd) Phase

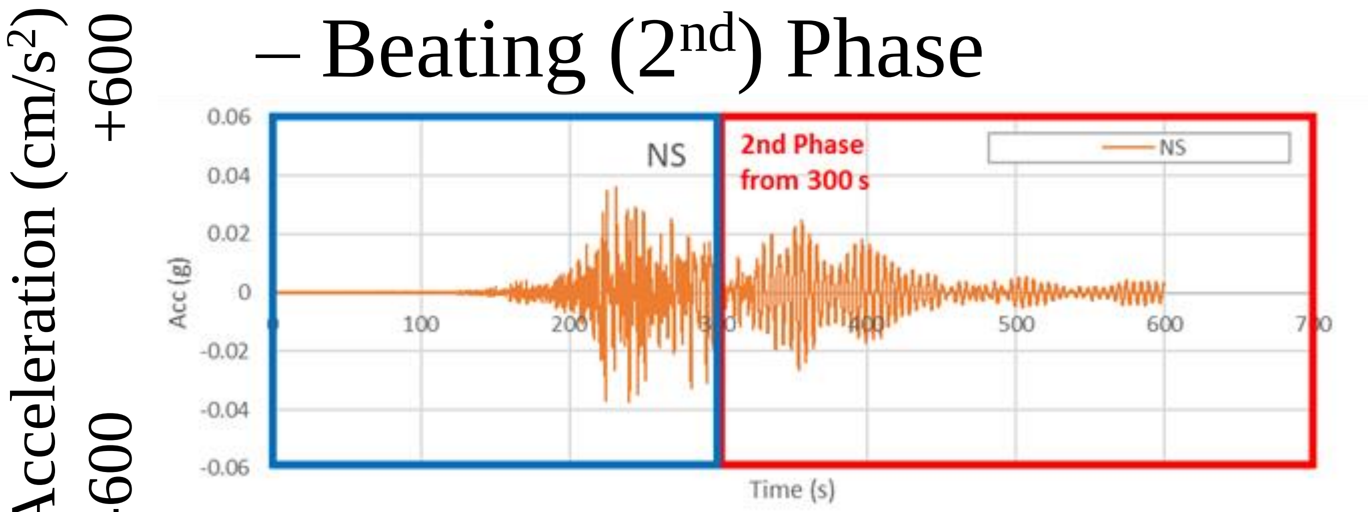

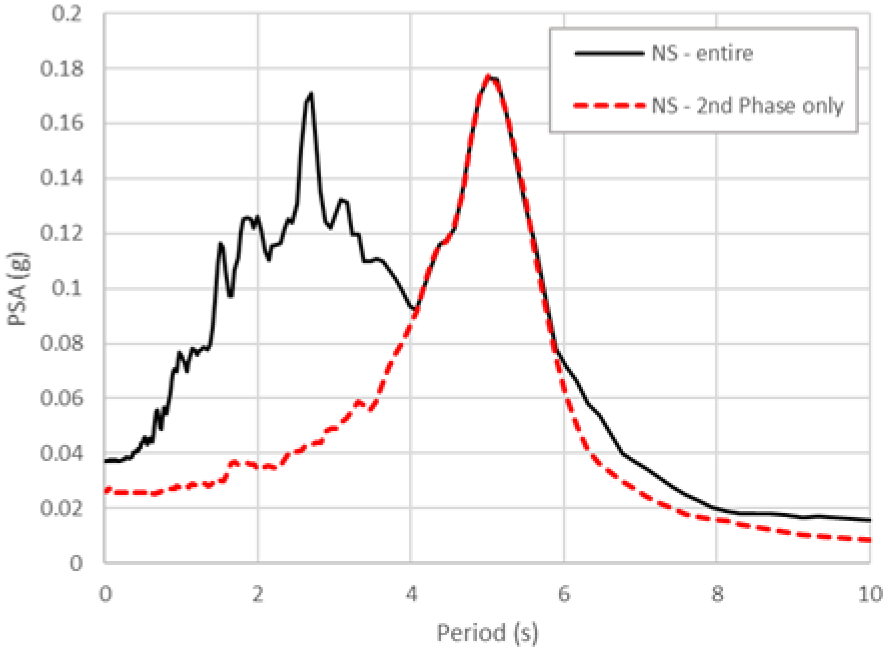

Seismograph records from UNAM (2017)

Gueguen et al (2002) Urban effect on ground motions (Mexico City)

Building-to-soil kinematic energy ratio

$$\frac{E_{kb}}{E_{ks}} = \sum_{i=1}^{n} \frac{S_{bi}}{S_s} \cdot \frac{h_{1i}}{H_s} \cdot \frac{f_s^2}{\tilde{f}_i^2},$$

urbanisation density   building height: soft soil thickness   resonance (soil:building)

$E_{kb}/E_{ks} = 0.87$ at Aux station site
(threshold for urban effect is 0.1, after Gueguen et al (2002))

CAO Station, urban lakebed zone, Mexico City - Beating 2nd Phase

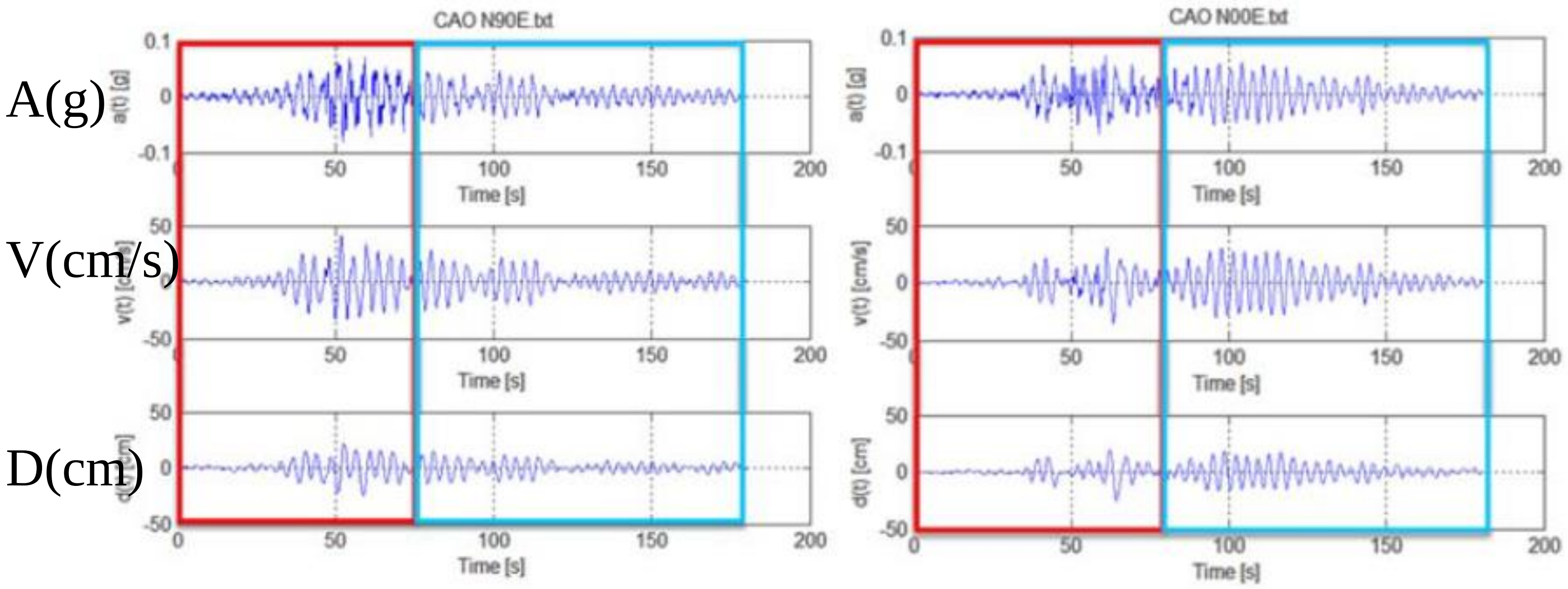

Minimum requirements for numerical analysis of dynamic soil-structure interaction: Non-Linear Response History Analysis software (O'Riordan & Almufti, 2015)

- Pressure- and rate-sensitive non-linear shear stress/strain soil properties
- Degrading G/Gmax curves for the soil
- Water pressures: recognise volumetric & shear strain rates at excavation/construction and dynamic excitation stages
- Accurate representation of foundation systems
- Interface layers between structural elements and the soil mass that represent disturbed soil
- Representation of structures, vehicles etc: equivalent mass, stiffness and damping to capture dynamic behaviour
- Representation of construction installation sequencing
- Soil domain sufficiently large that boundary effects are negligible during dynamic loading
- Able to provide 'rupture to rafters' (Ellison et al, 2017) process for seismic loadcases

ARUP

Repairable Limit State

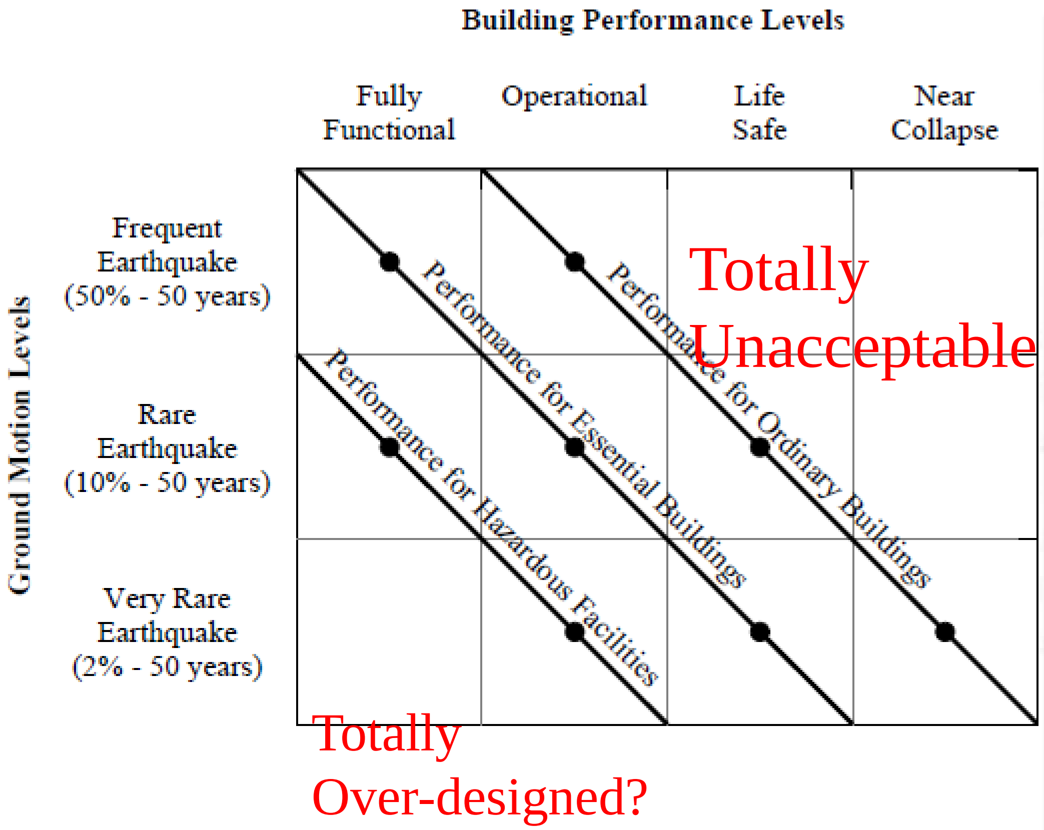

After SEAOC (1995)

Damage to a Structure →

Magnitude of Actions ↓

	Serviceability Limit State	Repairable Limit State	Ultimate Limit State
High freq. Low impact	◎ ○ △		
Medium freq. Med. Impact	◎ ○	△	
Low freq. High impact		◎	○ △

Note: ◎ Important Structure ○ Ordinary Structure
△ Easily Repairable Structure

After Honjo (2010)

Typical ‘backbone curve’ (modified after Atkinson, 2000)

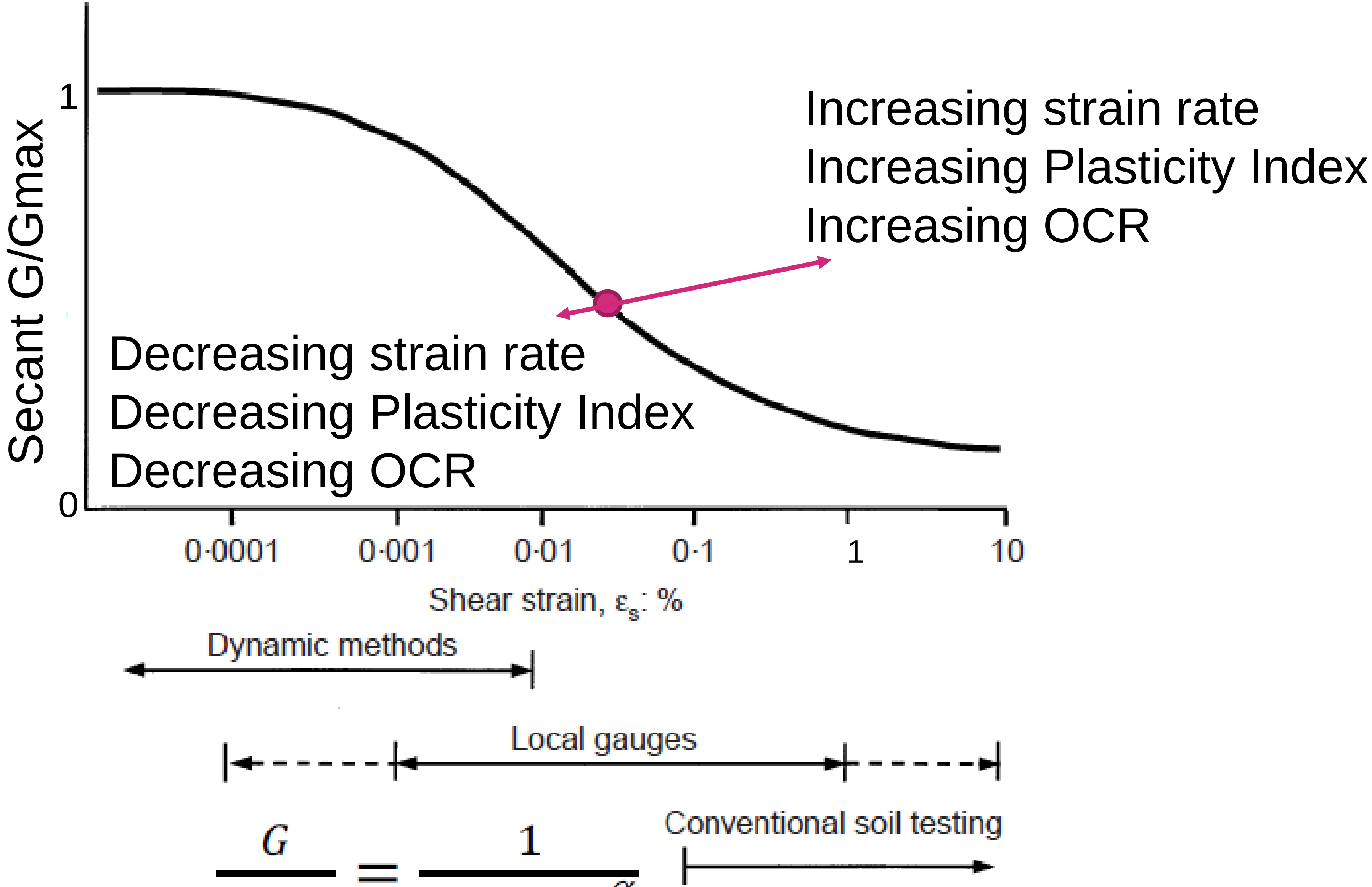

$$\frac{G}{G_{max}} = \frac{1}{1+\beta\left(\frac{\gamma}{\gamma_r}\right)^{\alpha}}$$

ARUP

Consequences for G/Gmax curves: ‘dynamic’ and ‘static’ soil behaviour

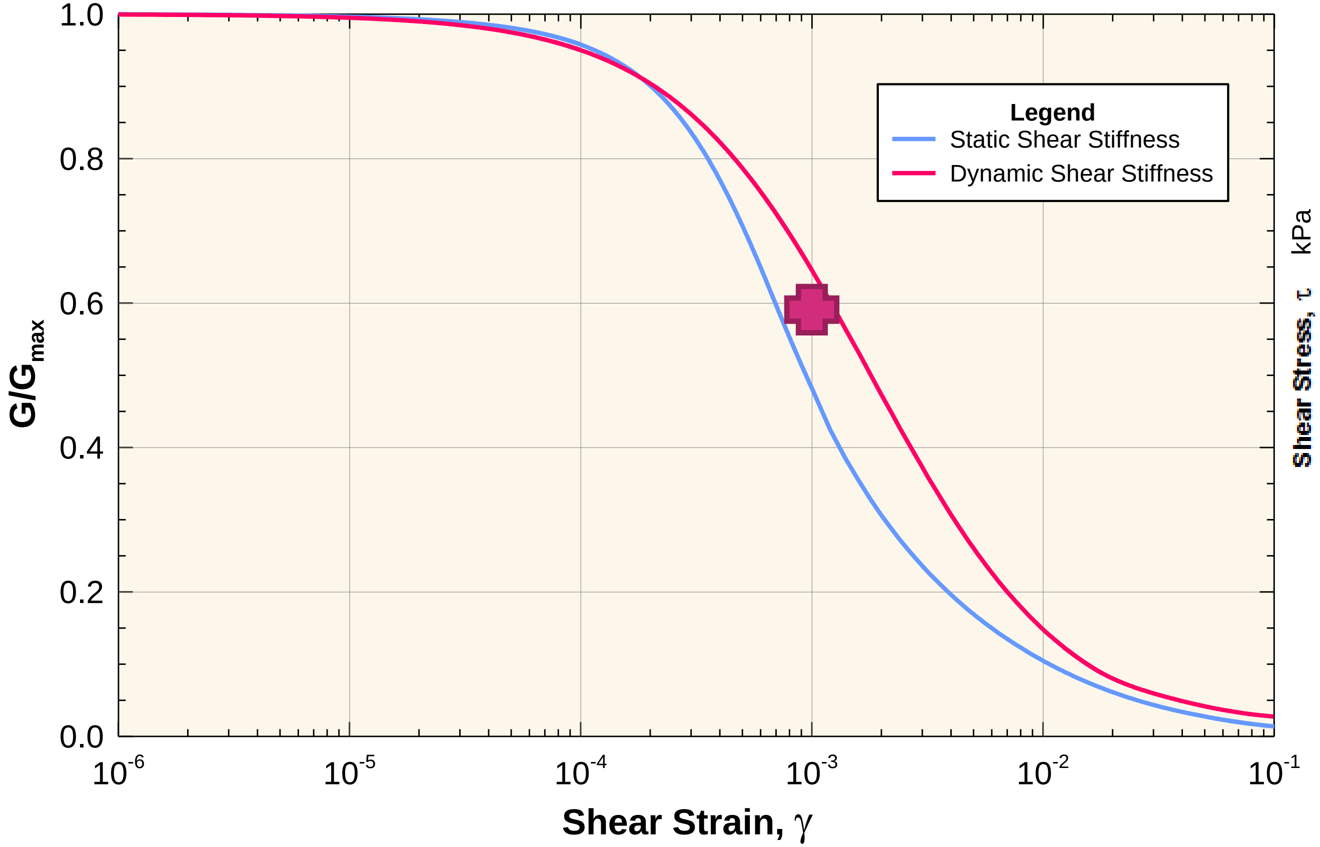

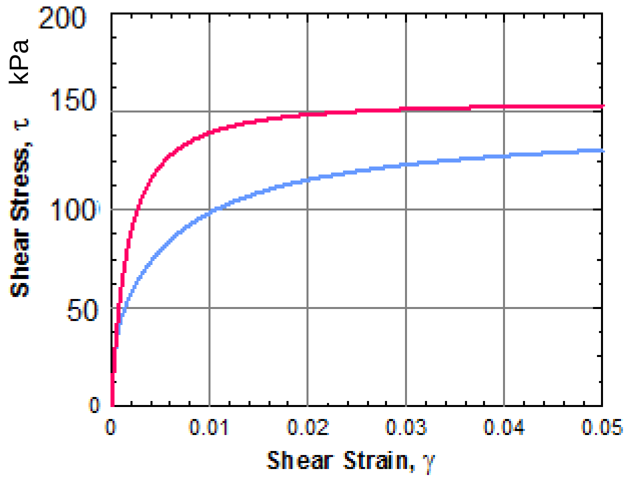

LS Dyna Mat_Hysteretic soil with strain rate controlled secant

shear modulus for SF Old Bay Clay (PI=40 to 50%, OCR=1.4)

ARUP

Consequences for G/Gmax curves

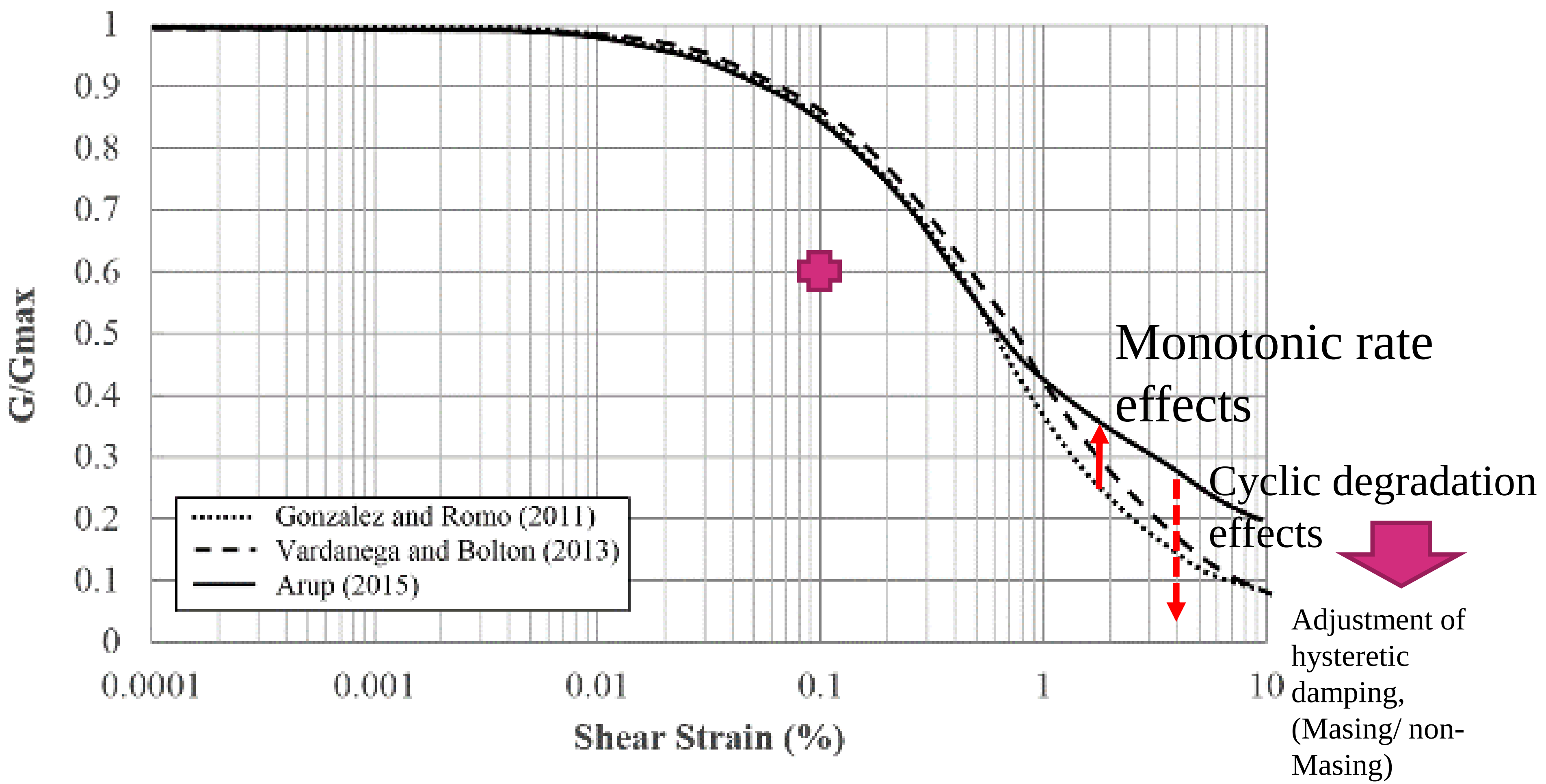

Mexico City Clays (PI=200%, OCR~1.5): backbone curve

for PLAXIS and LS DYNA analysis

ARUP

CPT in Mexico City clays in LS Dyna, with & without strain rate (SRE), with destructuration and variable velocity

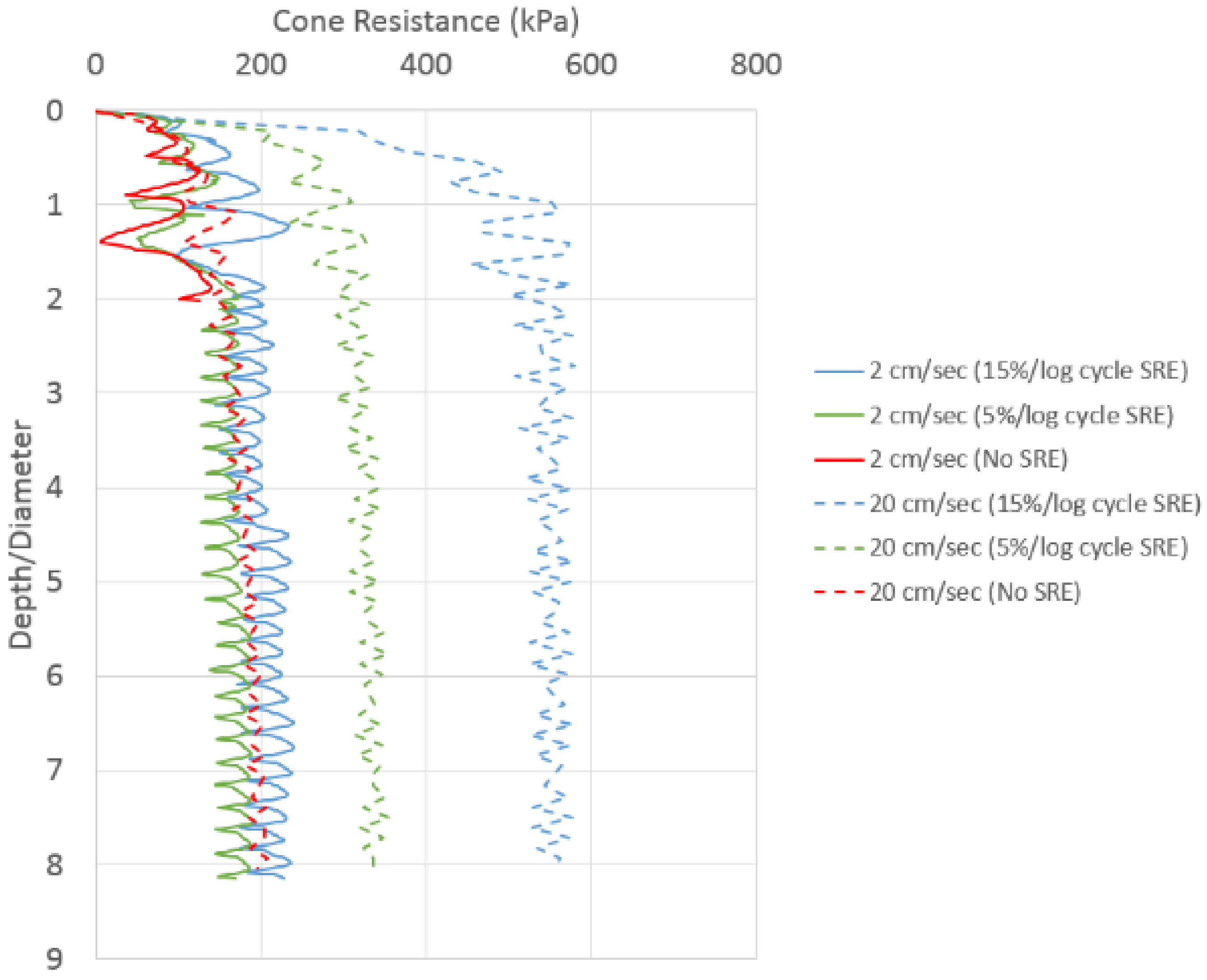

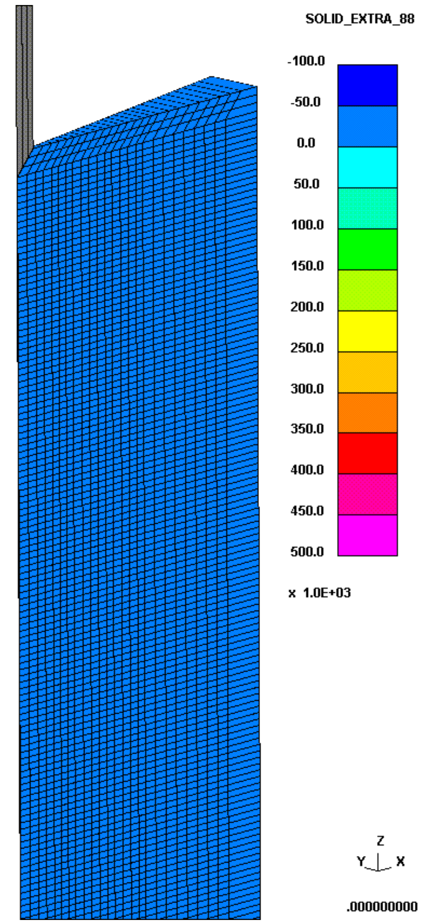

ARUP

Gautrain, Johannesburg>Pretoria

Gautrain: new railway for the soccer World Cup 2010

New Johannesburg> Pretoria railway crosses sinkhole-prone dolomite residuum on viaducts and ground slabs

Conventional GI technique is air-flush rotary, and measurement of drilling rate.

Limited published soils data, but ‘good’ history of sinkhole occurrence.

Viaduct Foundation

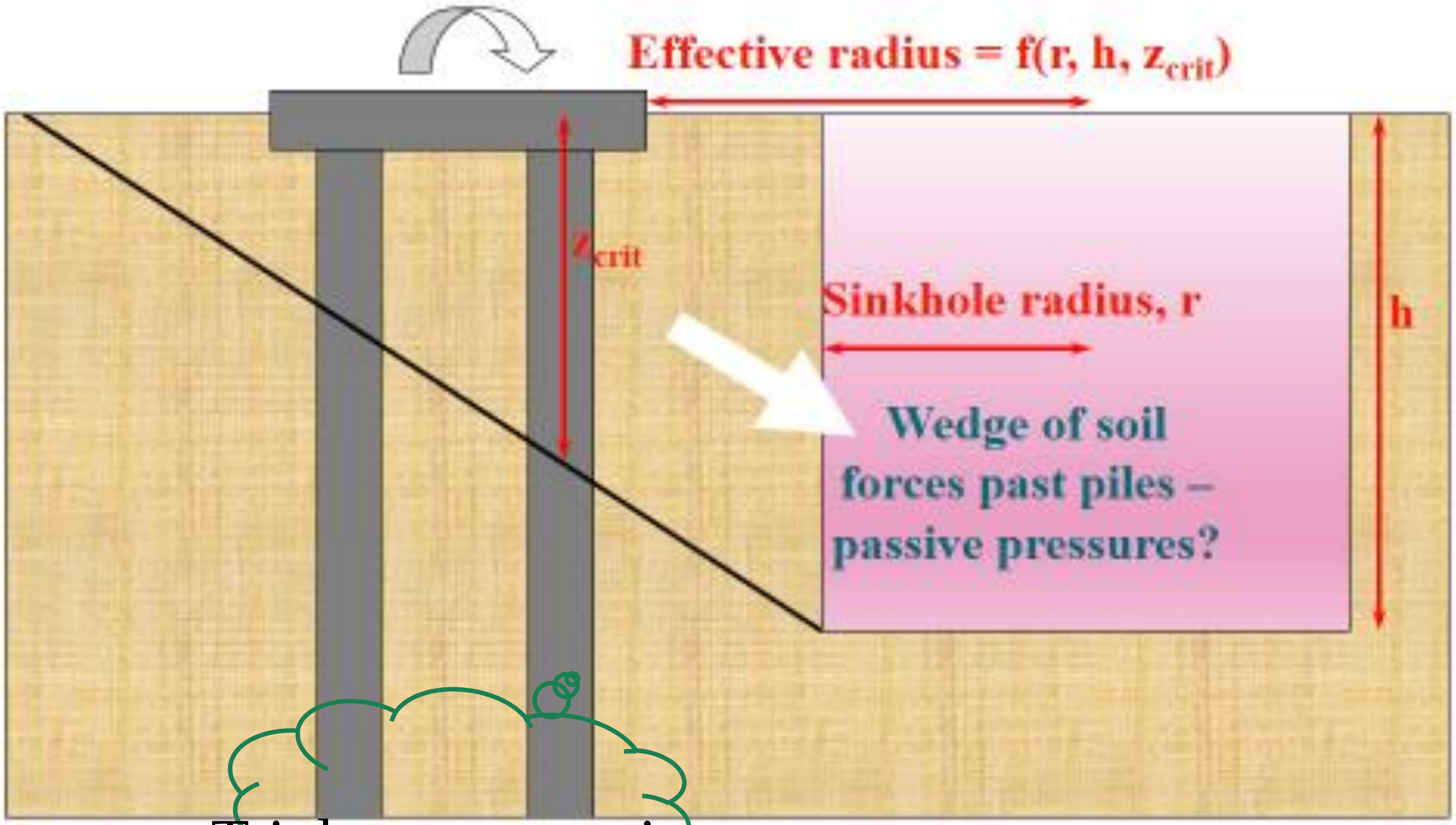

Triple-pass grouting

Pressuremeter test in Residuum/ ‘wad’

c’=7 kPa, Φ’ = 30^{o} elastic-plastic, Mohr-Coulomb

$\dot{\gamma}$ = 10^{-4} to 10^{-5} s^{-1} (~0.5 MPa/20s)

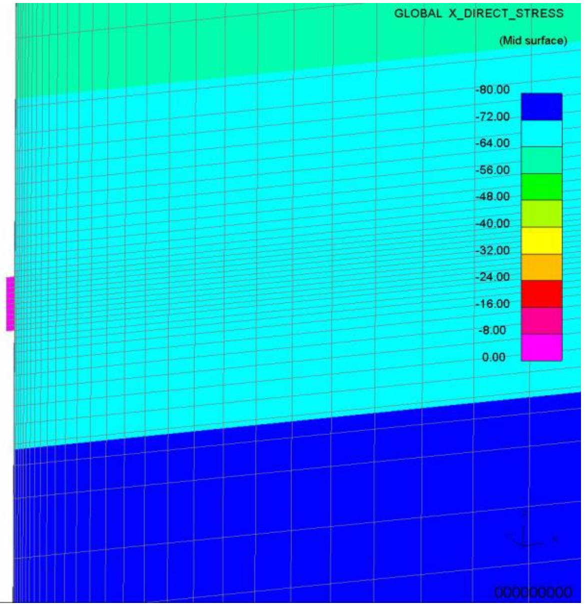

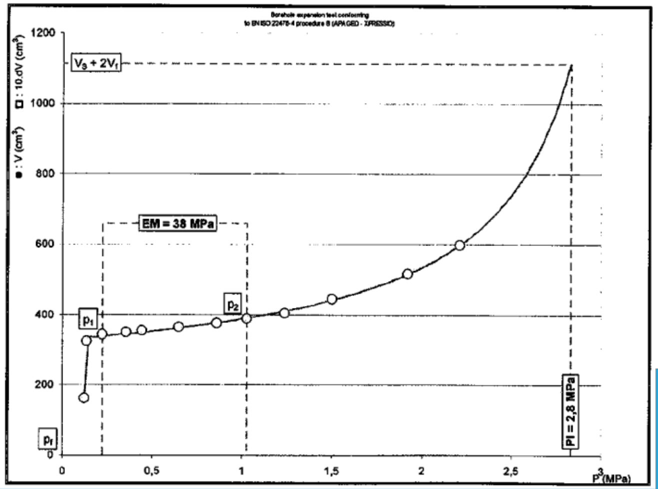

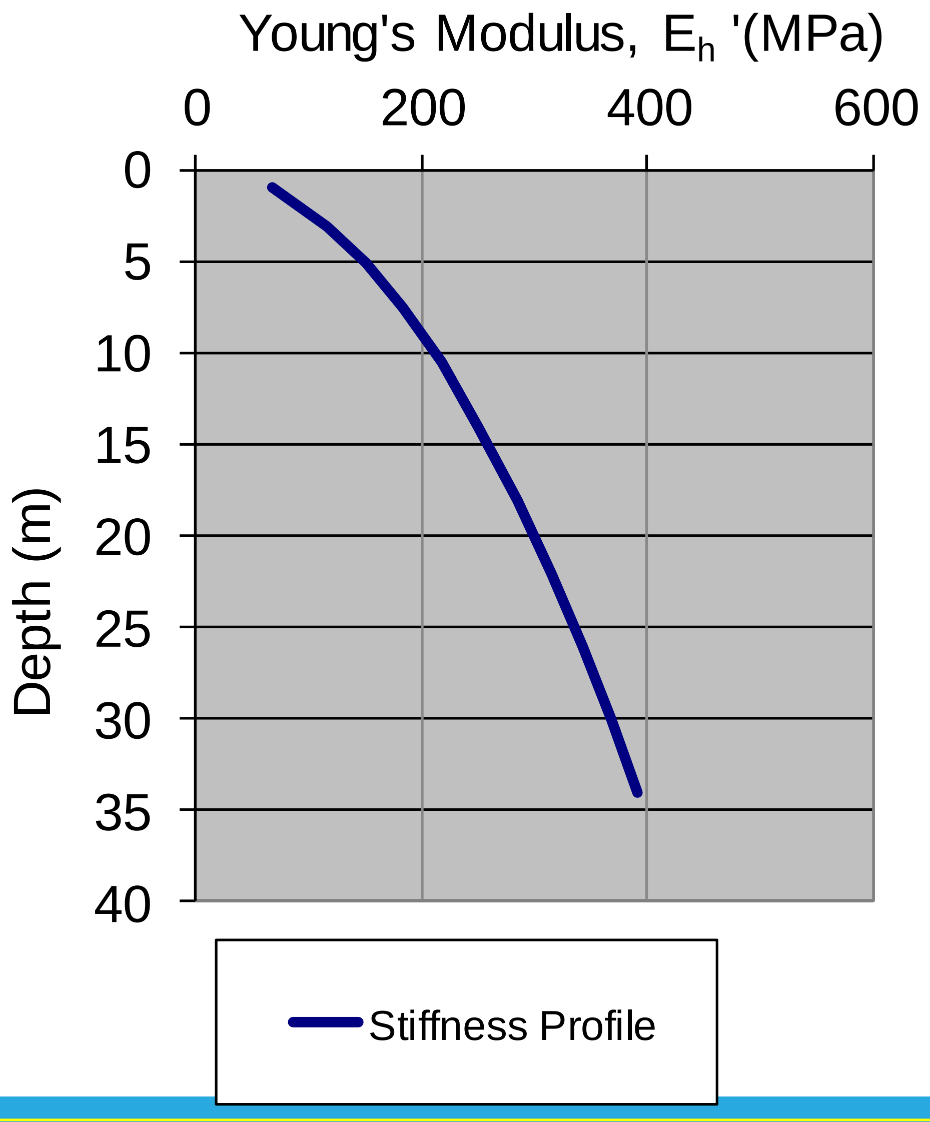

ARUP

Pressuremeter test in Residuum/ ‘wad’

c’=7 kPa, Φ’ = 30º elastic-plastic, Mohr-Coulomb

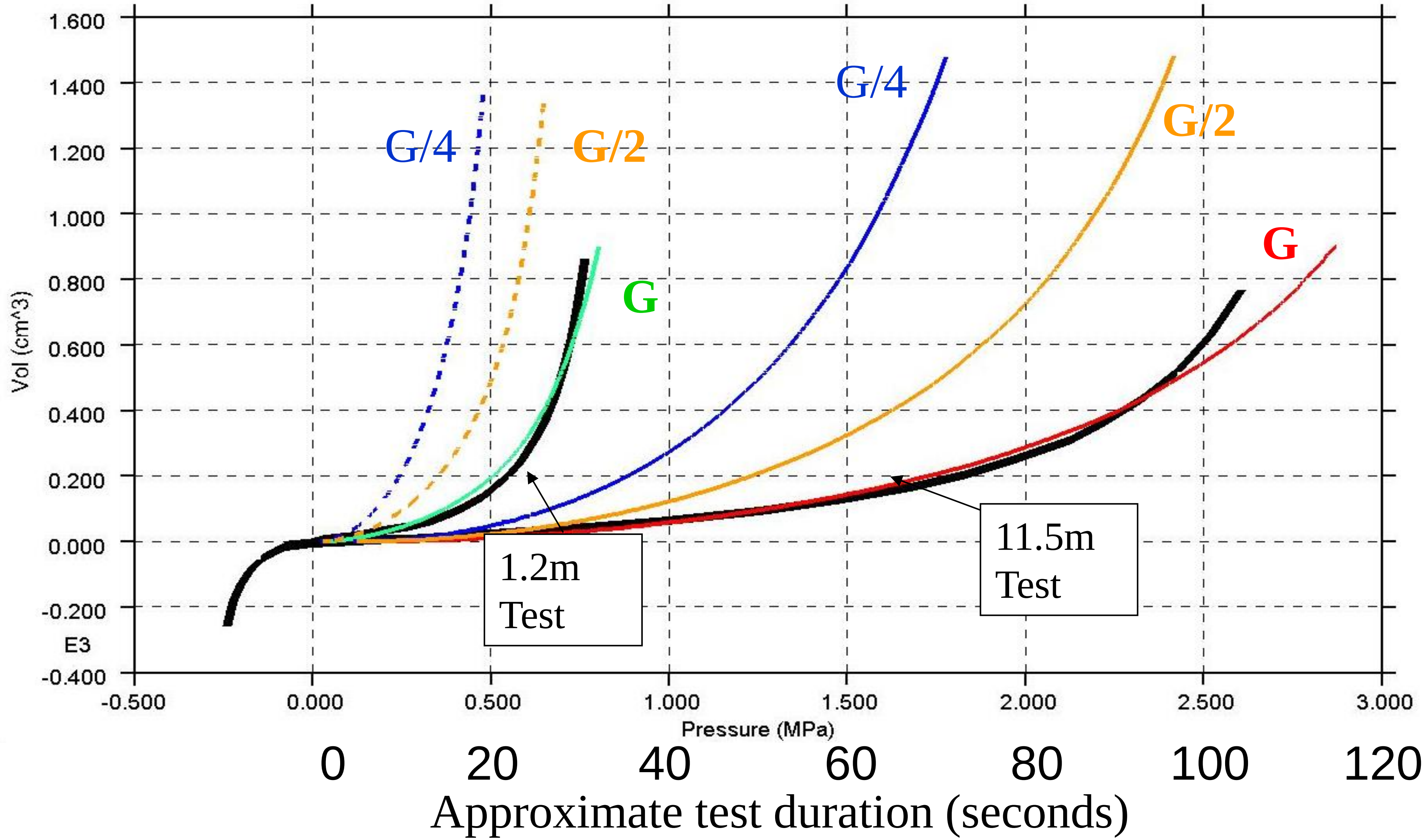

Shear modulus, G ~ Eh’/2.4

ARUP

Flow of soil into sinkhole, through pile group

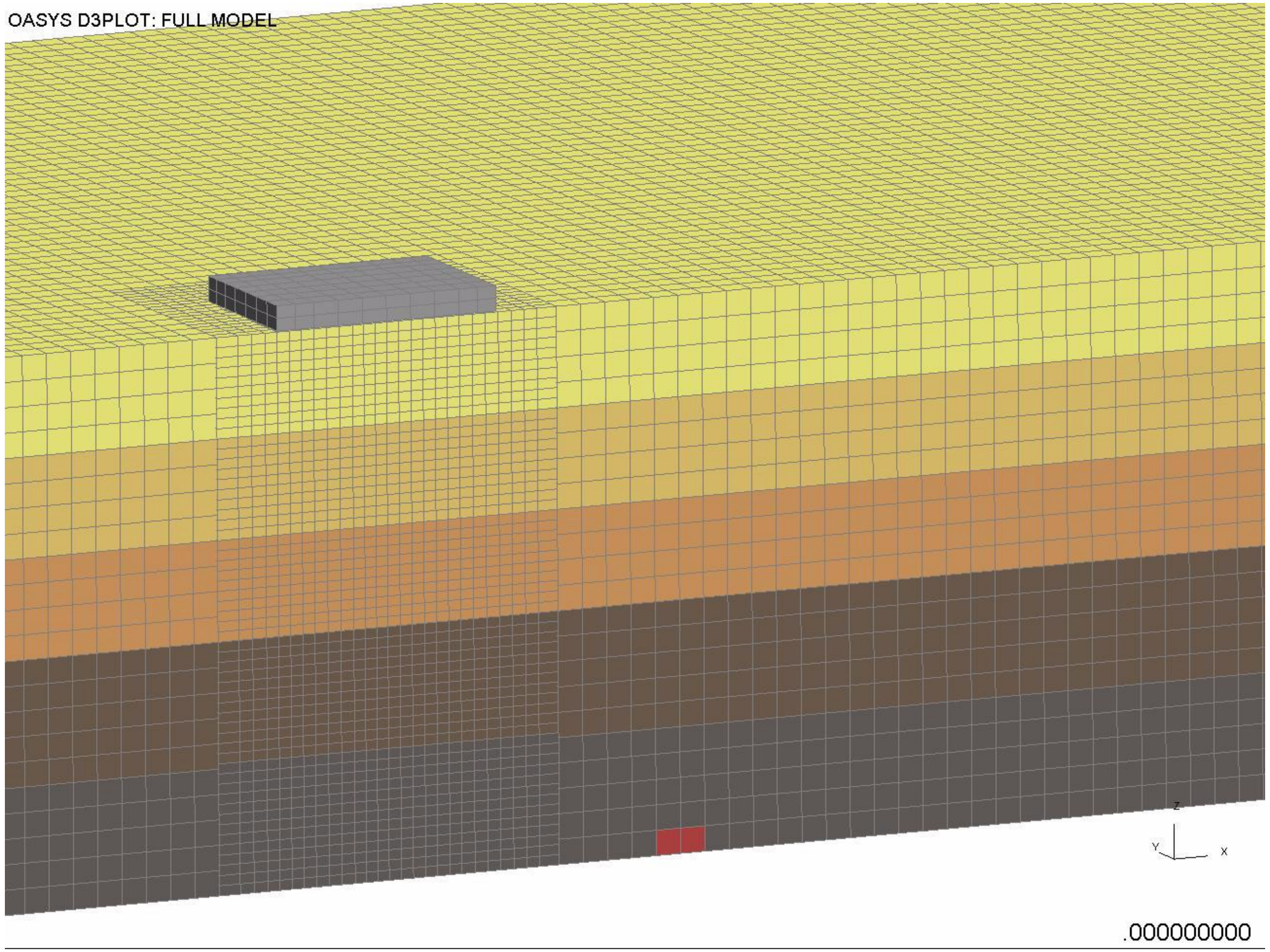

ARUP

Lateral pressures on pile during sinkhole collapse

After Sartain et al (2011)

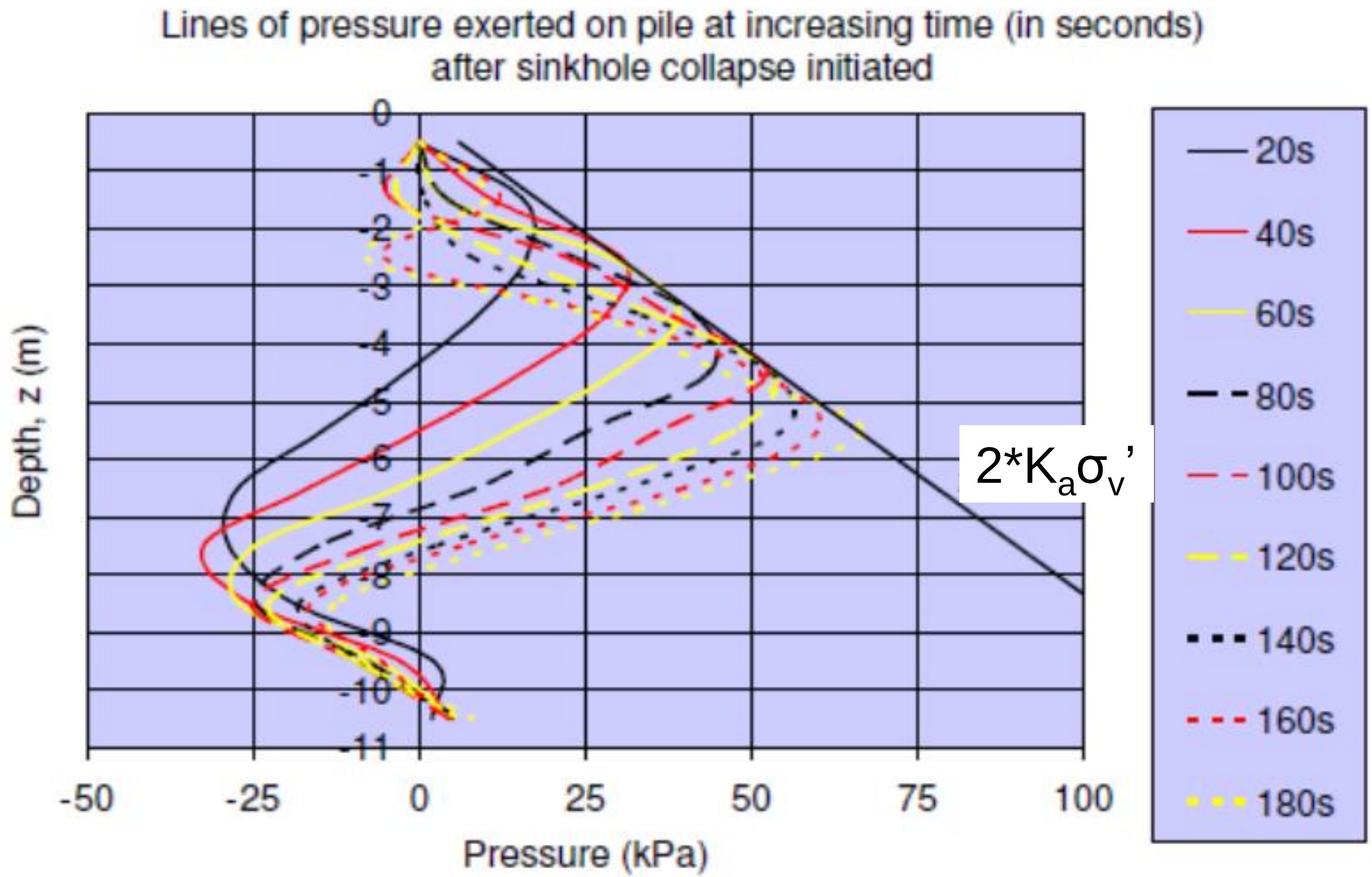

ARUP

3D SSI:
liquefaction effects prediction/simulation

a) heavy fluid, using Simplified Methods for triggering based upon CPT
b) bilinear soil with decoupled excess pore pressure generation, in offshore situations we can allow partial drainage during wave loading
c) non-linear critical state soil model such as SANISAND (Dafalias & Manzari, 2004) with coupled excess pore pressure generation and dissipation

Wave loading:
Generation of excess pore water pressure around offshore structures

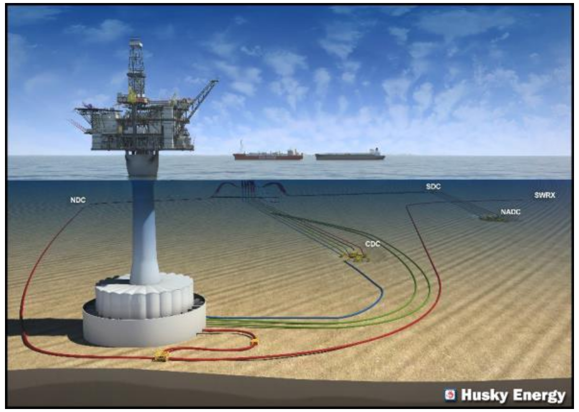

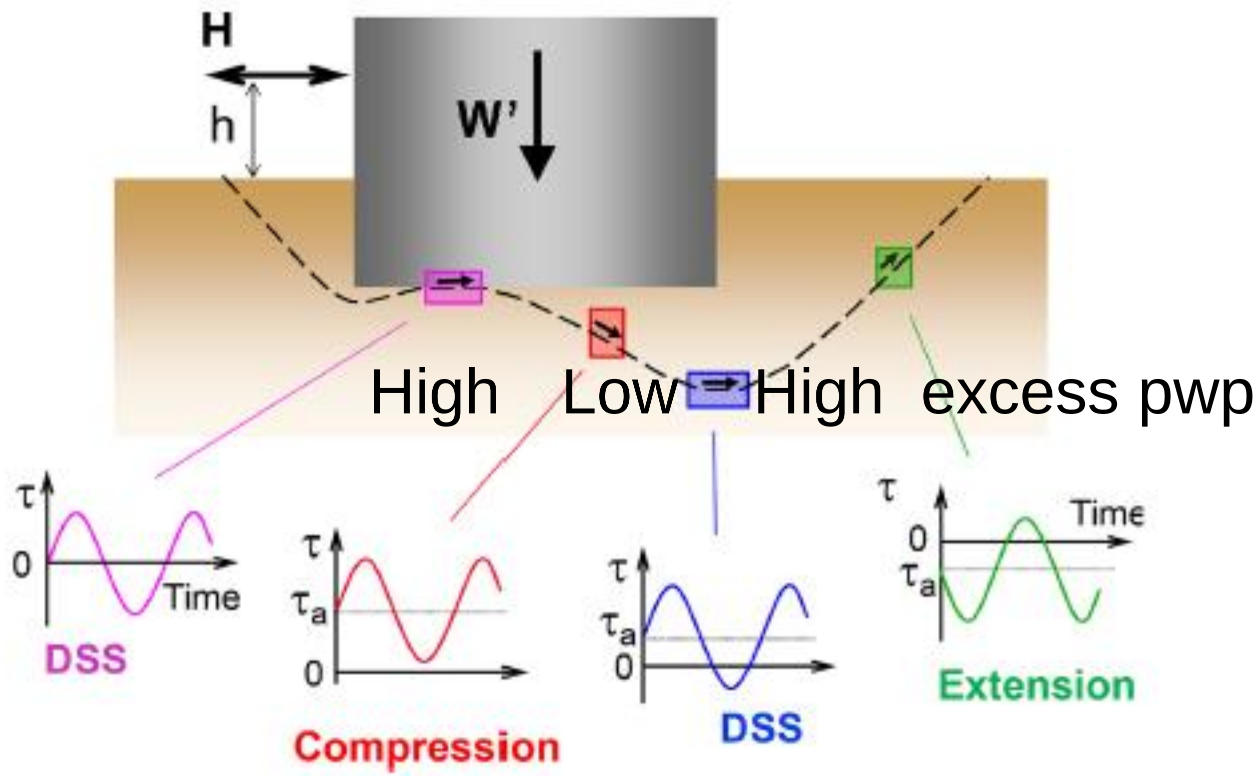

After Andersen (2015)

Excess pore pressure generation in sands undrained DSS loading

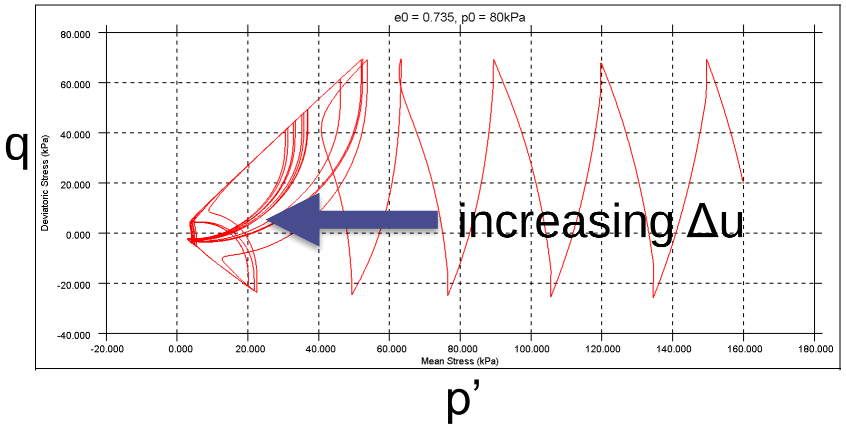

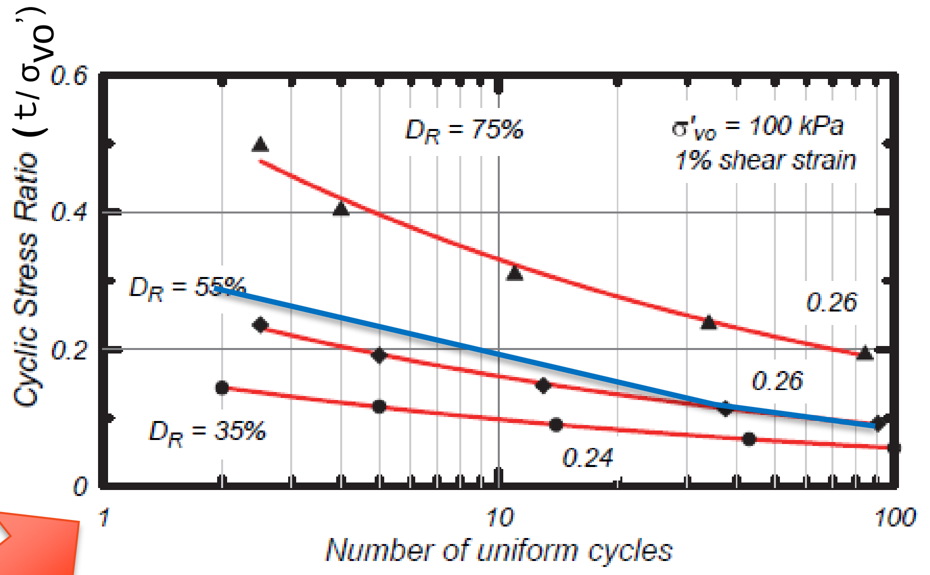

PM4 Sand in undrained DSS
(Boulanger & Ziotopoulou, 2015)

$$b=10^{(11.11\tau/\sigma_{vo}' - 2.67)}$$

where $b=\Delta u/(\sigma_{vo}'N)$

ARUP

FE analysis, shallow medium dense sands modelled as Elastic/ Mohr-Coulomb (G~100 MPa / ϕ'=36°)

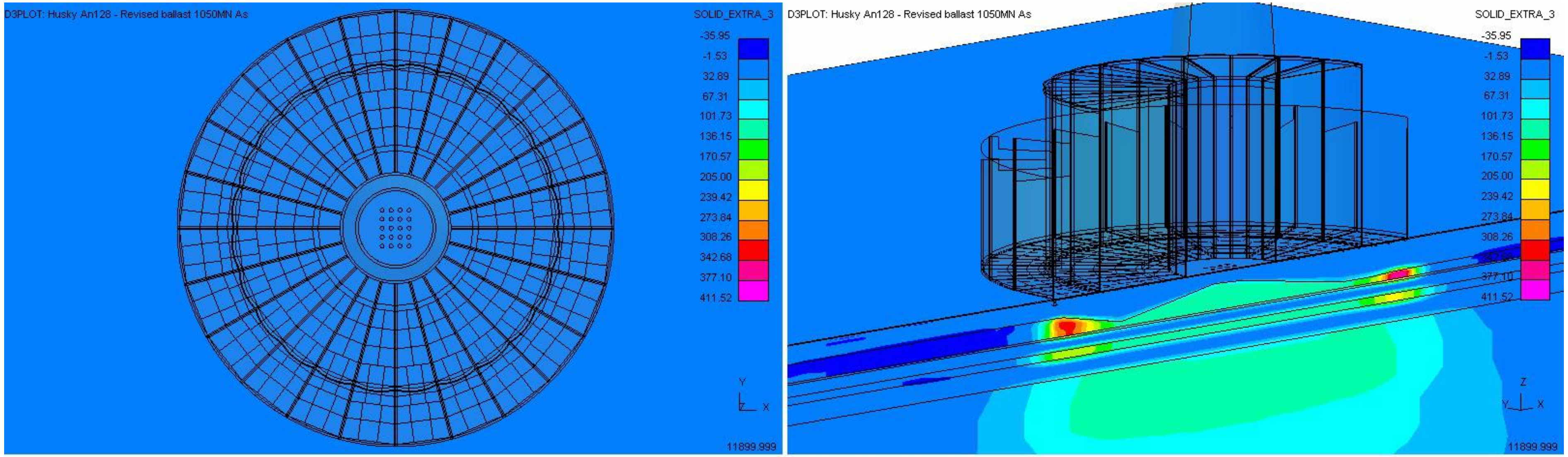

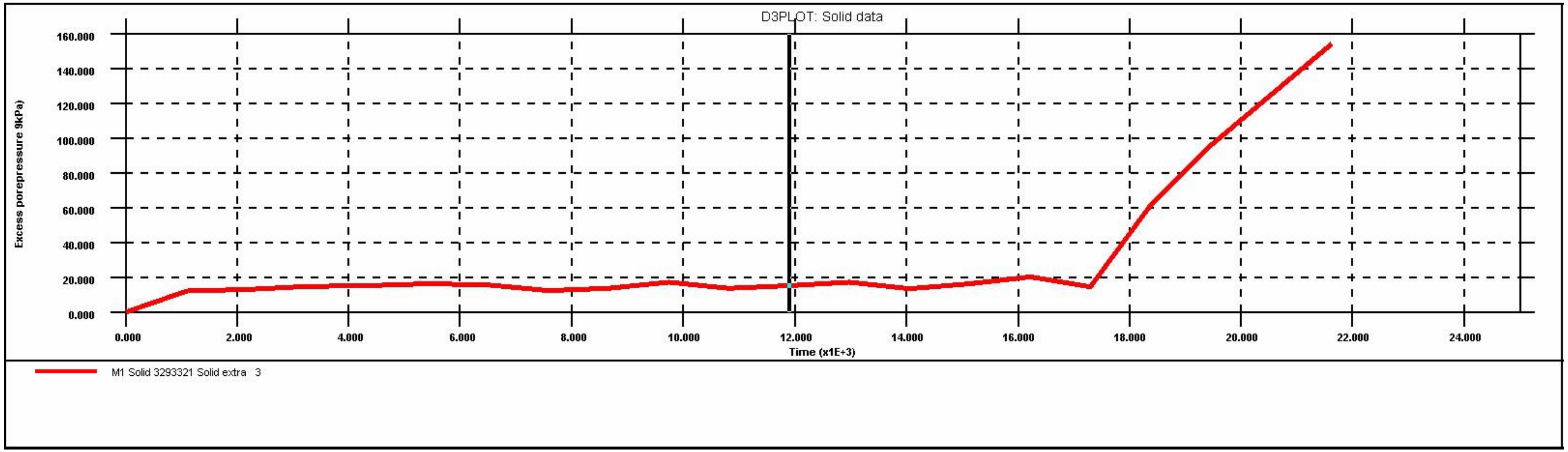

1 in 10,000 year storm wave loading on offshore gravity structure, with dissipation (after Dingle et al, 2017)

ARUP

Typical North Sea 6 hour design storm (after Hansteen, 1980)

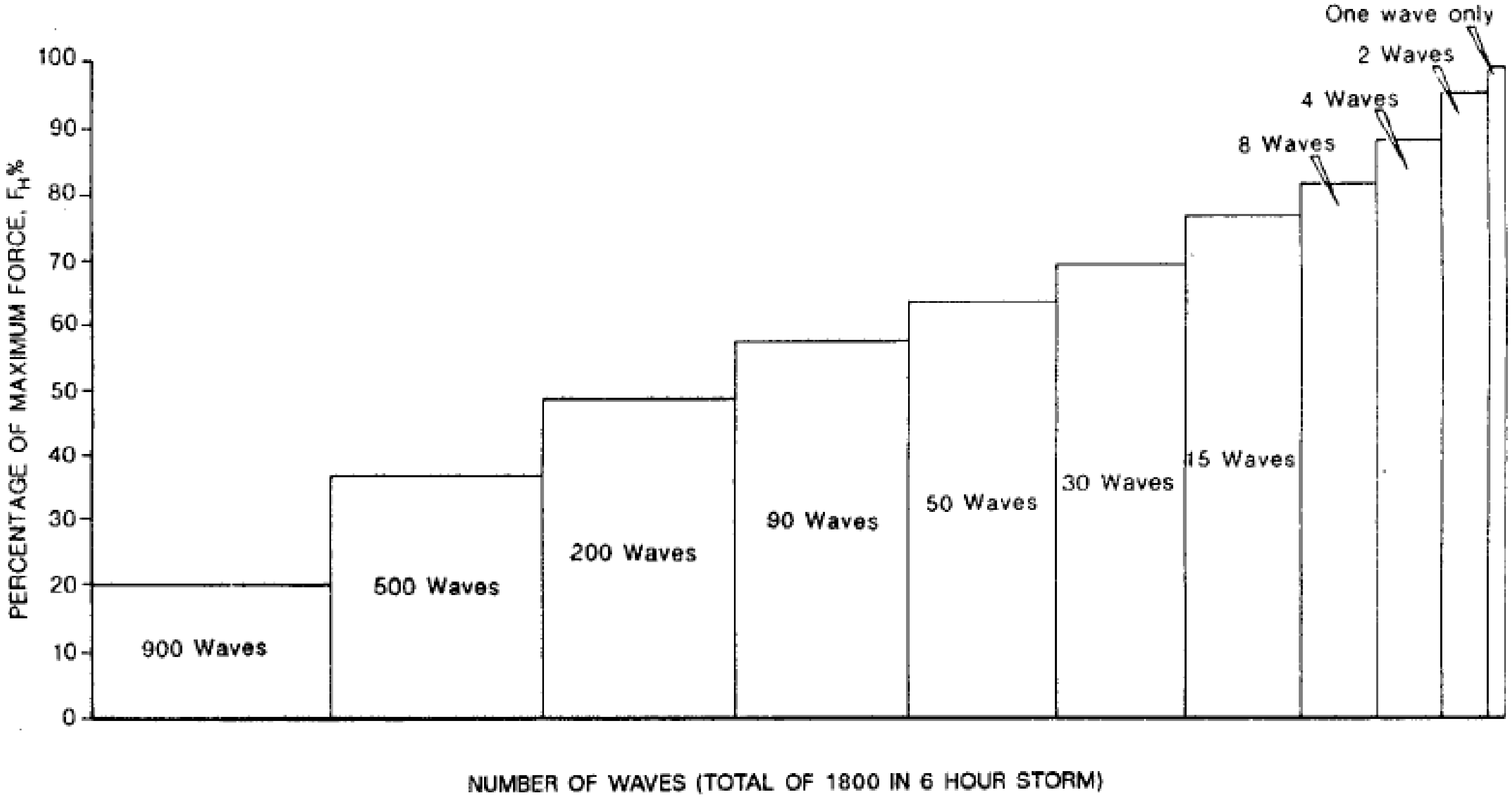

Average wave period = 12 seconds

ARUP

Probability Pj of waves > mean wave height occurring within a run of j waves during deep-water storms (Longuet-Higgins, 1984)

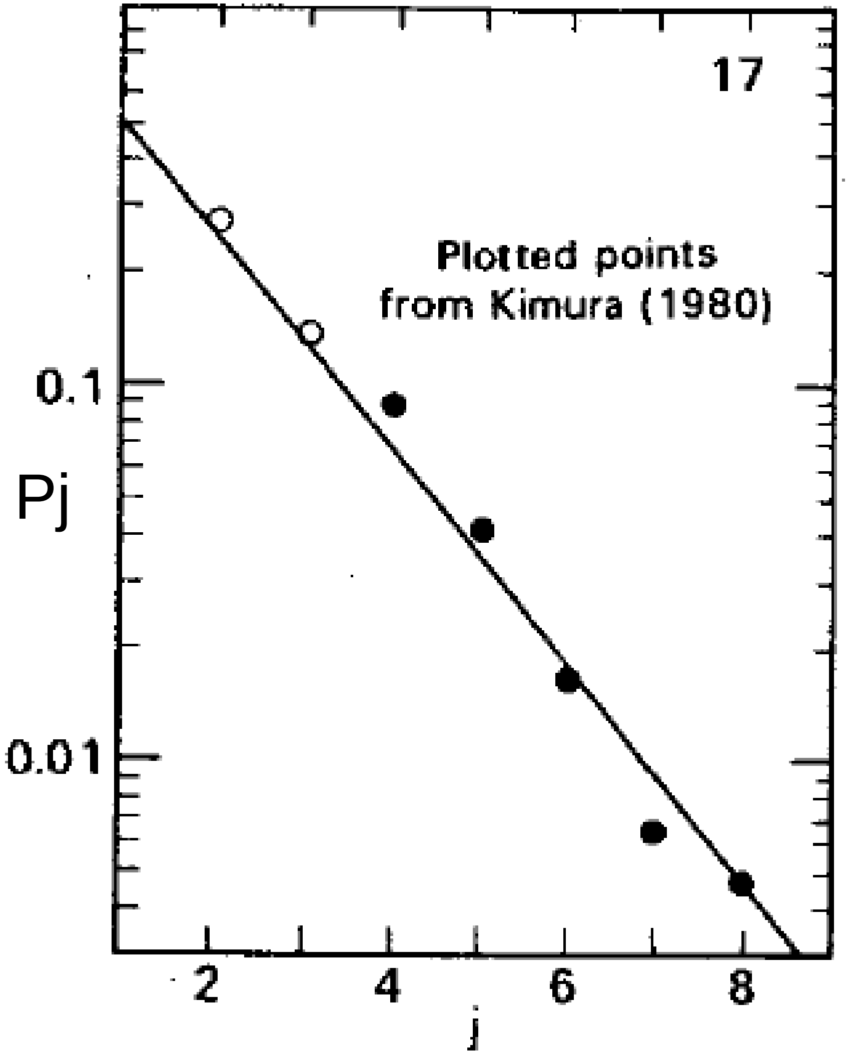

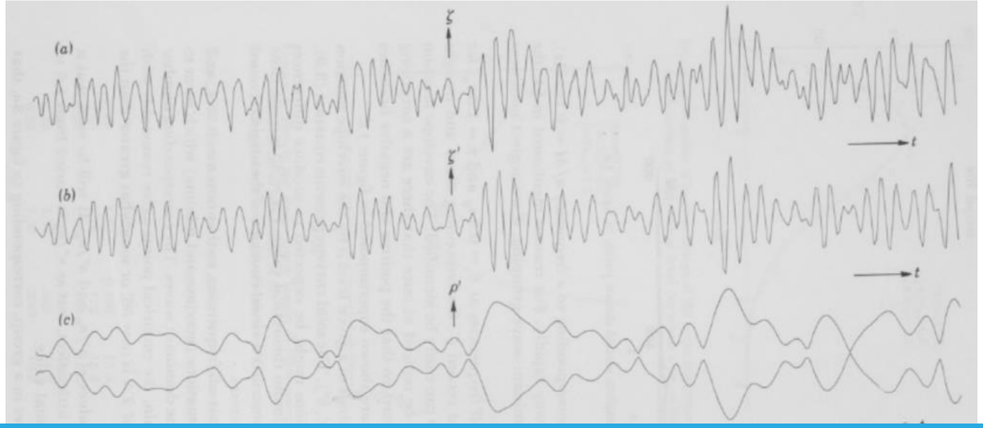

ARUP

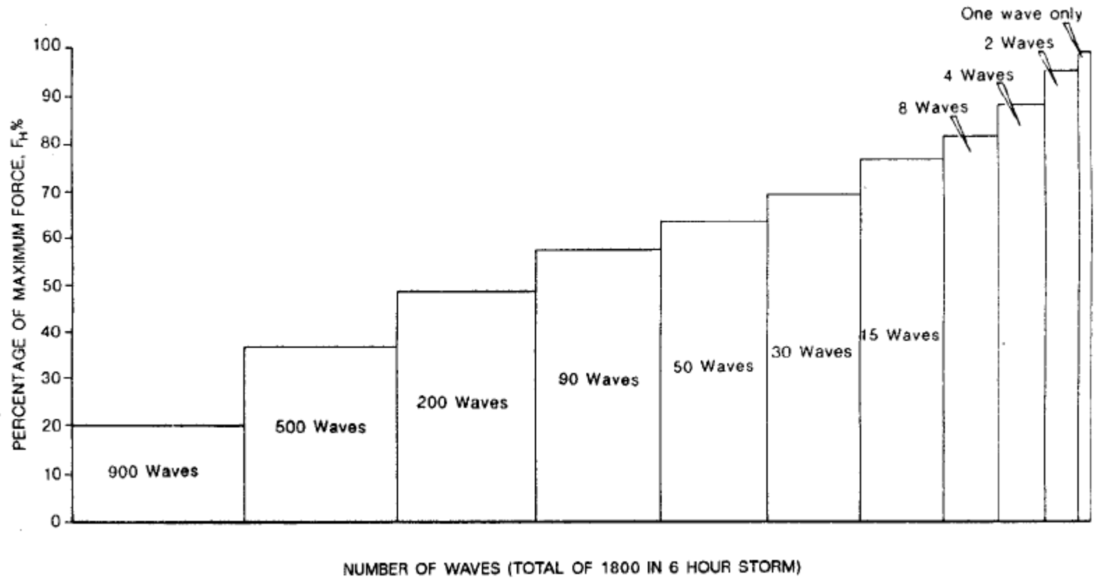

RANWAVE: greater realism, requiring a pseudo-random approach to storm wave composition

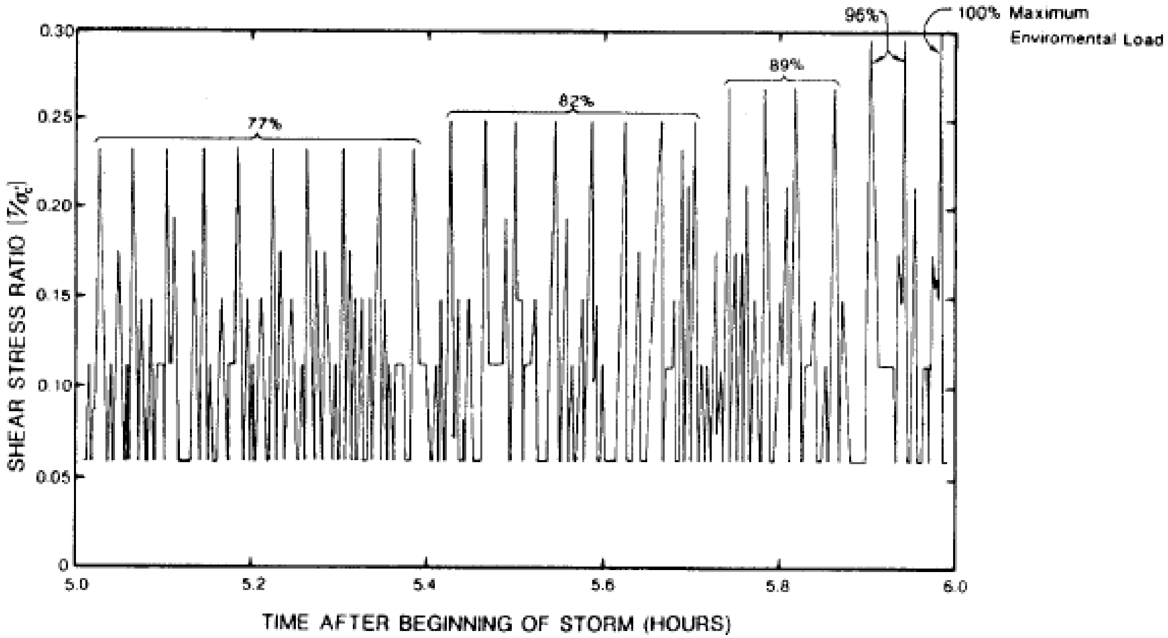

O’Riordan & Seaman (1993) 1 in 100 year storm

Statistical outcome from RANWAVE (O'Riordan & Seaman, 1993) and implementation in variety of FE platforms (Dingle et al, 2017)

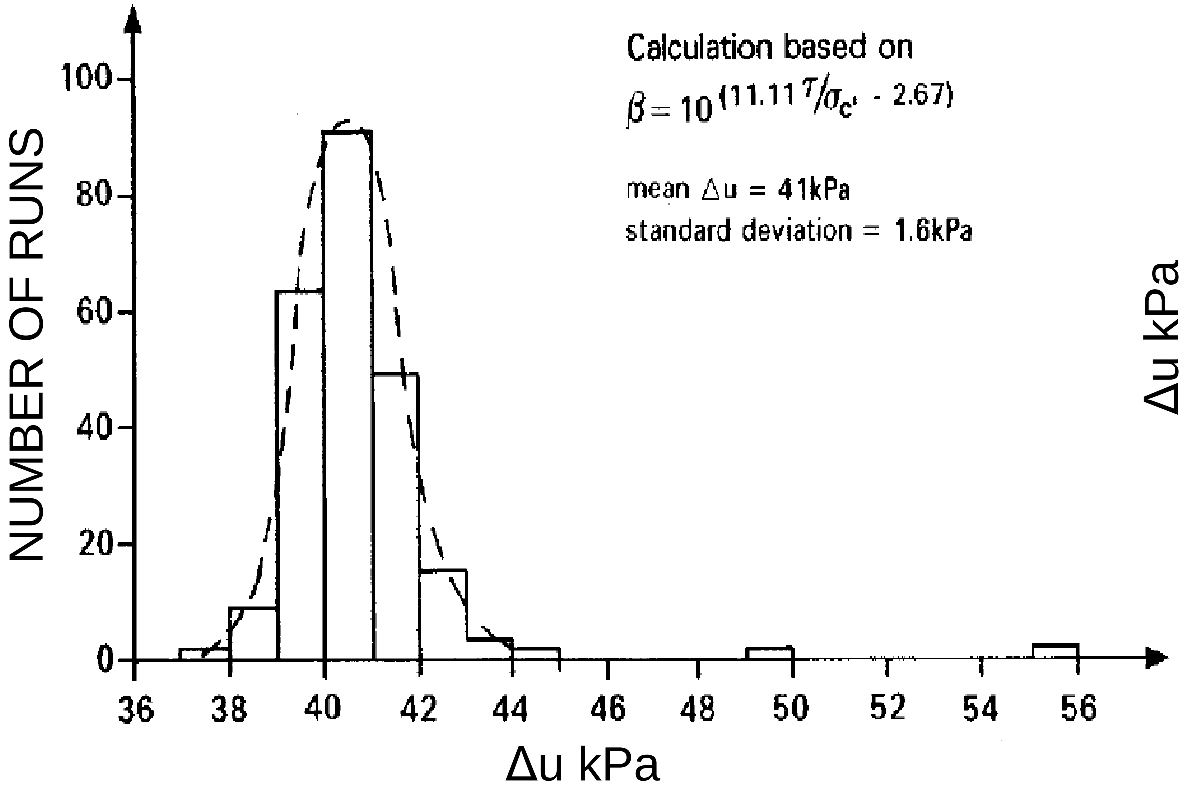

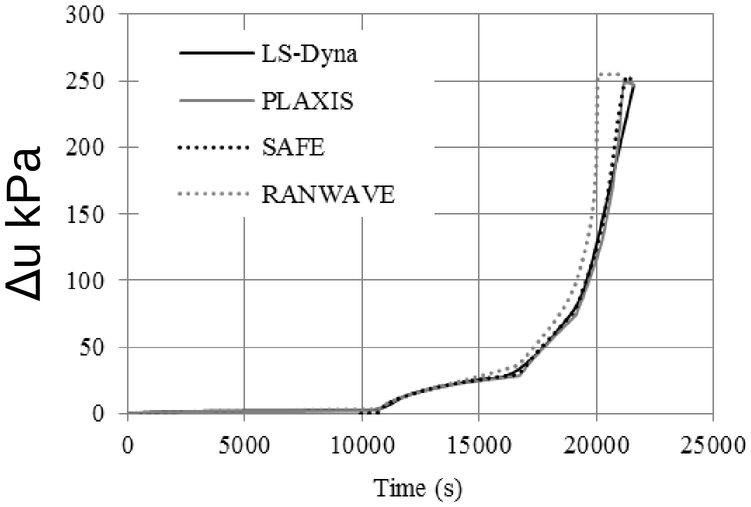

Comparison of RANWAVE with conventional ascending 'Hansteen' approach

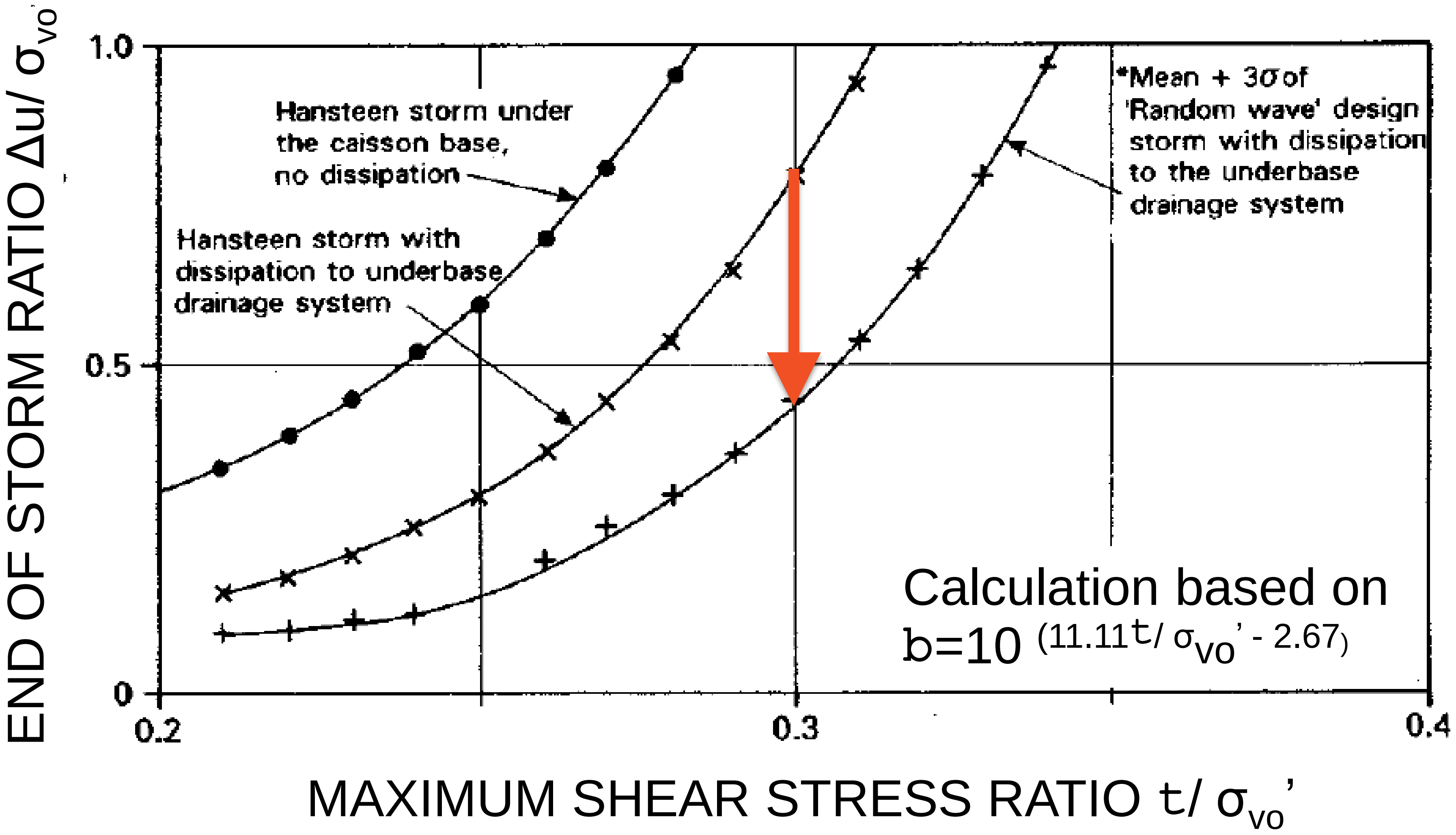

O'Riordan & Seaman (1993) 1 in 100 year return storm non-linear critical state soil model such as SANISAND (Dafalias & Manzari, 2004) with coupled excess pore pressure generation and dissipation

PEER blind liquefaction prediction competition 2018

Fig. 1: Laminar Soil Box at UCSD Powell Laboratory (H2.9m×L3.9m×W1.8m)

Total mass of box and contents ~ 46 tonnes

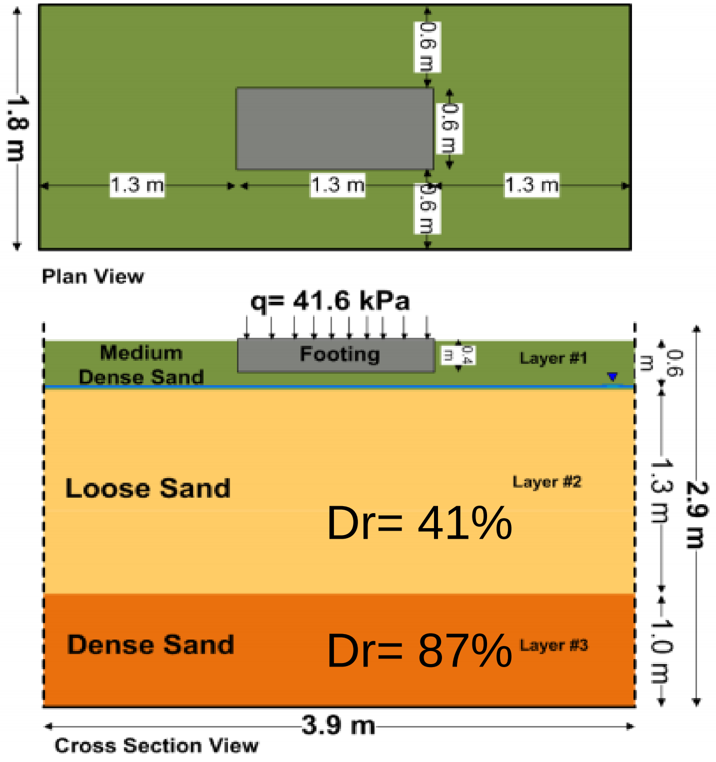

Fig. 1: Model ground configuration

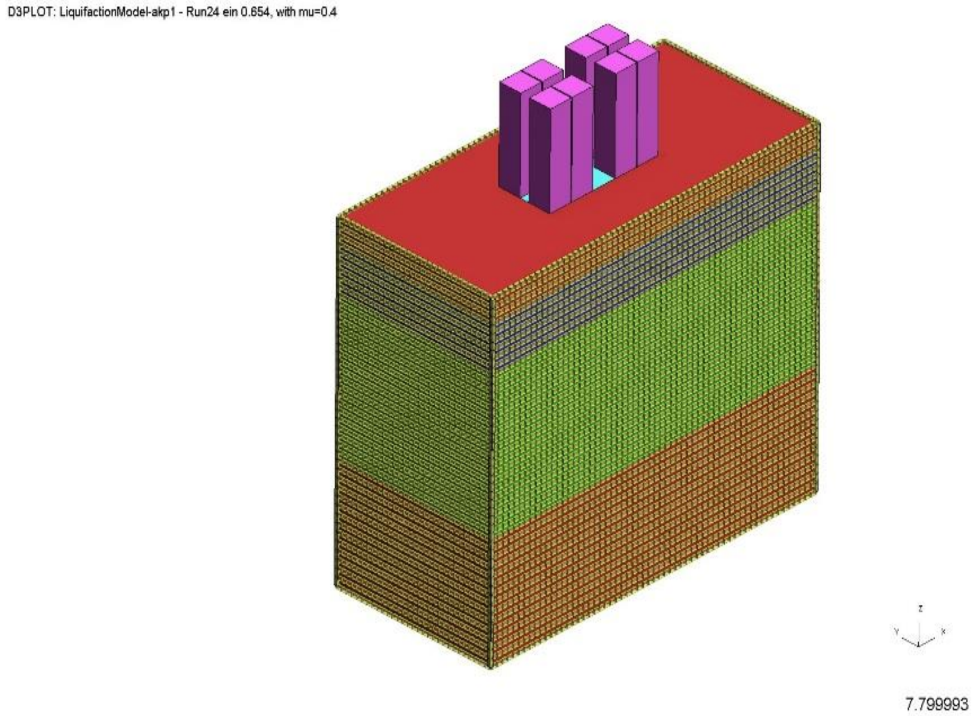

Input geometry (PEER,2018)

LSDyna model (hexagonal elements with single Gauss point for SANISAND elements)

Cyclic calibration : Test 17 (Dr=39%, CSR=0.1)

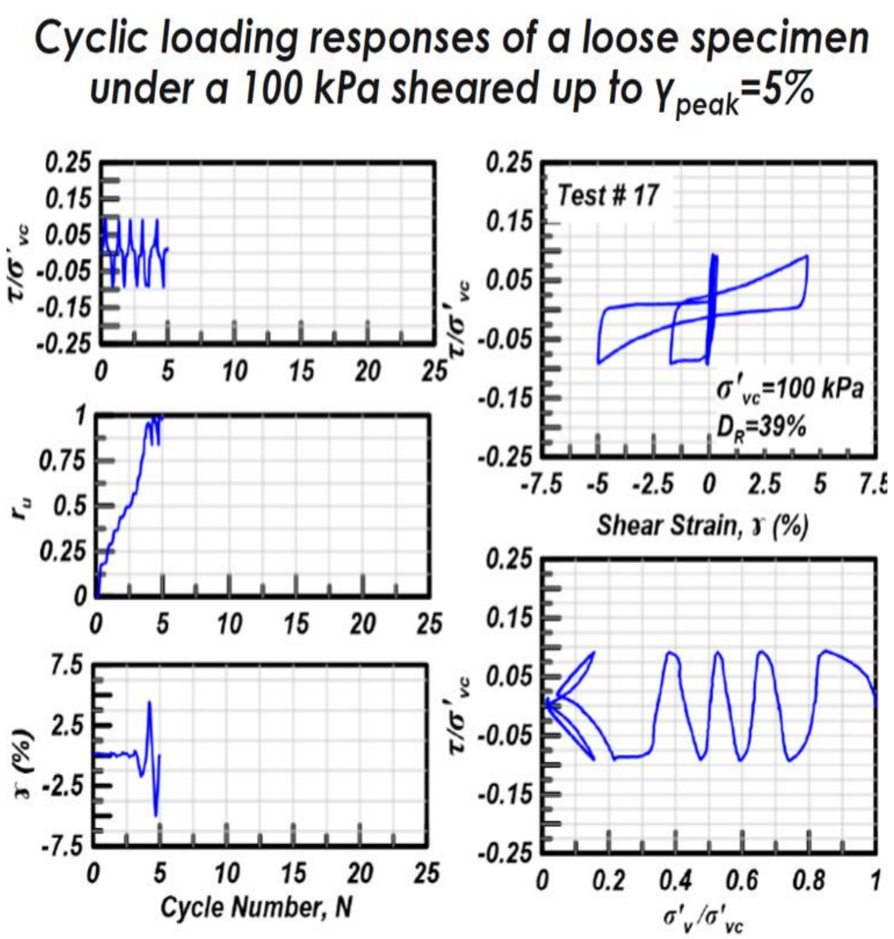

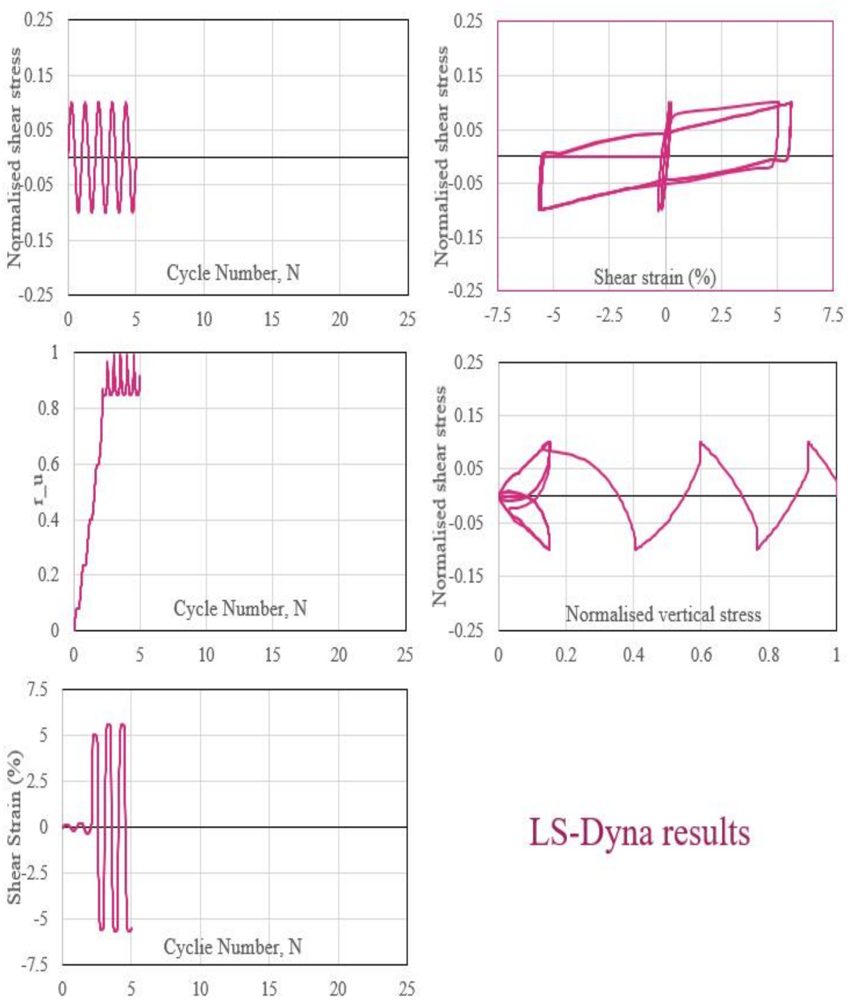

LS-Dyna results

Cyclic DSS tests (Bastidas, 2016): calibration results for LS Dyna SANISAND model (Dafalias & Manzari, 2004) shown in red. Overall calibration methodology informed by Ramirez et al (2018).

Cyclic calibration : Test 23 (Dr=77%, CSR=0.16)

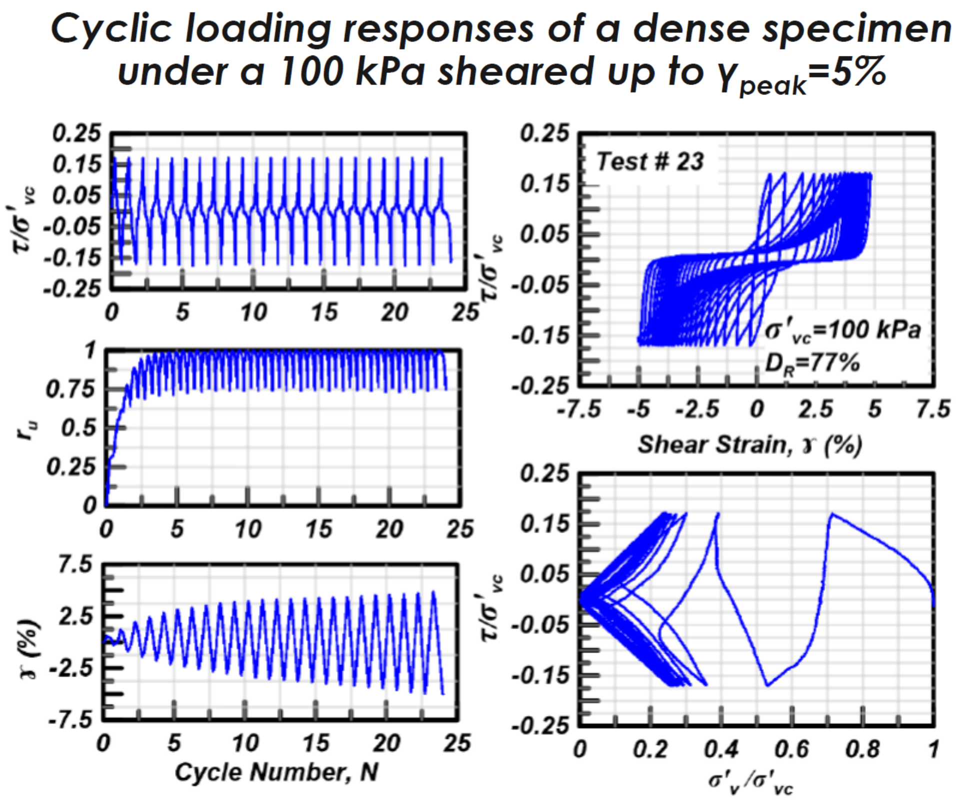

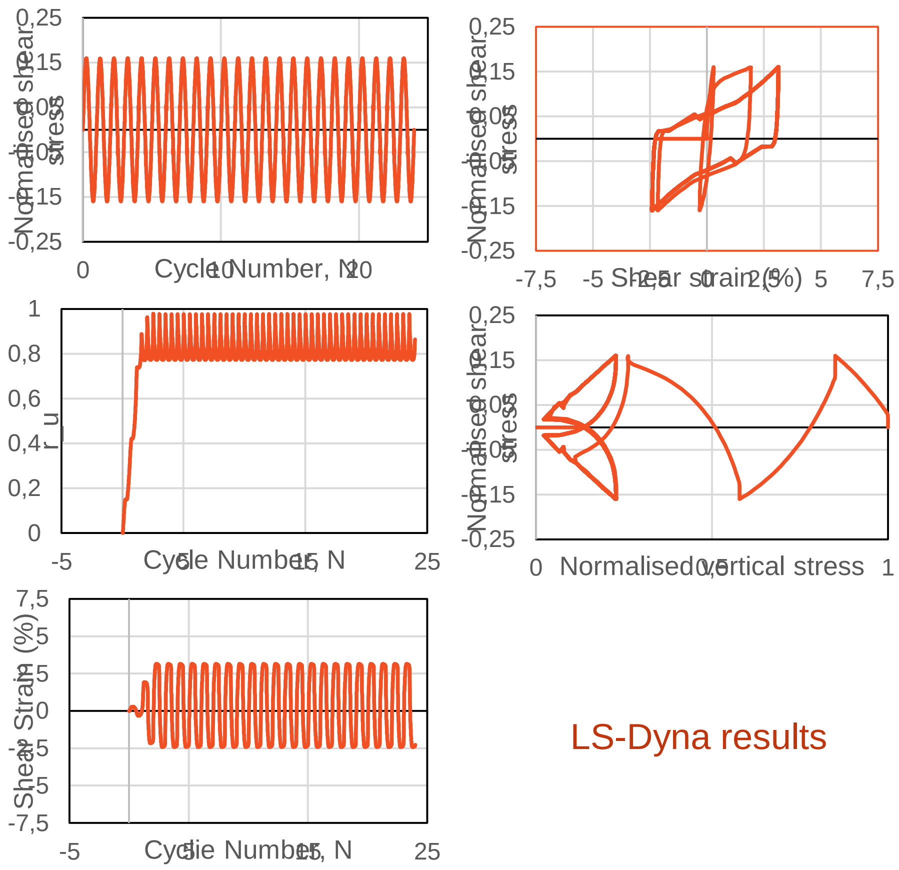

LS-Dyna results

ARUP

Ottawa F65 sand parameters derived for 3D Sanisand model (after Dafalias & Manzari, 2004)

LAYER	SIGVEFF	TERMINATE	CSR	ALPHA	FREQUENCY	K_0	RO	G0	K0	PREF	RHOC	THETA	X	EIN	ALPHAC	EA	LAMBDA	XI	NB	H0	CH	P0	CC	ND	A0	ANISO	KH	ZMAX	CZ	PAT	M	N	V
1	100	5	0.1	0	1	1	2	150	-0.05	5500	0.37	0.18	0.8	0.66	1.26	0.78	0.0287	0.7	0.6	5	0.968	55000	0.735	0.5	0.3	0.333	1	11	200	101.325	0.05	20	1000
2	100	14	0.11	0	1	1	2	150	-0.05	5500	0.37	0.18	0.8	0.70	1.26	0.78	0.0287	0.7	0.6	5	0.968	55000	0.735	0.5	0.3	0.333	1	11	200	101.325	0.05	20	1000
3	100	24	0.16	0	1	1	2	150	-0.05	5500	0.37	0.18	0.8	0.55	1.26	0.78	0.0287	0.7	0.6	5	0.968	55000	0.735	0.5	0.3	0.333	1	11	200	101.325	0.05	20	1000

Table 1 SANISAND soil parameters

Note: top 200mm of layer 1 replaced by Mohr-Coulomb material with G=10 MPa, Φ’ = 34deg

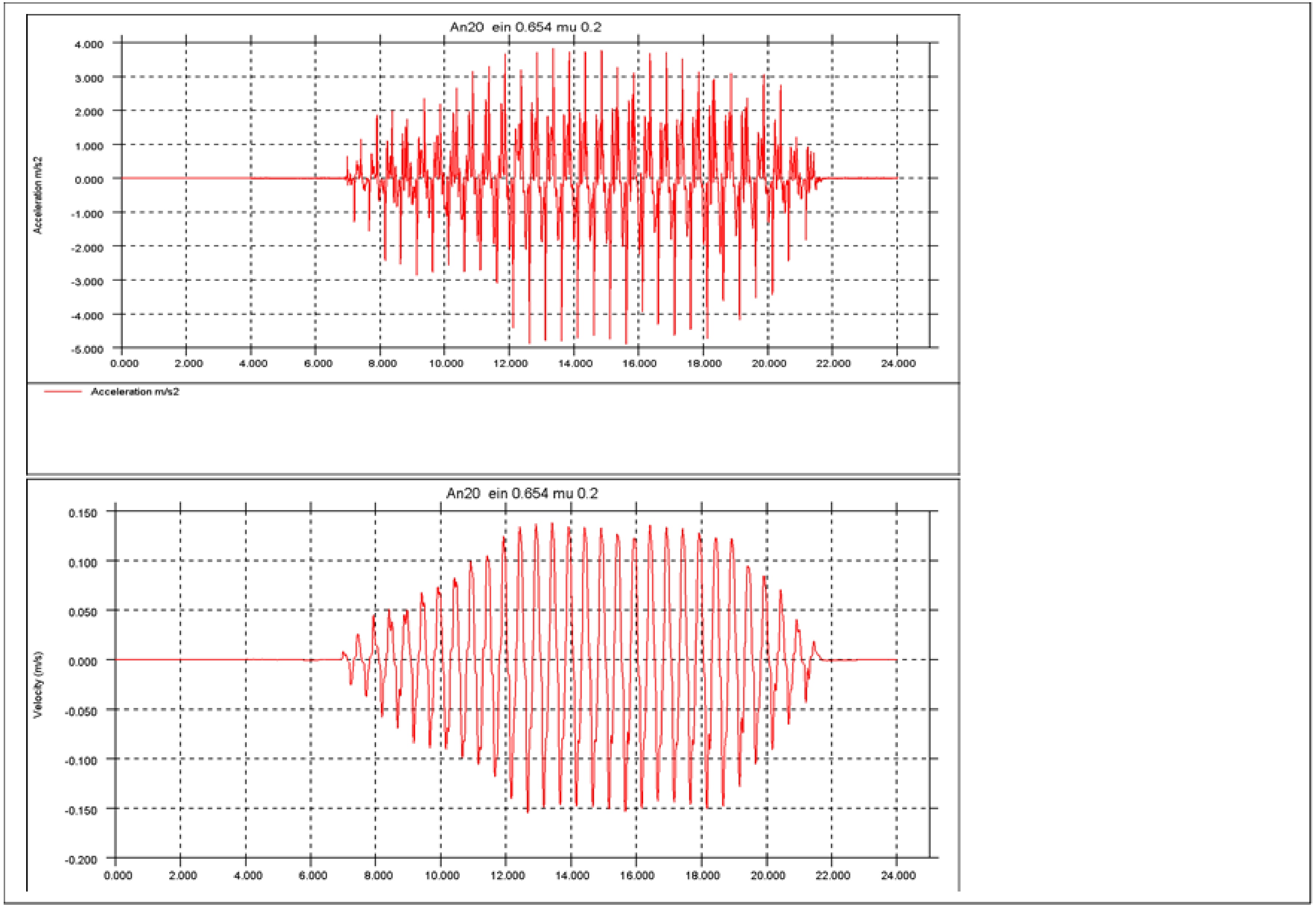

Base input time history: 16 seconds of shaking and up to **0.4 g** over 6 seconds

Time history for generation of excess pore pressures at various depths in the box (zero volumetric strain imposed)

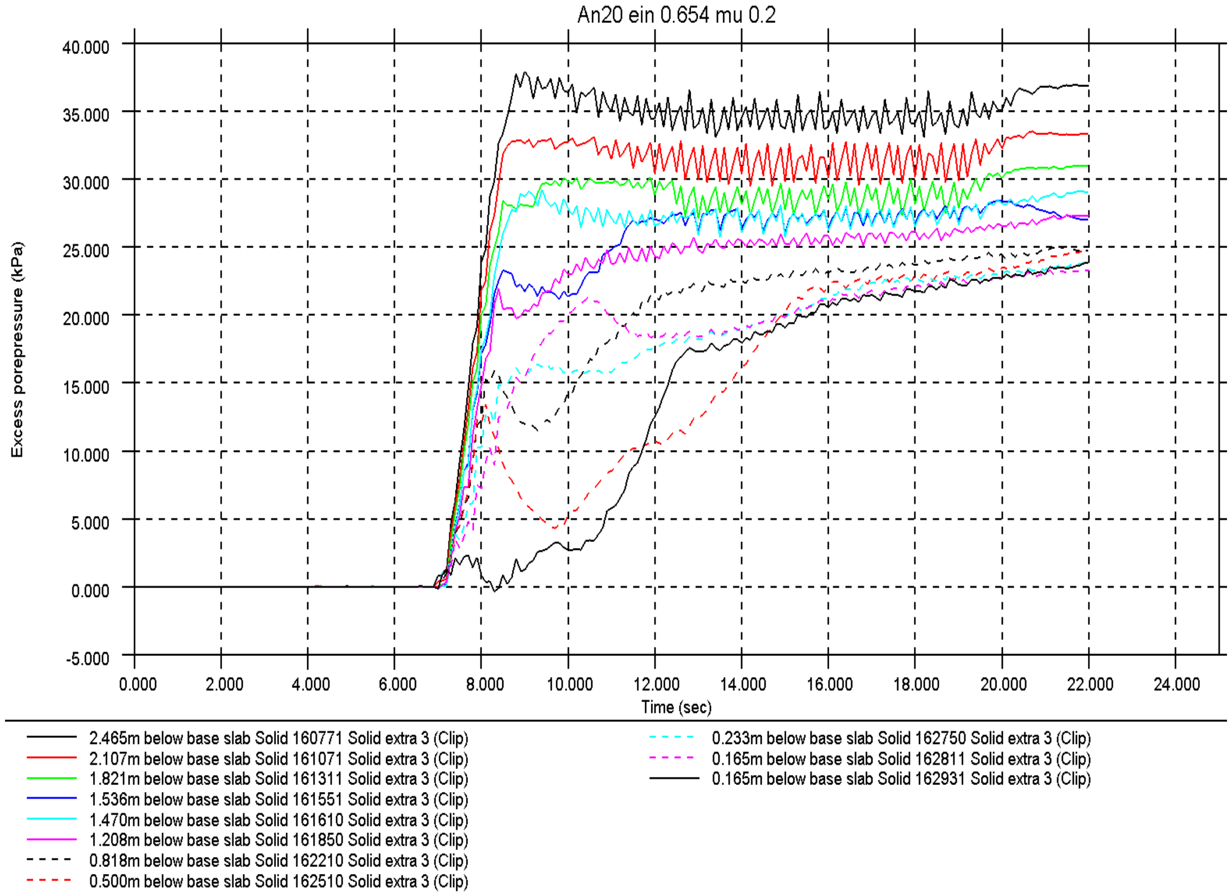

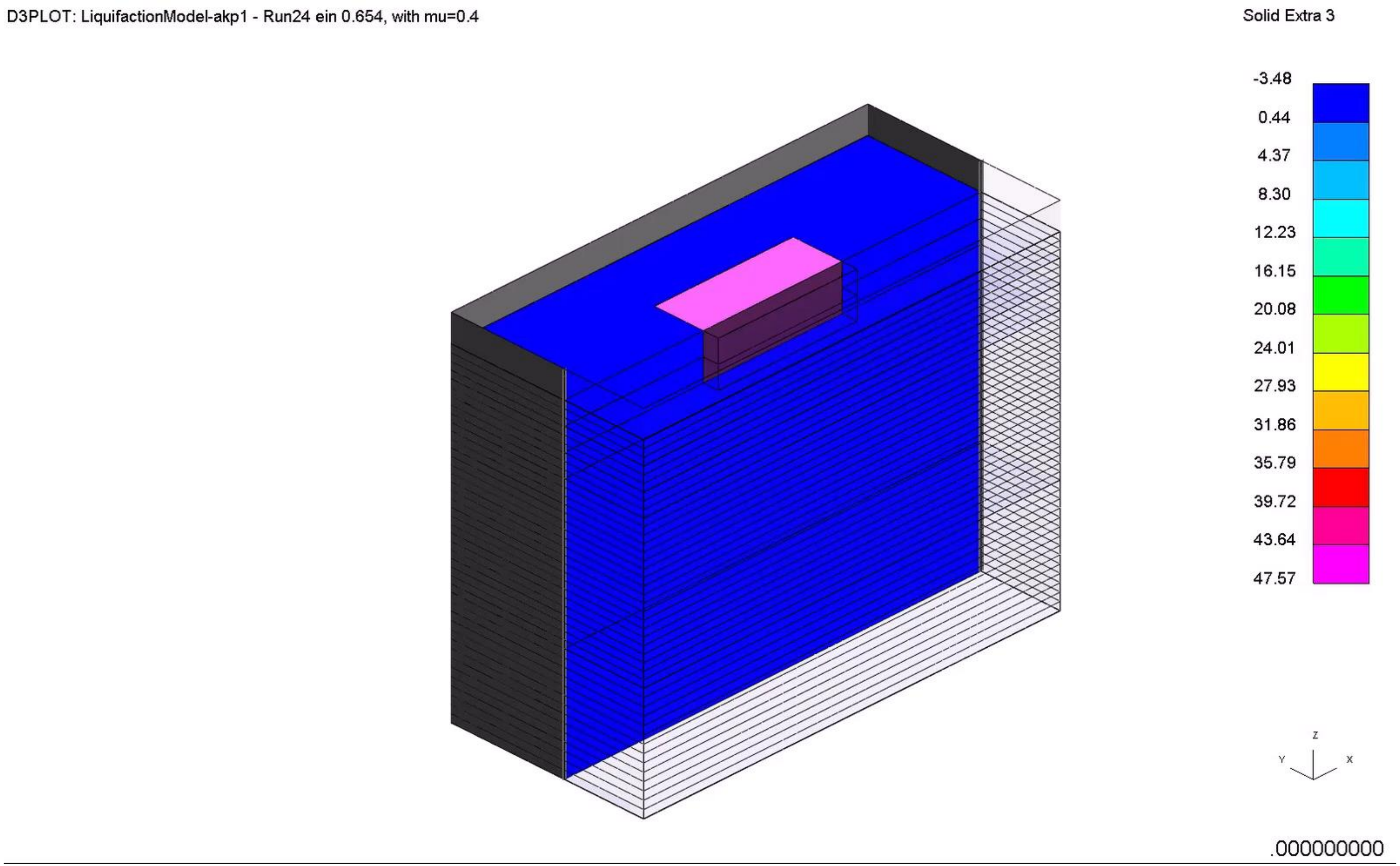

Excess pore pressures (in kPa) within model elements

Test#1: Predicted vertical movements

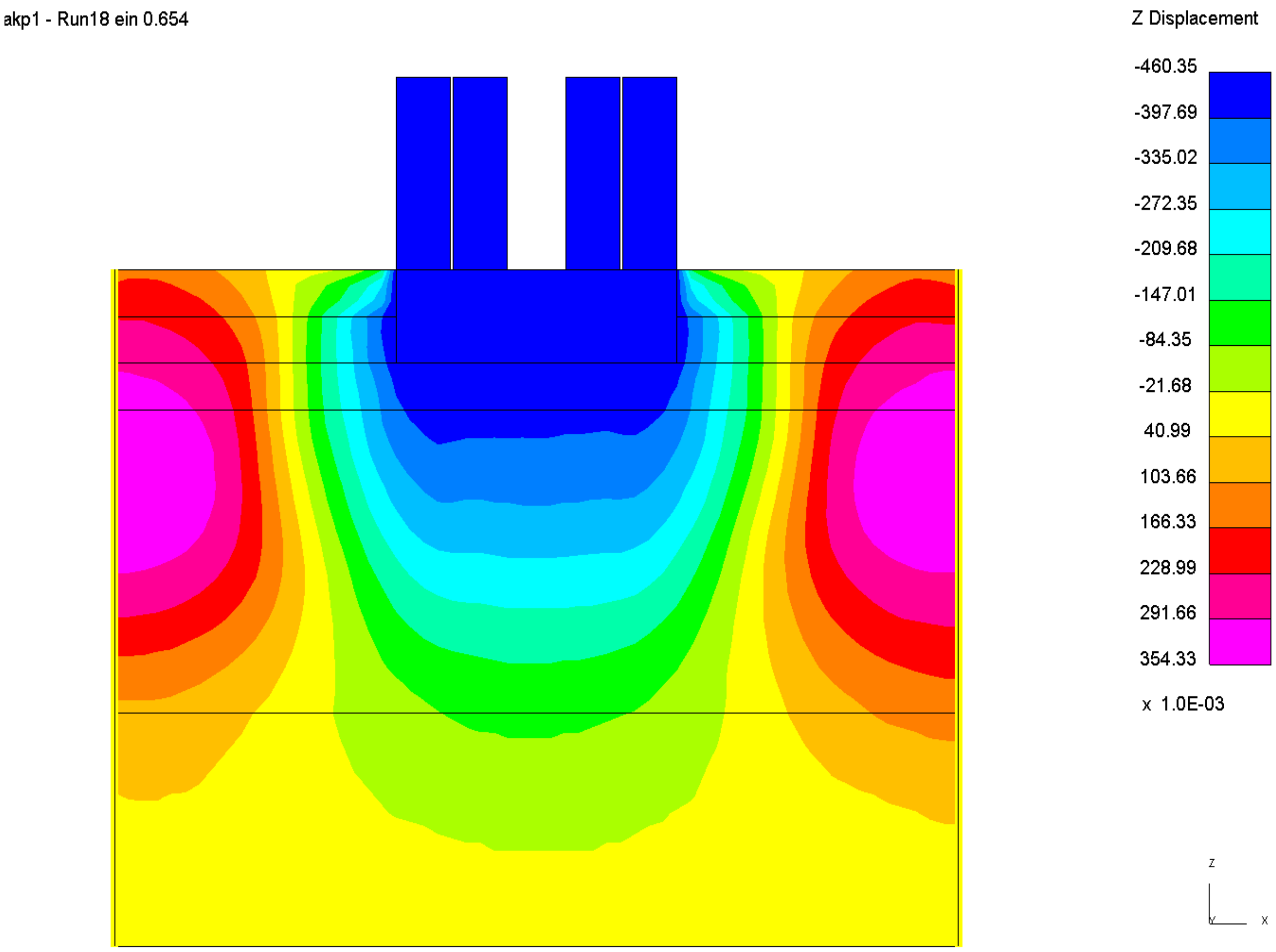

Predicted footing settlement= 460mm (thickness of 6 steel weights)
All excess pore pressures dissipate within 80 seconds after shaking

Measured footing settlement, Test#1: ~230mm

free-field settlement~ 25mm

'On average, the participating teams underestimated *the foundation settlement by a factor of 2, whereas they* overestimated *the free-field settlement by more than a factor of 3.' (Motamed et al, 2019)*

Test #2: PGA= 0.3g, GWT= 0.0m (Sand Ejecta)

Motamed, R. (2019) “Class B Blind Prediction of a Large-Scale Shake Table Test on a Shallow Foundation in Liquefied Soils” *PEER 2019 Annual Meeting: Seismic Resilience 25 Years after Northridge: Accomplishments and Challenges*, January 17-18 2019, UCLA Mong Auditorium, Los Angeles, CA.

ARUP

Very soft Mexico Clays: seismic performance and design

Regional subsidence: satellite image, 2014 (ESA Sentinel 1-A radar scans)

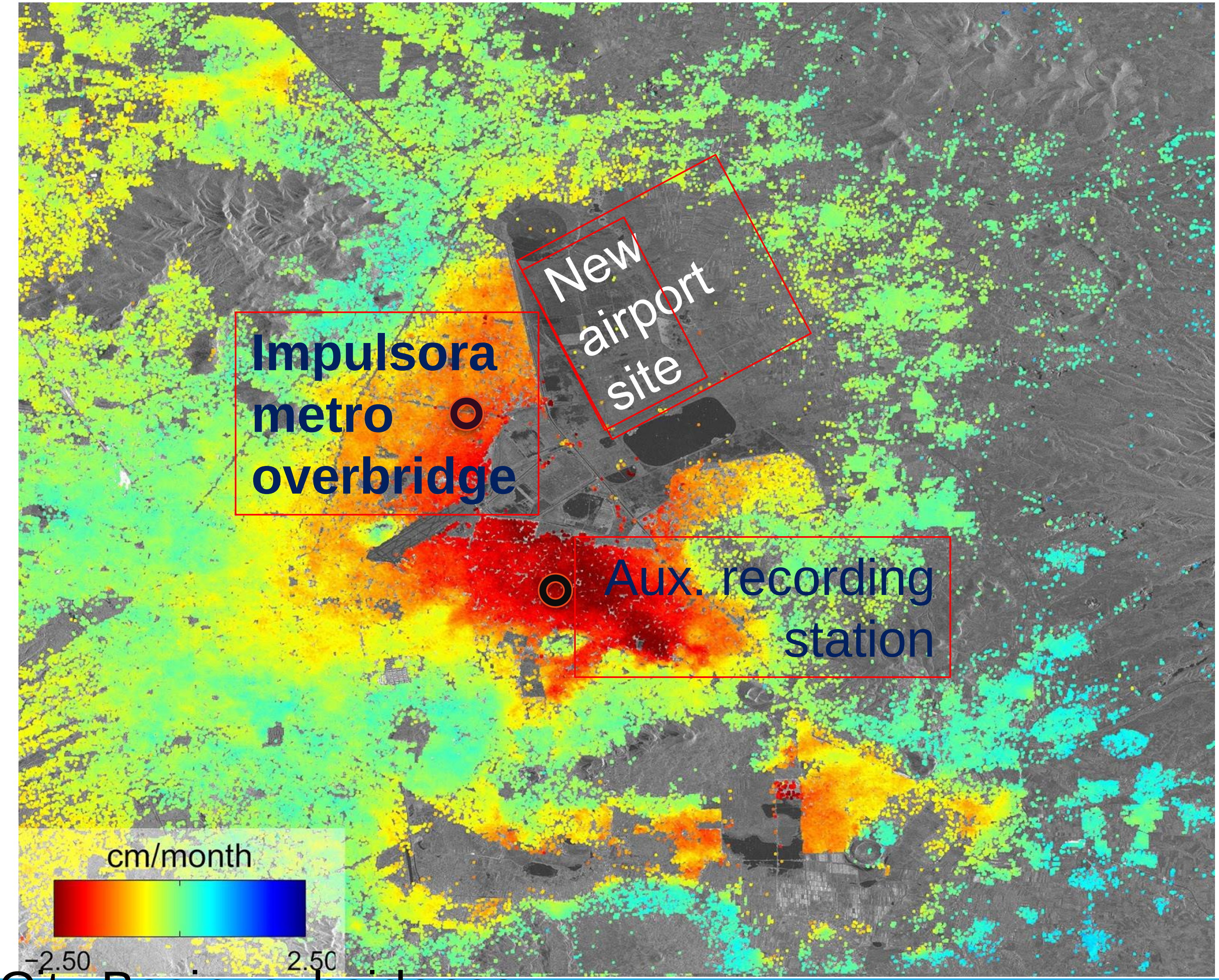

Mexico City Basin: subsidence due to groundwater extraction

10 km

ARUP

Impulsora metro station overbridge

ARUP

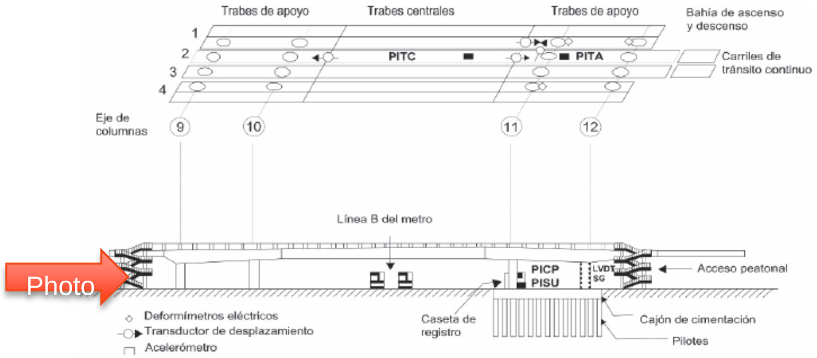

Alcantara et al (2005)

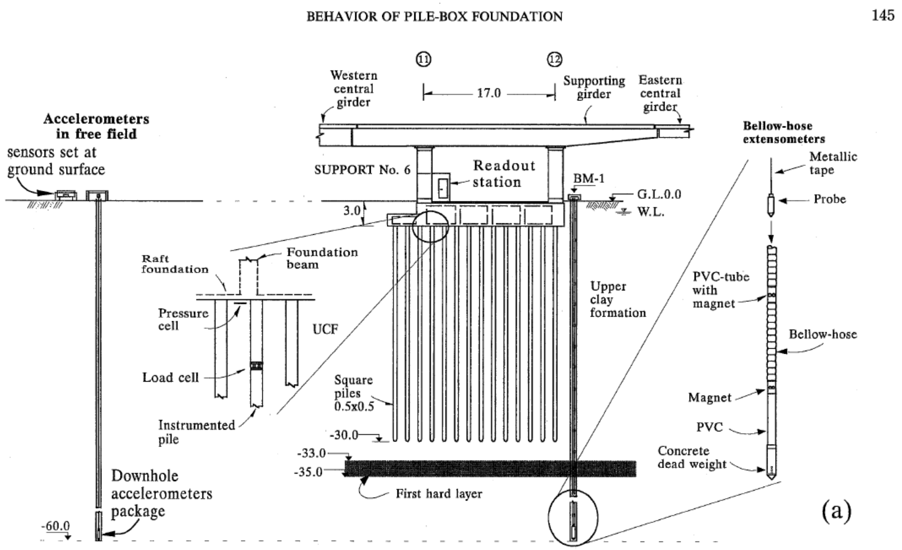

Mendoza et al (2000), *Static and seismic behaviour of a friction pile-box foundation in Mexico City Clay*
Soils and Foundations, JGS, Tokyo

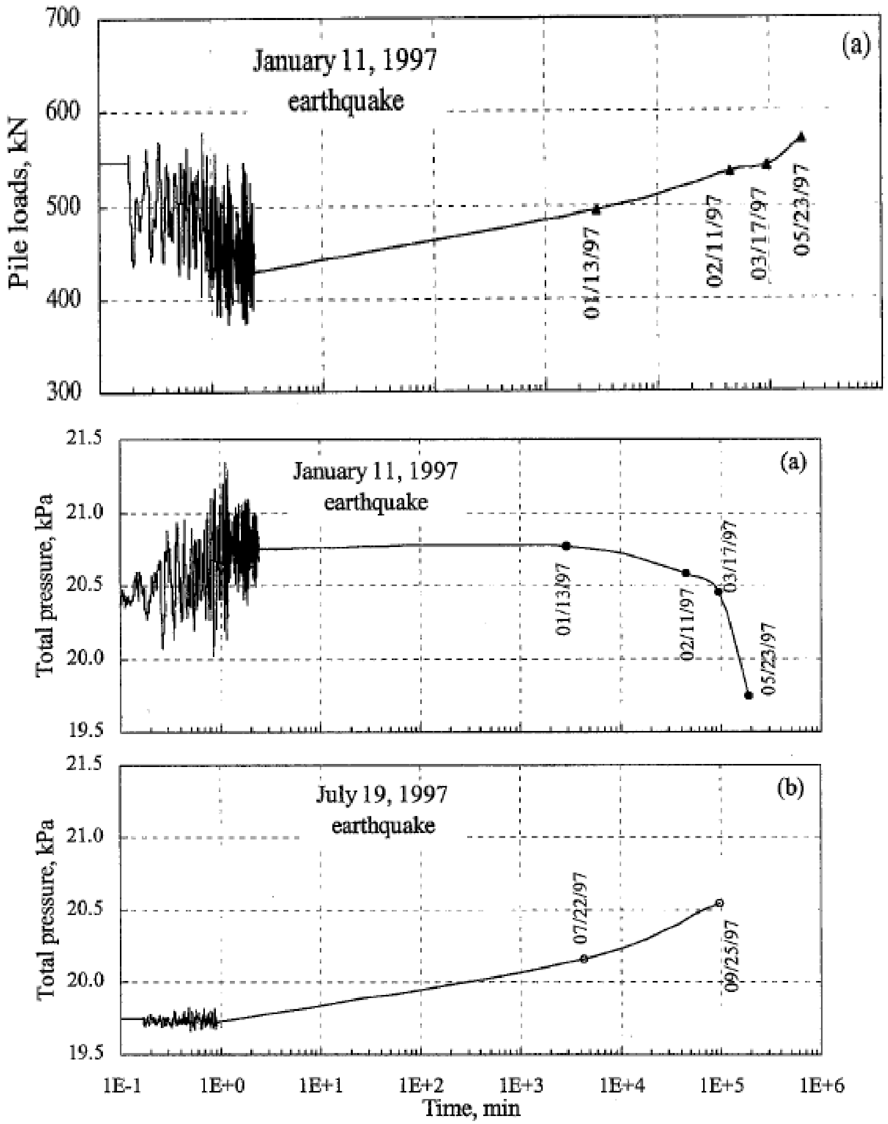

Fig. 9. History of vertical pressures at CP3 at R-S contact during seismic events A and B, and later evolutions

Mexico City (Impulsora metro overbridge) foundation

Mw=7.3, 450 km distant epicentre

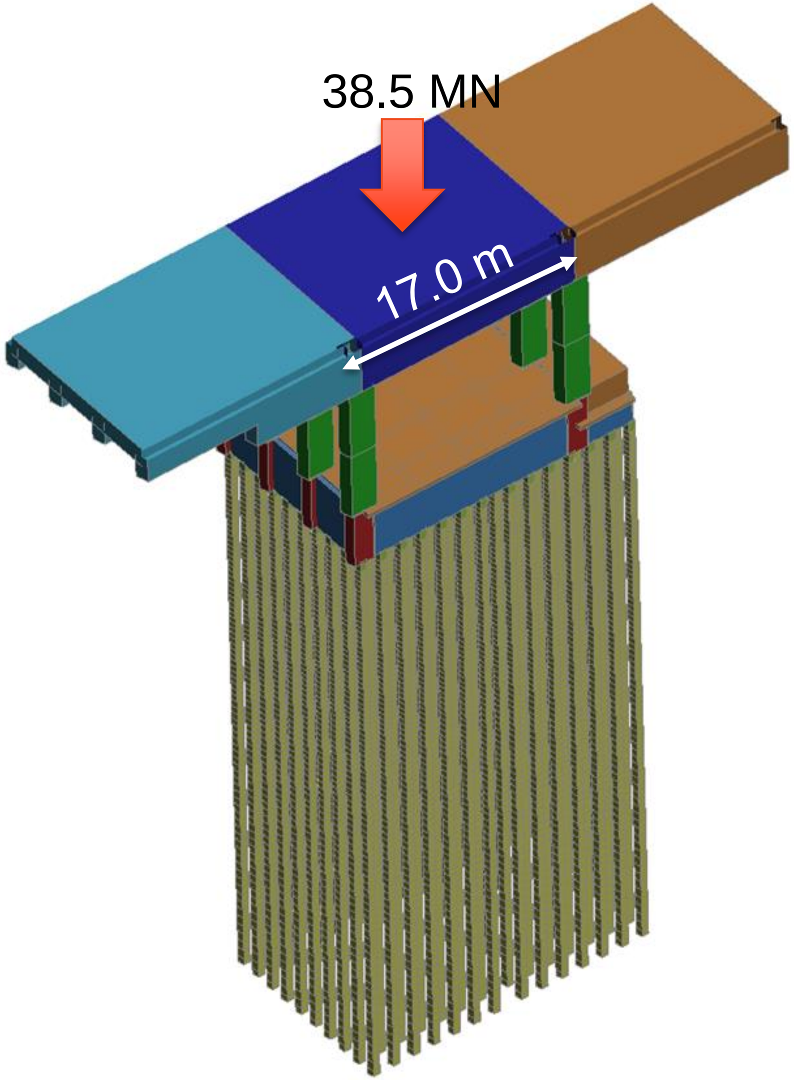
38.5 MN
17.0 m

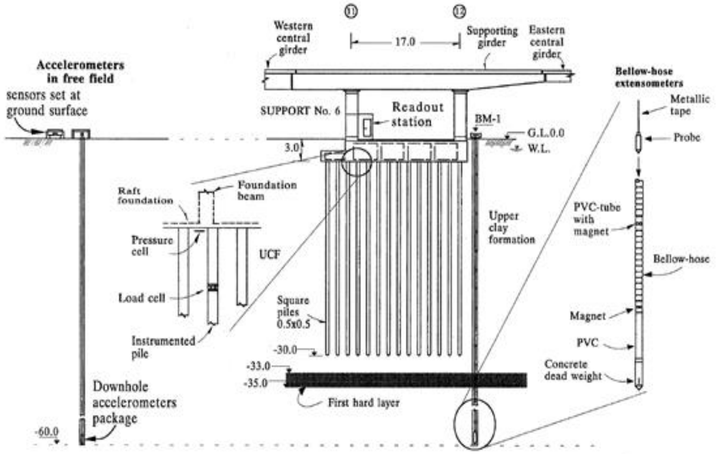
Western central girder
17.0
Supporting girder
Eastern central girder
Accelerometers in free field
sensors set at ground surface
SUPPORT No. 6
Readout station
BM-1
G.L.0.0
W.L.
Bellow-hose extensometers
Metallic tape
Probe
3.0
Raft foundation
Foundation beam
Pressure cell
UCF
Upper clay formation
PVC-tube with magnet
Bellow-hose
Load cell
Square piles 0.5x0.5
Magnet
PVC
Instrumented pile
-30.0
-33.0
-35.0
Concrete dead weight
Downhole accelerometers package
First hard layer
-60.0

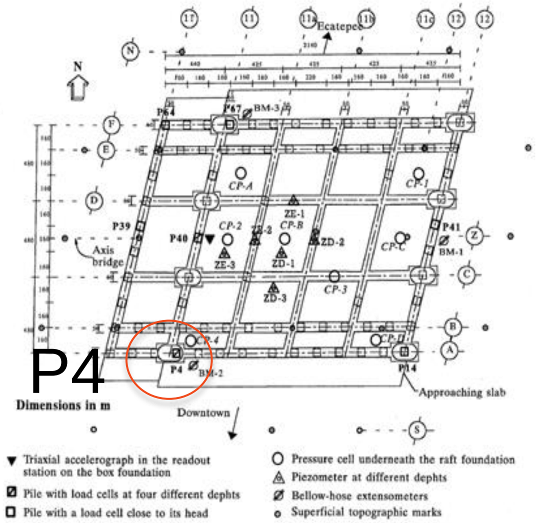
Ecatepec
N
P64
P67
BM-3
CP-A
CP-1
ZE-1
CP-B
P39
P40
CP-2
ZE-2
ZD-2
CP-C
P41
BM-1
Axis bridge
ZE-3
ZD-1
CP-3
ZD-3
CP-4
P4
BM-2
P14
P4
Dimensions in m
Approaching slab
Downtown
Triaxial accelerograph in the readout station on the box foundation
Pile with load cells at four different depths
Pile with a load cell close to its head
Pressure cell underneath the raft foundation
Piezometer at different depths
Bellow-hose extensometers
Superficial topographic marks

Force transfer ‘springs’ at pile-soil interface

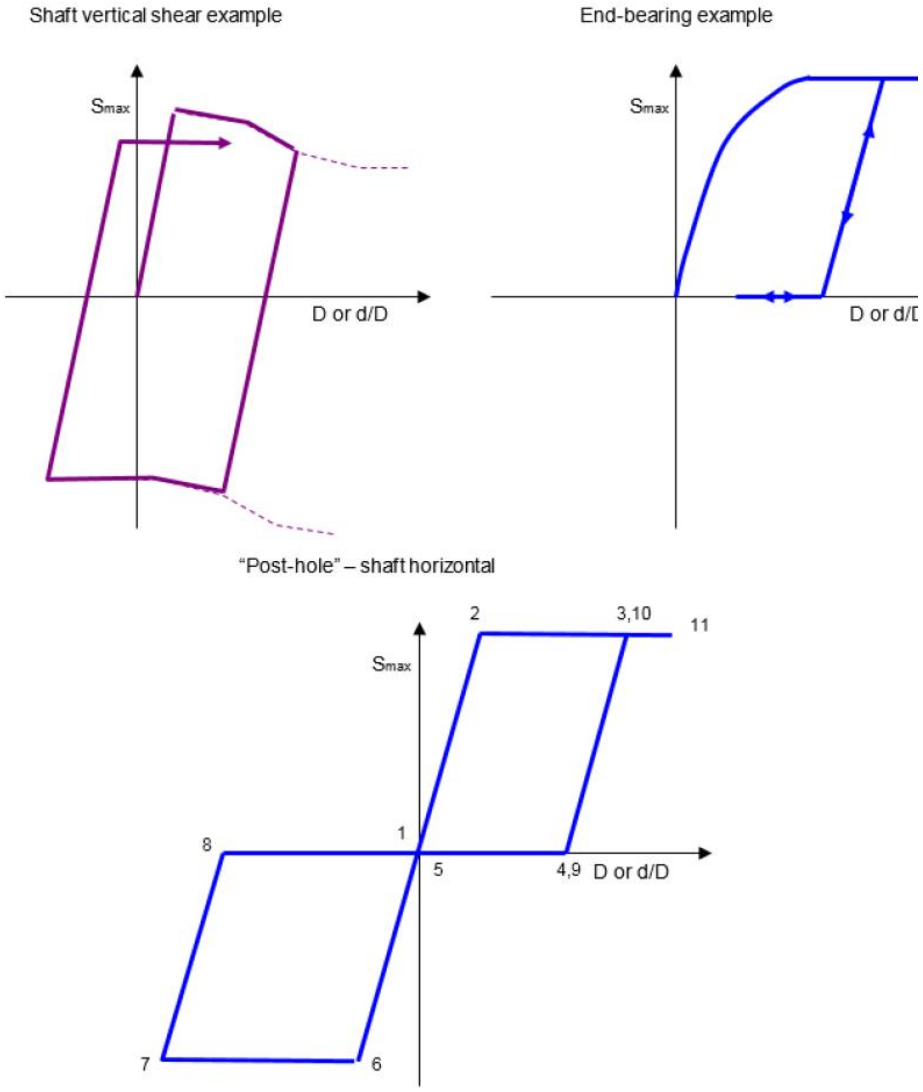

ARUP

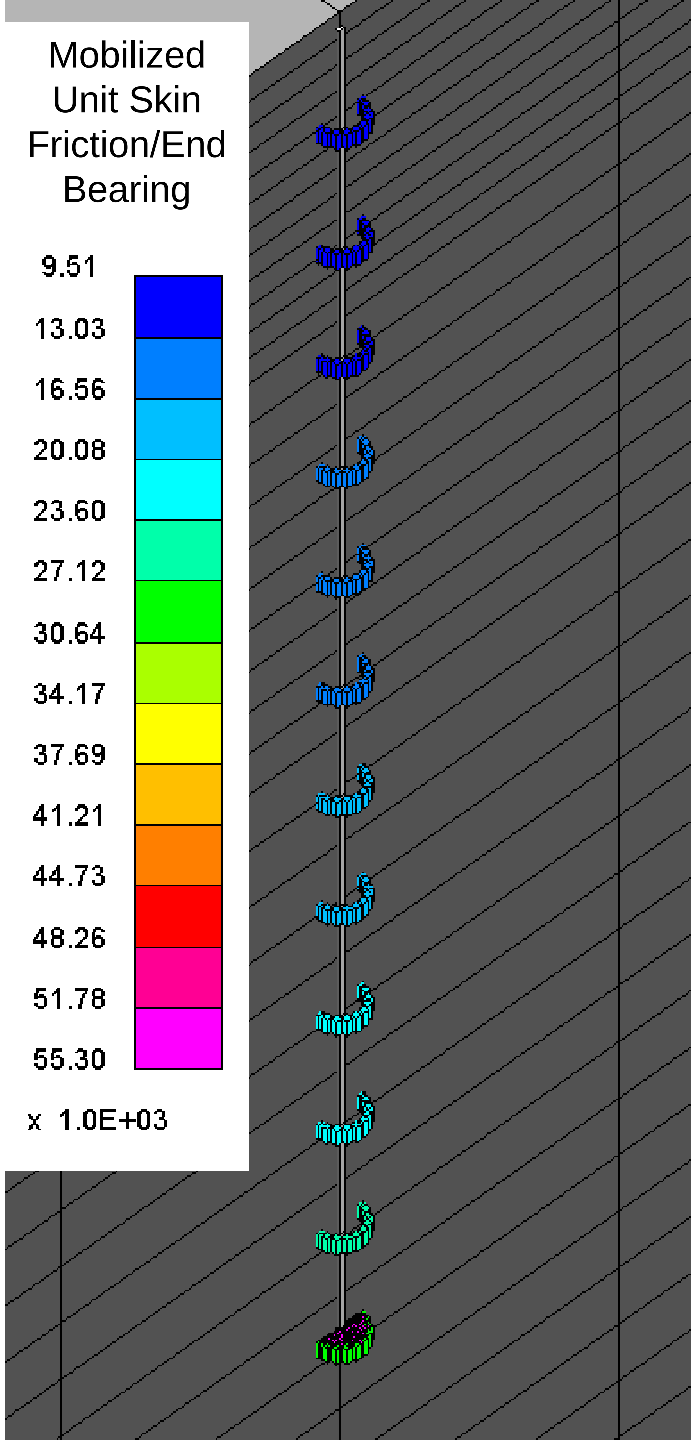
Mobilized
Unit Skin
Friction/End
Bearing
9.51
13.03
16.56
20.08
23.60
27.12
30.64
34.17
37.69
41.21
44.73
48.26
51.78
55.30
x 1.0E+03

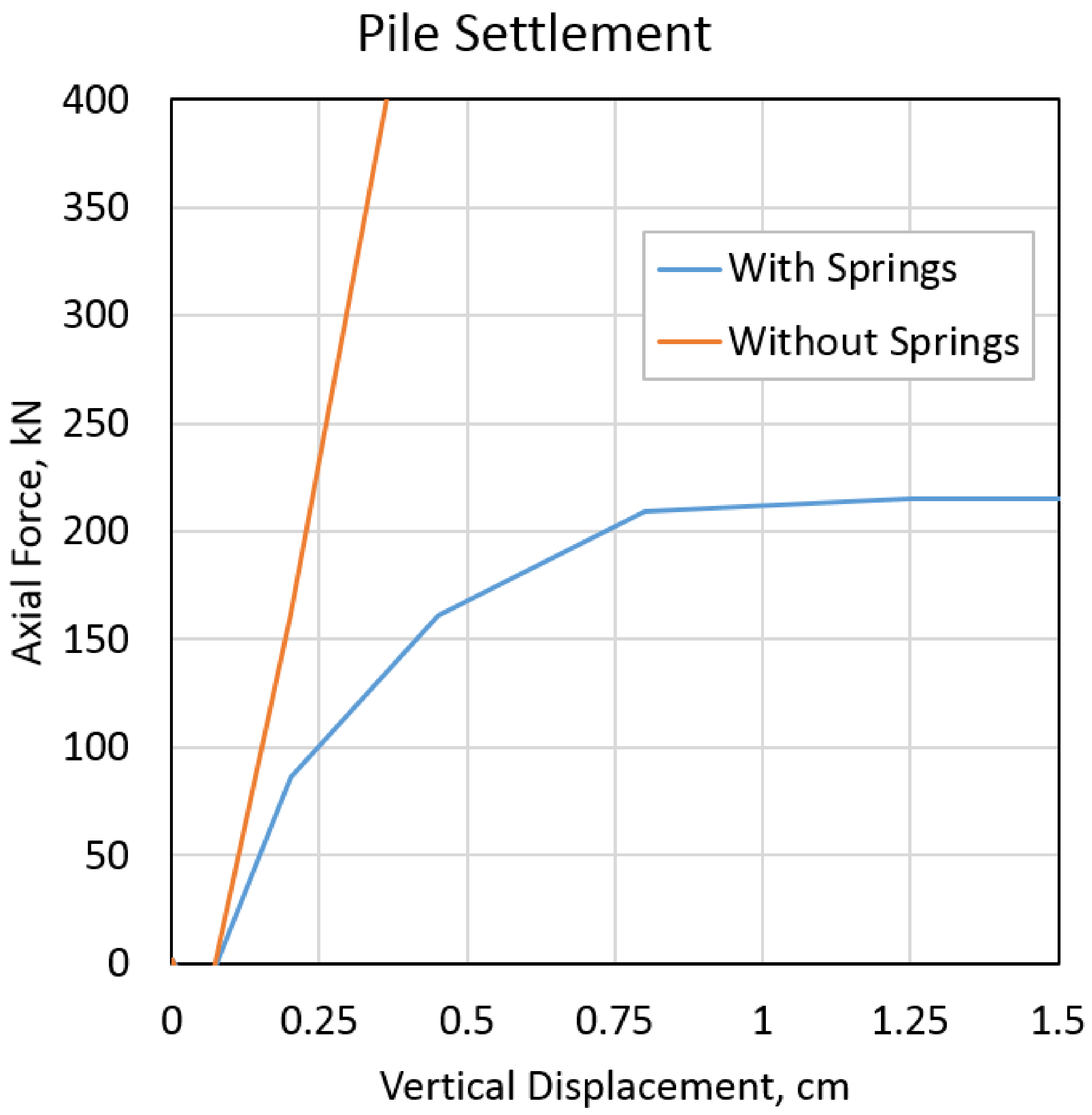
Pile Settlement
Axial Force, kN
400
350
300
250
200
150
100
50
0
With Springs
Without Springs
0
0.25
0.5
0.75
1
1.25
1.5
Vertical Displacement, cm

ARUP

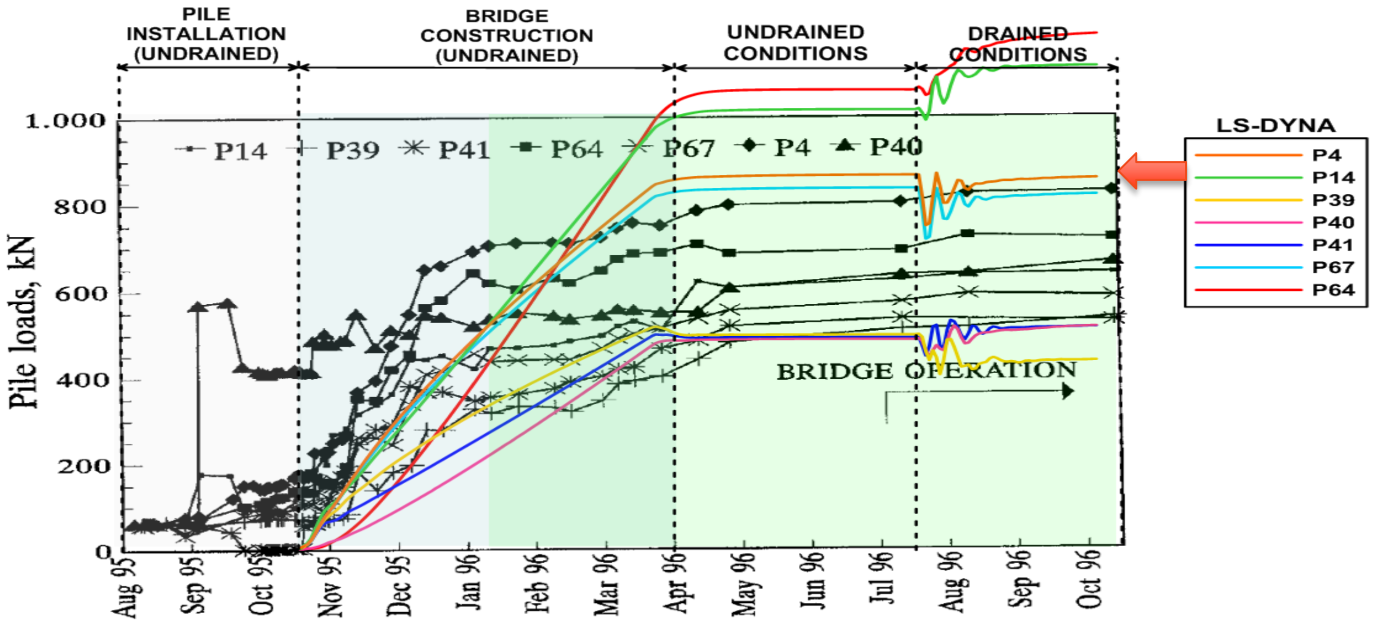

STATIC
PILE
LOADS

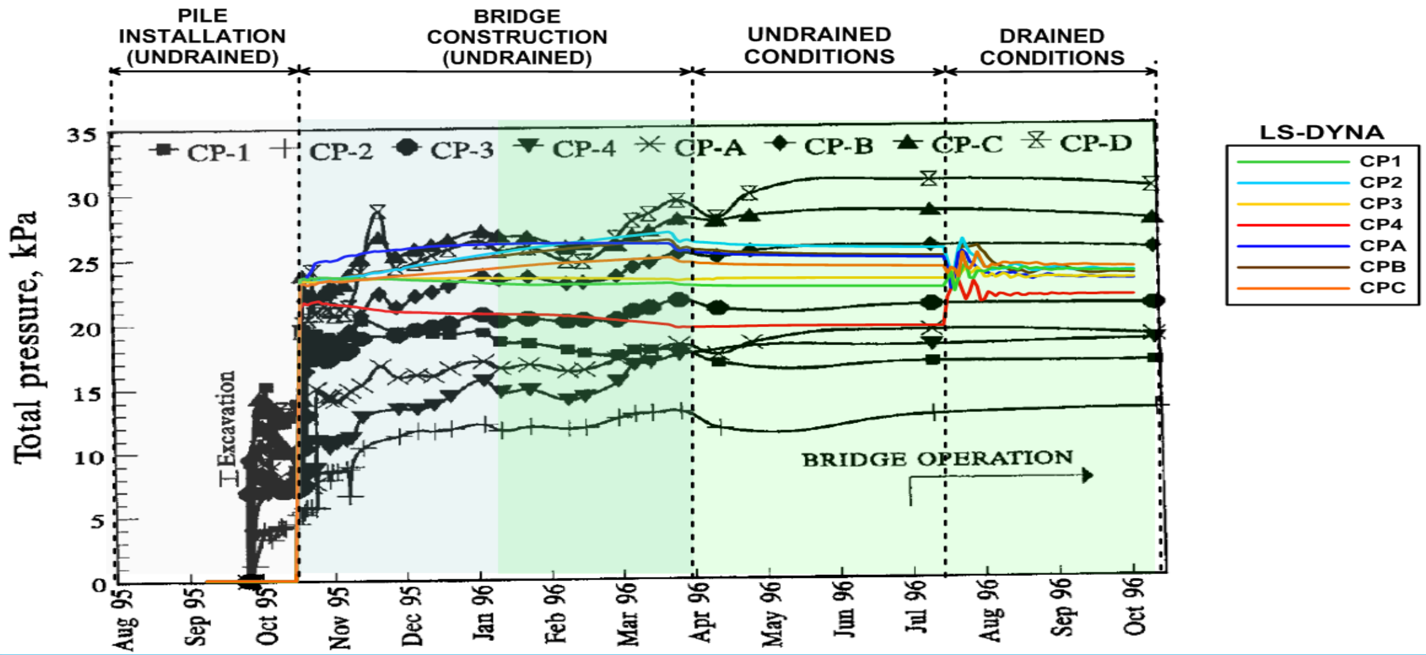

STATIC MAT/SOIL
INTERFACE
PRESSURES

Impulsora: LSDyna results over Mendoza et al (2000) data

ARUP

All instrumented pressure cells & piles at Impulsora: FE simulation

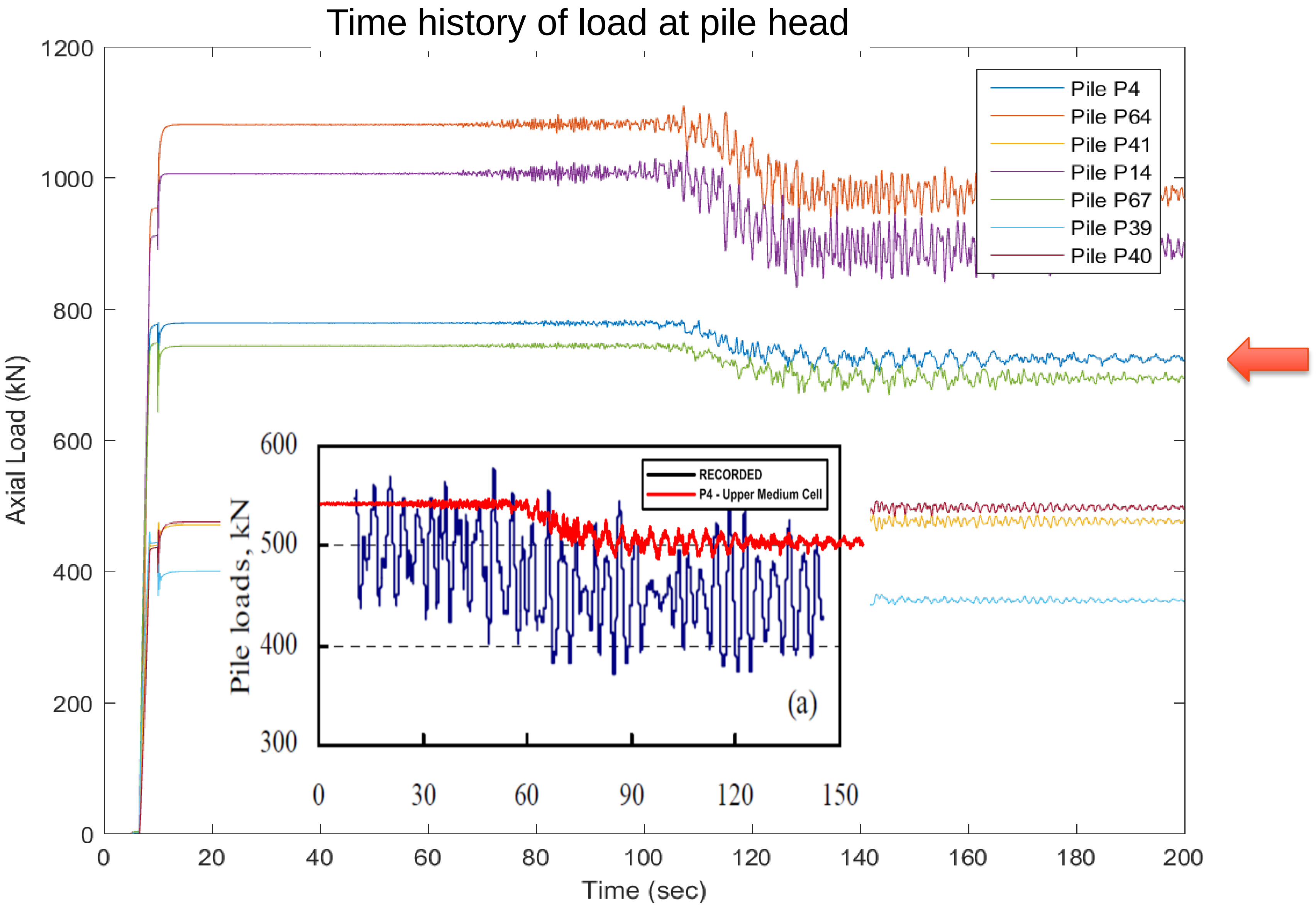

ARUP

All instrumented pressure cells & piles at Impulsora: FE simulation

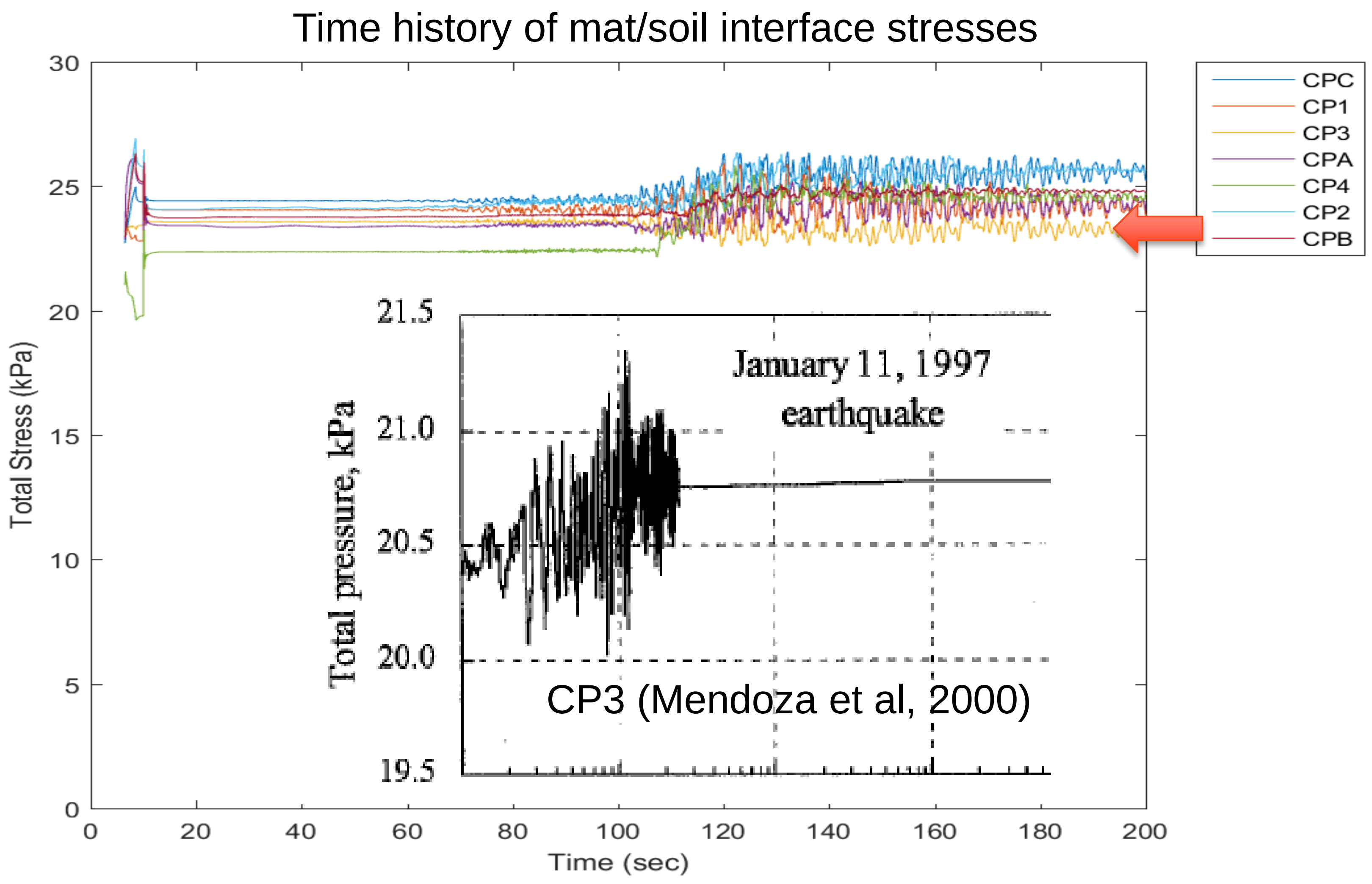

ARUP

New International Airport, Mexico City

Located on virgin Lake Texcoco clays

ARUP

NAIM Air traffic control tower

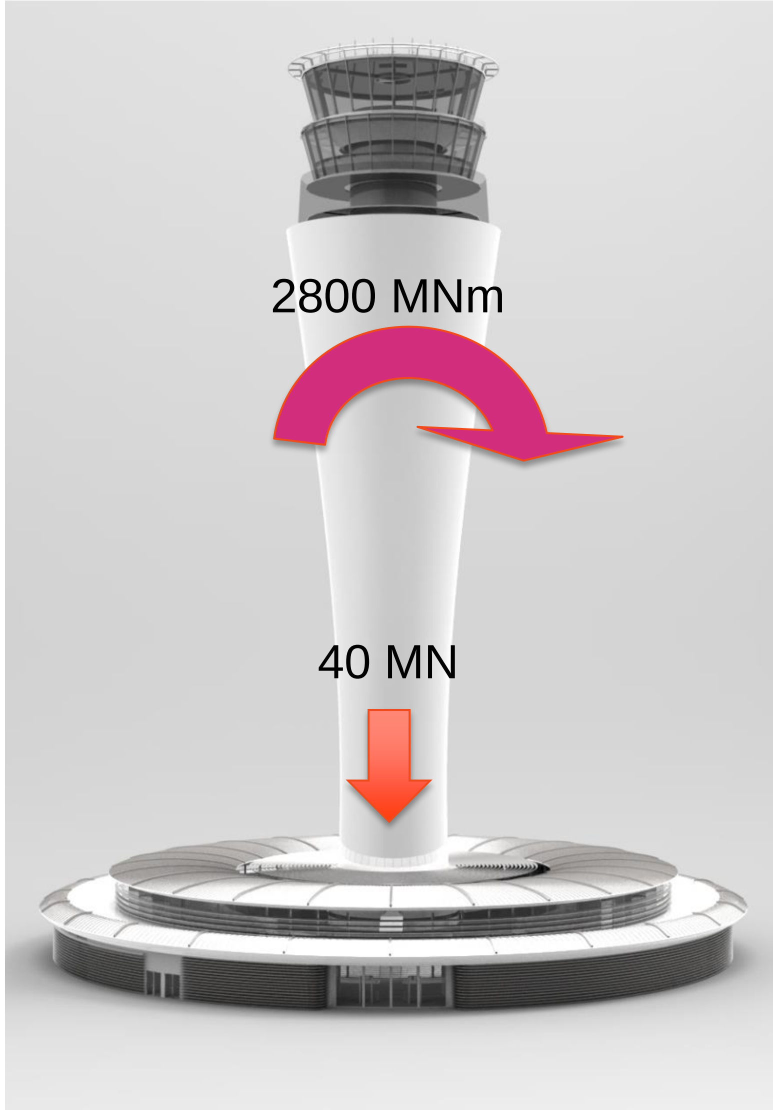

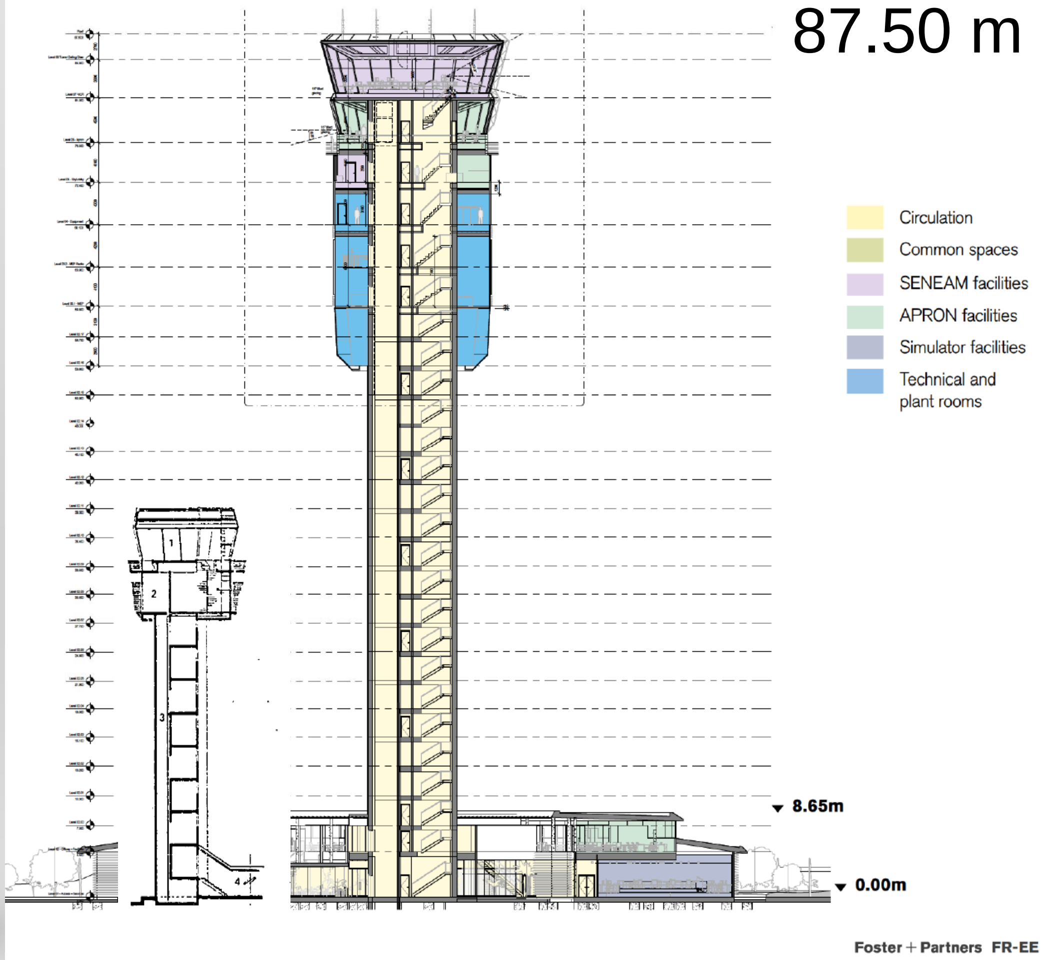

ARUP

Michouacan EQ Motion 19 Sept 1985, scaled to 1 in 2475 year return period

No Piles

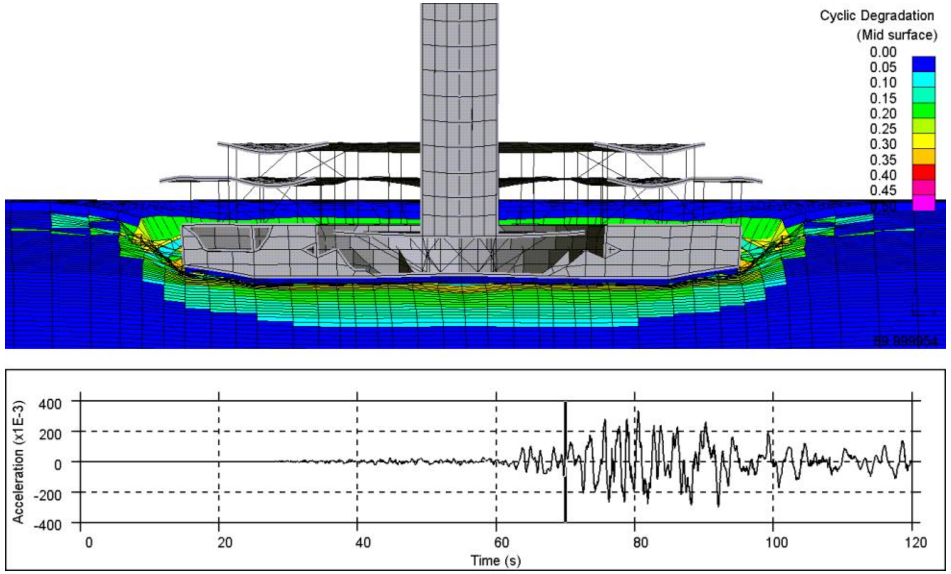

480 Lower Bound Piles

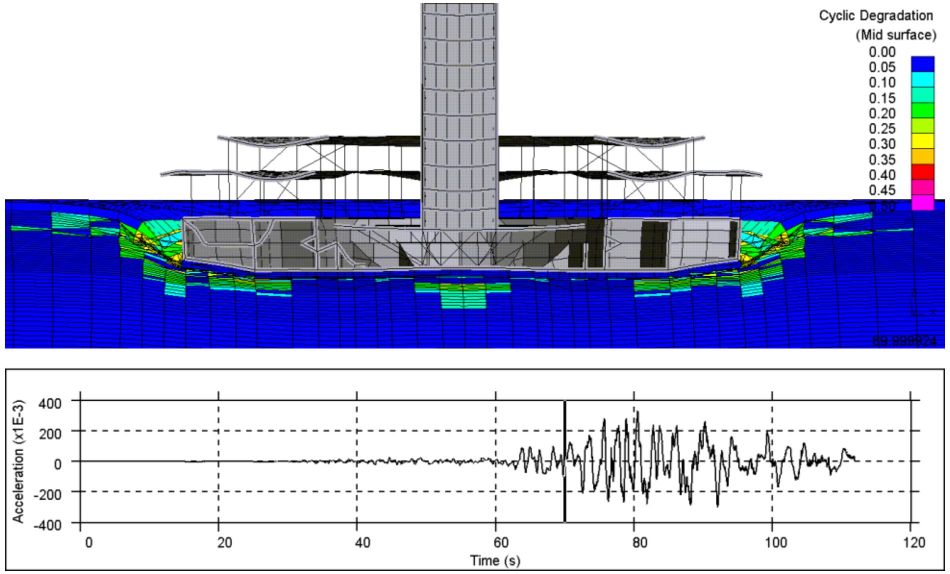

Soil modelled using backbone curves that degrade cyclically using a damage strain algorithm to mimic cyclic triaxial test behaviour

ARUP

NAIM Passenger terminal building under construction
January 2019

ARUP

IIUNAM measured excess pore pressures and settlements under PTB raft Puebla earthquake 19 September 2017

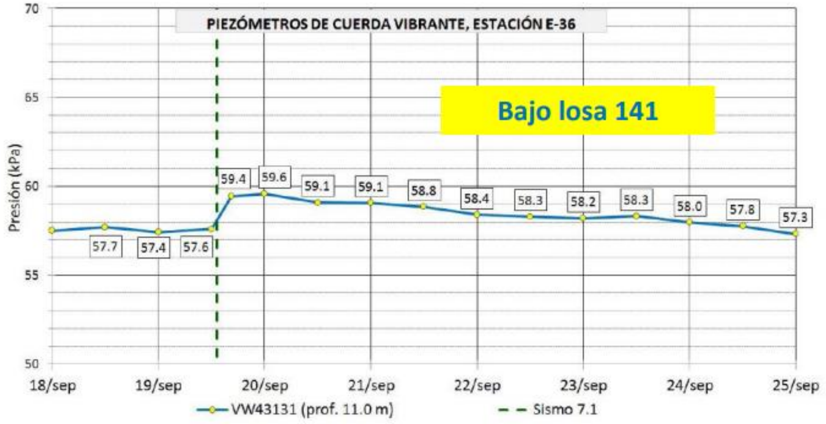

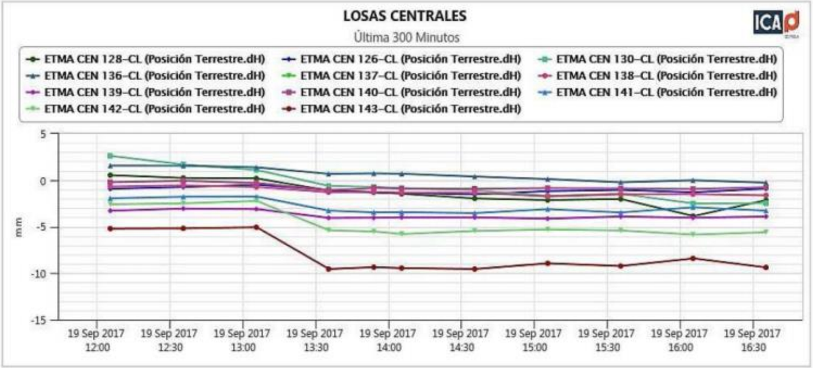

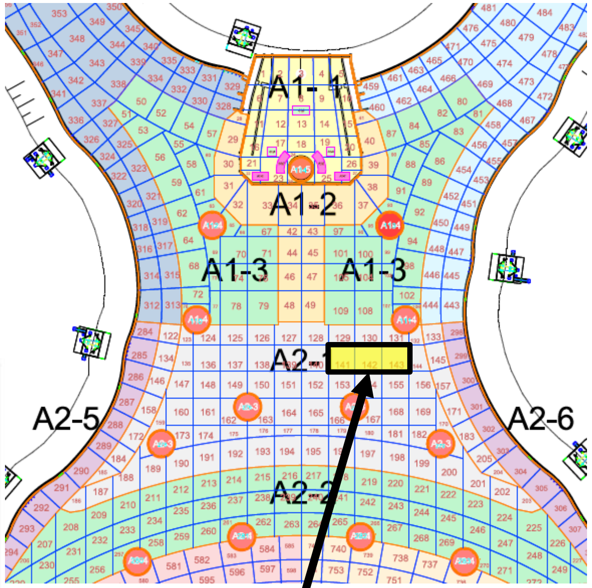

Pwp and movements reported by UNAM in this area

Bajo losas 141, 142 y 143

ARUP

Dynamic Soil Structure Interaction: extreme events, acute & repetitive

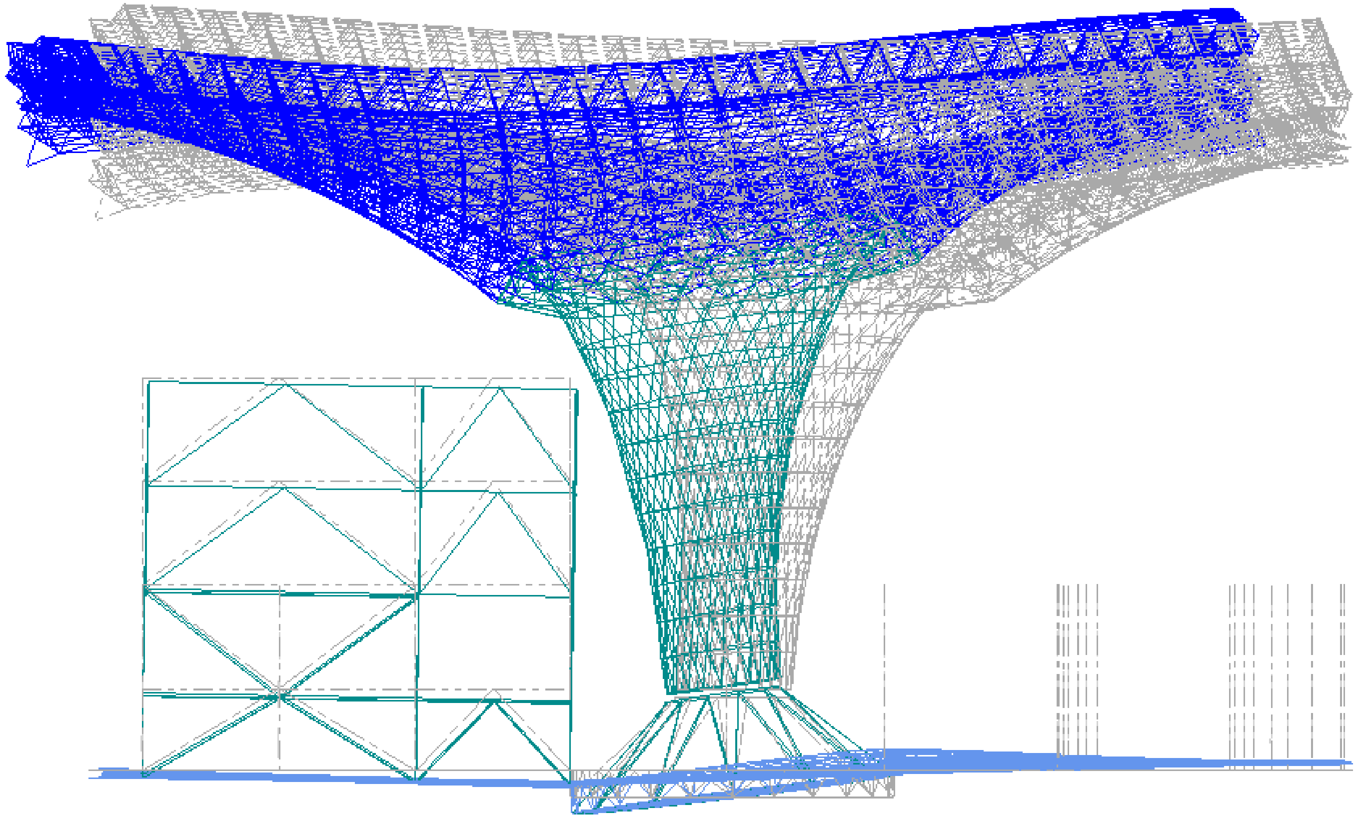

ARUP

- Increasing urbanisation has changed the nature of geotechnical engineering
- Everything is connected, and we can ‘instrument the Anthropocene’, beyond mere construction monitoring
- A resilient future will require much greater feedback from performance of foundation systems
- Dynamic numerical analysis can be used to calibrate soil models against extreme events
- This includes transient ‘extreme’ in-situ tests such as the CPT and Pressuremeter, as well as output from vertical arrays of seismic accelerometers

- Advanced, unified soil models and increasing computing power enable progress towards performance-based design and resilience
- We can look forward to increasing feedback from long term instrumentation systems: ‘Big *geotechnical* data’
- We now have the tools to articulate to stakeholders the consequences of extreme events on foundation systems through the use of digital ‘twins’

Sincere thanks are due to, in no particular order:

Yuli Huang, Iraklis Koutrouvelis, Kirk Ellison, Ibbi Almufti, Richard Sturt, Tom Wilcock, James Go, Jongwon Lee, Martin Walker, Eron Sudhausen, Chris Humpheson, John Seaman, Helen Dingle, Anton Pillai, Mike Long, Nick Sartain, William Powrie, Jeff Priest, Olivier Martin, Paul Vardanega, Tom Wilcock, Matt Clark, Youssef Hashash, Ed Cording, Demetrious Koutsoftas, Mike Long, Toni Canavate, Francisco Ciruela, Brian Simpson, Juan Mayoral, Jesus Mendoza, Gabriel Auvinet, Tom O'Rourke, Paul Morrison, Tim Chapman, Deepak Jayaram, Ulas Cilingir, Alan Phear

Thank you!